# Non-Dinosaurian Dinosauromorphs from the Chinle Formation (Upper Triassic) of the Eagle Basin, Northern Colorado: *Dromomeron romeri* (Lagerpetidae) and a New Taxon, *Kwanasaurus williamparkeri* (Silesauridae)

**Jeffrey W Martz** [Corresp., 1, 2], **Bryan J Small** [3]

[1] Department of Natural Sciences, University of Houston, Downtown, Houston, Texas, United States

[2] Denver Museum of Nature and Science, Earth Sciences, Denver, Colorado, United States

[3] The Museum of Texas Tech University, Lubbock, Texas, United States

Corresponding Author: Jeffrey W Martz
Email address: martzj@uhd.edu

The “red siltstone” member of the Upper Triassic Chinle Formation in the Eagle Basin of Colorado contains a diverse assemblage of dinosauromorphs falling outside of Dinosauria. This assemblage is the northernmost known occurrence of non-dinosaurian dinosauromorphs in North America, and probably falls within either the Revueltian or Apachean land vertebrate estimated biochronozones (215-202 Ma, middle Norian to Rhaetian). Lagerpetids are represented by proximal femora and a humerus referable to *Dromomeron romeri*. Silesaurids (non-dinosaurian dinosauriforms) are the most commonly recovered dinosauromorph elements, consisting of dentaries, maxillae, isolated teeth, humeri, illia, femora, and possibly a scapula and tibiae. These elements represent a new silesaurid, *Kwanasaurus williamparkeri*, gen. et sp. nov., which possesses several autapomorphies: a short, very robust maxilla with a broad ascending process, a massive ventromedial process, a complex articular surface for the lacrimal and jugal, and twelve teeth; fourteen dentary teeth; an ilium with an elongate and blade-like preacetabular process and concave acetabular margin; a femur with an extremely thin medial distal condyle and a depression on the distal end anterior to the crista tibiofibularis. The recognition of *K. williamparkeri* further demonstrates the predominantly Late Triassic diversity and widespread geographic distribution of silesaurids more derived than *Asilisaurus*, a clade here named Sulcimentisauria. Silesaurid dentition suggests a variety of dietary specialization from small vertebrates and invertebrates to herbivory, and the extremely robust maxilla and folidont teeth of *K. williamparkei* may represent relatively strong herbivorous dietary specialization among silesaurids.

# NON-DINOSAURIAN DINOSAUROMORPHS FROM THE CHINLE FORMATION (UPPER TRIASSIC) OF THE EAGLE BASIN, NORTHERN COLORADO: *DROMOMERON ROMERI* (LAGERPETIDAE) AND A NEW TAXON, *KWANASAURUS WILLIAMPARKERI* (SILESAURIDAE)

JEFFREY W. MARTZ[1] AND BRYAN J. SMALL[2]

[1]Department of Natural Sciences, University of Houston-Downtown, 1 Main Street, Houston, TX 77002 USA; Department Earth Sciences, Denver Museum of Nature and Science, 2001 Colorado Boulevard, Denver, CO 80205, USA

[2]The Museum of Texas Tech University, 3301 4th St., Lubbock, TX 79409-3191, USA

Corresponding Author:

Jeffrey W. Martz[1]

Email address: martzj@uhd.edu

## ABSTRACT

The “red siltstone” member of the Upper Triassic Chinle Formation in the Eagle Basin of Colorado contains a diverse assemblage of dinosauromorphs falling outside of Dinosauria. This assemblage is the northernmost known occurrence of non-dinosaurian dinosauromorphs in North America, and probably falls within either the Revueltian or Apachean land vertebrate estimated biochronozones (215-202 Ma, middle Norian to Rhaetian). Lagerpetids are represented by proximal femora and a humerus referable to *Dromomeron romeri*. Silesaurids (non-dinosaurian dinosauriforms) are the most commonly recovered dinosauromorph elements, consisting of dentaries, maxillae, isolated teeth, humeri, illia, femora, and possibly a scapula and tibiae. These elements represent a new silesaurid, *Kwanasaurus williamparkeri*, gen. et sp. nov., which possesses several autapomorphies: a short, very robust maxilla with a broad ascending process, a massive ventromedial process, a complex articular surface for the lacrimal and jugal, and twelve teeth; fourteen dentary teeth; an ilium with an elongate and blade-like preacetabular process and concave acetabular margin; a femur with an extremely thin medial distal condyle and a depression on the distal end anterior to the crista tibiofibularis. The recognition of *K. williamparkeri* further demonstrates the predominantly Late Triassic diversity and widespread geographic distribution of silesaurids more derived than *Asilisaurus*, a clade here named Sulcimentisauria. Silesaurid dentition suggests a variety of dietary specialization from small vertebrates and invertebrates to herbivory, and the extremely robust maxilla and folidont teeth of *K. williamparkei* may represent relatively strong herbivorous dietary specialization among silesaurids.

## INTRODUCTION

By the final years of the 20th century, the diversity of dinosauromorphs across Pangea was thought to follow a simple pattern during the Triassic Period. The non-dinosaurian dinosauromorphs were restricted to the Middle Triassic of South America (*Sereno & Arcucci, 1994a,b*), and Dinosauria was restricted to the Late Triassic with theropods, sauropodomorphs, and ornithischians all having a global distribution that included western North America (*e.g. Lucas, Hunt & Long, 1992; Long & Murry, 1995; Padian & May, 1999*).

This picture began to change drastically in the 21st century with the description of *Silesaurus opolensis* (*Dzik, 2003*) from the Carnian or Norian Krasiejów beds of Poland, which revealed that non-dinosaurian dinosauriforms survived into the Late Triassic. This prompted an extensive re-evaluation of the record of putative dinosaur fossils from the Upper Triassic Chinle Formation of New Mexico and Arizona, and the equivalent Dockum Group of Texas (*Ezcurra, 2006; Nesbitt, Irmis & Parker, 2007, Nesbitt et al., 2009a, Nesbitt & Chatterjee, 2008; Irmis et al., 2007; Martz et al., 2013; Sarigül, 2016*).

In addition to revealing that ornithischians and sauropodomorphs were probably absent in North America prior to the Jurassic (*Nesbitt, Irmis & Parker, 2007; Irmis et al., 2007*), this work led to a previously unrecognized diversity of non-dinosaurian dinosauromorphs surviving into the Late Triassic of North America. The lagerpetid dinosauromorphs *Dromomeron romeri* (*Irmis et al., 2007*) and *D. gregorii* (*Nesbitt et al., 2009a*) extended the record of the Lagerpetidae from the Middle Triassic of South America into the Norian stage of the Late Triassic of North America (*Irmis et al., 2007; Nesbitt, Irmis & Parker, 2007;Marsh, 2018*). Moreover, the taxa *Eucoelophysis baldwini* (*Sullivan & Lucas, 1999*) from the Chinle Formation of New Mexico (*Ezcurra, 2006; Nesbitt, Irmis & Parker, 2007; Irmis et al., 2007; Breeden et al., 2017*) and

*Technosaurus smalli* (*Chatterjee, 1984*) and *Soumyasaurus aenigmaticus* (*Sarigül, Agnolin & Chatterjee, 2018*) from the Dockum Group of Texas demonstrate that silesaurids occurred in North America during the Late Triassic (*Nesbitt, Irmis & Parker, 2007; Martz et al., 2013*). Lagerpetids and silesaurids have also been discovered in Upper Triassic strata outside of Poland and western North America, giving both groups a global record spanning the Middle to Late Triassic (*e.g. Langer et al., 2013; Martinez et al., 2015; Müller, Langer & Da Silva, 2018*), and both groups coexisted with dinosaurs in Gondwana by the late Carnian (*Martinez et al., 2013; Garcia et al., 2018*).

The Eagle Basin of Colorado (Fig. 1A) contains some of the northernmost exposures of the Chinle Formation (*Poole & Stewart, 1964; Dubiel, 1992*), a unit that has been studied more extensively in the Colorado Plateau (*e.g. Stewart, Poole & Wilson, 1972; Blakey & Gubitosa, 1983; Lucas, 1993; Dubiel, 1994; Martz et al., 2017*). During the Late Triassic, the Eagle Basin was separated from the Colorado Plateau depocenter by the Ancestral Front Range and Ancestral Uncompahgre Highlands (*e.g. Dubiel, 1992, 1994*). Over twenty years of collection from Eagle Basin localities by the junior author has yielded an abundance of vertebrate fossils, mostly consisting of isolated elements (*Small & Sedlmayr, 1995; Small, 2001, 2009; Martz, Mueller & Small, 2003; Small & Martz, 2013; Martz & Small, 2016; Pardo, Small & Huttenlocker, 2017*), that include rare fish, the stem caecilian *Chinlestegophis jenkinsi Pardo, Small, & Huttenlocker, 2017*, a possible metoposaurid, a leptopleuronine procolophonid similar to *Libognathus Small, 1997*, a variety of small diapsids, rare phytosaur elements that cannot be assigned to alpha taxa, the aetosaur *Stenomyti huangae Small and Martz, 2013*, another aetosaur that may be referable to *Rioarribasuchus Lucas, Hunt, & Spielmann, 2006*, shuvosaurids, rauisuchids, crocodylomorphs,

and dinosauromorphs. A variety of plant macrofossils have also been recovered from the area (*B.J. Small and J.W. Martz, unpublished data*).

Here we describe the first occurrence of the lagerpetid *Dromomeron romeri* from the Chinle Formation of the Eagle Basin of Colorado, which represents the northernmost occurrence of the genus, and a new genus and species of silesaurid, *Kwanasaurus williamparkeri*. This new taxon is based primarily on isolated elements (Table 1) exhibiting a distinctive suite of derived characters not recognized in any other silesaurid. *Kwanasaurus* is the fourth silesaurid alpha taxon recognized from North America, and the northernmost silesaurid known from the Americas. Material from the Eagle Basin localities referable to Neotheropoda (*Small, 2009*) will be described in detail elsewhere.

## GEOLOGIC SETTING

The fossils that are the focus of this study come from the middle of the informally named "red siltstone member" of the Chinle Formation (Fig. 1B-E), a 100-150 meter section of steep, bench forming red beds that overlie the Gartra Member, a conglomeratic sandstone considered to form the base of the Chinle Formation. The Eagle Basin Chinle Formation unconformably overlies the Permian Maroon Formation and Early Triassic State Bridge Formation, and is unconformably overlain by the Early Jurassic Entrada Formation (*Poole & Stewart, 1964; Stewart, Poole & Wilson, 1972; Dubiel & Skipp, 1989; Dubiel, 1992*).

The red siltstone member contains sandstones and conglomerate lenses interbedded with siltstones and very fine sandstones showing abundant evidence of pedogenic modification; these beds have been interpreted as moderate to high sinuosity channels sandstones and overbank deposits (*Dubiel, 1992*). The red siltstone member shows a subtle fining upward sequence in

which the upper part of the sequence is almost entirely siltstone to very fine-grained sandstone with more evidence of pedogenic development than seen in the lower part of the member (Fig. 1B; *J.W. Martz & B.J. Small, unpublished notes*). Although *Poole & Stewart (1964)* correlated the red siltstone member with the Church Rock Member of Utah, the sedimentological transition from the lower to upper red siltstone member (Fig, 1B-C) resembles the shift from the Petrified Forest Member to the Owl Rock Member in the Colorado Plateau (*e.g. Blakey & Gubitosa, 1983; Martz et al., 2017*). However, the current authors have not pursued sufficiently detailed lithostratigraphic correlations between the Eagle Basin and the Colorado Plateau to resolve the precise relationships between these units.

Vertebrate specimens from the Eagle Basin have primarily been recovered from the lower half of the red siltstone member, 50-60 meters below the top of the Chinle Formation, in the coarser-grained "Petrified Forest-like" facies (Fig. 1B). Specimens have been recovered from the highly productive Main Elk Creek locality near Newcastle, Colorado (DMNS loc. 1306), as well as the Derby Junction (DMNH loc. 692; Dubiel, 1992, p. W16), Lost Bob (DMNH loc. 3980), Lost Bob East (DMNH loc. 4629), Burrow Cliff (DMNH loc. 4340) and Shuvosaur Surprise (DMNH loc. 3492) localities. All localities occur at about the same stratigraphic horizon near Derby Junction, Colorado (Fig. 1B). Specimens consist mostly of isolated bones, with occasional associated remains and rare articulated elements, recovered from small conglomeratic lenses (Fig. 1E) probably representing small channels transporting remains under high energy conditions (*Small & Martz, 2013, unpublished data*). The finer-grained overbank siltstones (Fig. 1D) represent lower energy conditions and have yielded some of the best-articulated material (e.g. the holotype of *Stenomyti huangae*; *Small & Martz, 2013*).

The precise age of the Eagle Basin Chinle localities is difficult to determine, as these strata have not yet yielded a diagnostic palynoflora, phytosaur cranial material, or radioisotopic dates required for definitive biostratigraphic or chronostratigraphic correlations with the better-calibrated Chinle Formation of the Colorado Plateau and Dockum Group of the southern High Plains (e.g. *Irmis et al., 2011; Martz & Parker, 2017*). However, specimens possibly referable to the leptopleuronine procolophonid *Libognathus* (DMNH EPV. 56657), the aetosaur *Rioarribosuchus* (e.g. DMNH EPV.48018, 48019), and the lagerpetid *Dromomeron romeri* (DMNH EPV.54826) all provide circumstantial evidence that the fossil localities may fall within the Revueltian estimated biochronozone (*Small, 2009; sensu Martz & Parker, 2017*) which is probably Alaunian to Sevatian (middle to late Norian) (*Martz & Parker, 2017*). Moreover, the aetosaur *Stenomyti huangae* (*Small & Martz, 2013*) is very similar to *Aetosaurus* material from European strata that are probably also Norian (*Wild, 1989; Heckert & Lucas, 2000; Bachmann & Kozur, 2004*), and *Aetosaurus*-like osteoderms have been identified from the Revueltian and Apachean estimated biochronozones elsewhere in the western United States (*Lucas, 1998; Heckert et al., 2007; Martz, 2008*).

## METHODOLOGY

All material described below from the Main Elk Creek, Lost Bob, Shuvosaur Surprise, Burrow Cliff, and Derby Junction localities are isolated and associated elements from larger bone assemblages. We rely primarily on an apomorphy-based approach for identification of vertebrates from the Eagle Basin localities following the framework established for other Upper Triassic localities (*Nesbitt & Stocker, 2008; Martz et al., 2013*). This testable approach utilizes the presence of discrete apomorphies in a phylogenetic framework to determine the taxonomic

158 placement of individual specimens (*Bever, 2005; Bell, Gauthier & Bever, 2010*). Incomplete
159 specimens lacking clear autapomorphies may in some cases be tentatively assigned to particular
160 taxa based on close association or similarity with more complete specimens possessing
161 autapomorphies. Moreover, we have designated voucher specimens for all identified taxa, which
162 are usually the most complete or best preserved specimens (Table 1). Measurements for selected
163 appendicular elements are given in Table S1, illustrated in Fig. S1, and described in Appendix 1.
164 The electronic version of this article in Portable Document Format (PDF) will represent a
165 published work according to the International Commission on Zoological Nomenclature (ICZN),
166 and hence the new names contained in the electronic version are effectively published under that
167 Code from the electronic edition alone. This published work and the nomenclatural acts it
168 contains have been registered in ZooBank, the online registration system for the ICZN. The
169 ZooBank LSIDs (Life Science Identifiers) can be resolved and the associated information viewed
170 through any standard web browser by appending the LSID to the prefix http://zoobank.org/. The
171 LSID for this publication is: urn:lsid:zoobank.org:pub:20FCEEA6-4512-42FD-BAE9-
172 A570BF4611F4. The online version of this work is archived and available from the following
173 digital repositories: PeerJ, PubMed Central and CLOCKSS.
174
175 **SYSTEMATIC PALEONTOLOGY**
176
177 **Dinosauromorpha** *Benton, 1985 sensu Sereno, 1991*
178 **Lagerpetidae** *Arcucci, 1986 sensu Nesbitt et al., 2009a*
179 ***Dromomeron*** *Irmis et al., 2007*
180 ***Dromomeron romeri*** *Nesbitt, Irmis & Parker, 2007*

181

182 **Referred specimens**. DMNH EPV.54826 (Fig. 2), proximal left femur (voucher specimen);
183 DMNH EPV.63873 (Fig. 3), proximal right femur (and other associated elements, at least some
184 of which are pseudosuchian); DMNH EPV.29956 (Fig. 4), right humerus.

185 **Description and discussion**.

186 **Femur**

187 Two proximal femora (Figs. 2-3; DMNH EPV.54826; DMNH EPV. 63873) recovered from
188 Main Elk Creek possesses several apomorphies of the lagerpetid *Dromomeron* (*Irmis et al.,*
189 *2007; Nesbitt et al., 2009a; Langer et al., 2013*). The femoral heads are distinctly hook-shaped
190 with a ventrolateral emargination (ve in Figs. 2-3) as in *Dromomeron romeri*, *Lagerpeton*
191 *chanarensis,* and *Ixalerpeton polesinensis* (*Nesbitt et al., 2009a; Cabreira et al., 2016*) and a
192 well-developed posteromedial tuber (pmt in Fig. 2-3) that is much larger than the anteromedial
193 tuber (amt in Fig. 2-3), which is barely discernible (autapomorphies of Lagerpetidae; *Nesbitt, et*
194 *al., 2009a*). The proximal end of the femora forms the smooth arc characteristic of lagerpetids,
195 with the facies articularis antitrochanterica (faa in Figs. 2-3) extending more ventrally on the
196 posteromedial side of the proximal femur as in other dinosauromorphs (*Nesbitt et al., 2009a*). An
197 anterolateral tuber is absent so that the lateral side of the proximal femur head is relatively
198 flattened in DMNH EPV.54826 (Fig. 2B), a feature shared by lagerpetids and shuvosaurids
199 (*Nesbitt, 2011*), although the region is nonetheless somewhat swollen in DMNH EPV. 63873.
200 There is no indication of the roughened anterior trochanter or posteromedial muscle scar
201 diagnostic of *Dromomeron gigas* (*Martinez et al., 2015*). The anterolateral edge of the proximal
202 end of the femora is sharper than the posteromedial edge of the proximal end, although it does
203 not form the distinct dorsolateral trochanter present in dinosauriforms (*Nesbitt, 2011, 307-0*).

Below this sharp edge, the anterolateral surface of the proximal end of the femur in DMNH EPV.54826 is slightly concave (cnc in Fig. 2A), although the region is not fully prepared in DMNH EPV.63873. This concavity distinguishes *Dromomeron* from *Lagerpeton*, in which the anterolateral surface is flattened (*Nesbitt et al., 2009a, p. 502*). At least in DMNH EPV.54826, where some of the shaft is preserved, both lesser (anterior) and fourth trochanters are completely absent (autapomorphy of *Dromomeron romeri*; *Nesbitt et al., 2009a*). The posteromedial surface of the femur shaft is flattened and a scar for M. caudifemoralis longus cannot be clearly discerned (Fig. 2D), while the anterolateral surface of the shaft is more convex (cnv in Fig. 2B).

**Humerus**

The only non-dinosauriform dinosauromorph humeri known are for *Ixalerpeton*, which was figured but not described in detail (*Cabreira et al., 2016: figure 1F*) and a passing mention by *Nesbitt (2011, p. 125)* of a humerus he assigned to *Dromomeron gregorii* (TMM 31000-1329) without description. A slender right humerus (DMNH EPV. 29956; Fig. 4) from the Main Elk Creek locality may also belong to *Dromomeron*.

The proximal end and deltopectoral crest of DMNH EPV. 26656 (dc in Fig, 4B, D) are strongly mediolaterally expanded relative to the shaft as in most archosauriforms, including *Ixalerpeton* (*Cabreira et al., 2016*) and the dinosauriforms *Asilisaurus*, *Lewisuchus*, and *Marasuchus* (*Langer et al., 2013*). The proximal end and deltopectoral crest are both much less expanded in the derived silesaurids *Silesaurus* and *Diodorus*, as well as shuvosaurids (*Dzik, 2003; Nesbitt, 2011; Kammerer, Nesbitt & Shubin, 2012; Langer et al., 2013*).

The expanded proximal part of the humerus is medially inclined (Fig. 4A, D). The proximal end bears two distinct swellings, possibly the ectotuberosity and entotuberosity of *Welles (1984)* (ec and en in Fig. 4A-B), and a pointed medial or internal tuberosity (mt in Fig.

227 4A-C). The medial tuberosity is slightly displaced distally relative to the proximal edge of the
228 head as in most dinosauromorphs including *Ixalerpeton* (*Cabreira et al., 2016: figure 1F*), but
229 not in *Silesaurus* (*Dzik, 2003: figure 9*), and *Herrerasaurus* (*Sereno, 1994: figure 3*), where the
230 medial tuberosity is level with the proximal edge of the humerus.

231 The deltopectoral crest of DMNS EPV.29956 (dc in Fig. 4) is separated from the
232 proximal end of the humerus by a thin crest of bone (tc in Fig. 4A, D-E) as in dinosaurs (*Nesbitt,*
233 *2011*). However, as with most non-dinosaurian dinosauriforms, the deltopectoral crest retains the
234 plesiomorphic state of being subtriangular with the apex less than a third the length of the shaft
235 from the proximal end (*Nesbitt, 2011*); the deltopectoral crest in dinosaurs is subrectangular and
236 extends more than a third of the length of the humerus from the proximal end (*Langer & Benton,*
237 *2006; Nesbitt, 2011*). The lagerpetid *Ixalerpeton* differs from most non-dinosaurian
238 dinosauriforms in that the crest also extends more than a third the length of the humerus
239 (*Cabreira et al., 2016*).

240 Compared to *Marasuchus lilloensis* (*Bonaparte, 1975, fig. 9*), the shaft of the humerus in
241 DMNH EPV. 29956 is very slender compared to the distal end, much like *Ixalerpeton* (*Cabreira*
242 *et al., 2016, figure 1F*). A faintly preserved ectepicondylar flange and groove are present as in
243 phytosaurs and pseudosuchian archosaurs (ecf in Fig. 4B, E), although these are absent in nearly
244 all ornithodirans (*Nesbitt, 2011*). However, *Nesbitt (2011, p. 125)* noted that an ectepicondylar
245 groove was present in the humerus he assigned to *Dromomeron gregorii* (TMM 31000-1329);
246 whether or not a groove is present in *Ixalerpeton polesinensis* is unclear (*Cabreira et al., 2016:*
247 *figure 1F*). The ectepicondyle (lateral distal condyle) projects more distally than the
248 entepicondyle (medial condyle) (ect and ent in Fig. 4B-E) as it does in *Ixalerpeton* (*Cabreira et*

*al., 2016: figure 1F*). The posterior side of the distal end is deeply concave, with the concavity tapering proximally (cnc in Fig. 4C-D).

Viewed proximally, the long axes of the distal and proximal ends of the humerus are not parallel, but offset at an angle of about 45° (Fig. 4E-F). The presence of torsion between the proximal and distal ends of the humerus is variable amongst dinosauromorphs. It is present to at least some extent in *Eoraptor lunensis*, sauropodomorphs, and most basal theropods (*Tykowski, 2005: 172-1*), but absent (i.e. the long axes of the proximal and distal ends are parallel in proximal view) in *Marasuchus Herrerasaurus*, and basal ornithischians (*Tykowski, 2005*).

Given the presence of a single putative dinosaurian autapomorphy (a thin crest of bone separating the deltopectoral crest form the proximal end, also shared with *Ixalerpeton*) combined with a plesiomorphy absent in dinosaurs (subtriangular deltopectoral crest that does not extend far down the shaft), and the lack of any autapomorphies diagnosing any other archosauriform clade, DMNH EPV. 29956 is tentatively assigned to *Dromomeron*. The humerus is very distinct from those of both silesaurids and dinosaurs (see below).

**Dinosauriformes** *Novas, 1992*

**Referred specimens**. DMNH EPV.67956 (Fig. 5), partial right scapula; DMNH EPV.63875, complete right tibia (Fig. 6), several worn proximal left femora (all unfigured): DMNH EPV.27699, DMNH EPV.43126, and DMNH EPV.43588; DMNH EPV.56652 (Fig. 7A), worn proximal tibia; DMNH EPV.63872 (Fig. 7B-F), proximal right tibia; DMNH EPV.67955 (Fig. 7G-K), proximal left tibia.

**Description and discussion**. Some elements in the Eagle Basin collection possess dinosauriform apomorphies but cannot be assigned with certainty to a more specific group. These elements are

consistent with either silesaurids or basal (non-neotheropod) theropods (*e.g. Nesbitt et al., 2009b*), but lack autapomorphies that would allow them to be assigned definitively to either group. They are discussed here as potential silesaurid elements.

**Scapula**

DMNH EPV.67956 (Fig. 5) is a mostly complete right scapula from Lost Bob missing the much of the ventral anterior edge and the dorsal apex. The scapula is mediolaterally thickest ventrally at the articular glenoid (ag in Fig. 5C, E), and thins dorsally. In ventral view, the posteroventrally-facing surface of the glenoid is ovate, slightly concave, surfaced with spongy bone, and projects somewhat posterolaterally (Fig. 5E). Anterior to the glenoid, the element forms a subtriangular articular surface for the coracoid (co.ar in Fig. 5B, E). The posterior surface of the thickened part of the scapula immediately above the glenoid is flattened (Fig. 5C), the medial surface is slightly concave (cnc in Fig. 5B), and the lateral surface is slightly convex (cnv in Fig. 5D). The anterior part of the scapula prominence, including the preglenoid fossa, is not preserved except for part of the sharp-edged, posterodorsally-sloping, thin crest connecting the dorsal edge of the prominence to the anterior side of the shaft (tc in Fig. 5A-B, D). The absence of the scapula prominence is unfortunate, as the size of the ridge bordering the preglenoid fossa dorsally is much more sharper and narrower in at least some silesaurids compared to dinosaurs (*Langer & Ferigolo, 2013*), and may allow the two to be distinguished.

The anterior and posterior edges of the scapula shaft diverge slightly dorsally, indicating a widened dorsal apex, although most of the apex not preserved (asc in Fig. 5). However, it is evident that the blade length of the element is more than three times its distal width. Such "strap-like" scapulae occur in silesaurids and neotheropods (*Nesbitt, 2011: 218-1*), but also occurs in *Tawa hallae* (*Nesbitt et al., 2009b: figure 2B*). The lateral surface of the scapula shaft

is convex and the medial surface is slightly more flattened. Both surfaces are covered with faint longitudinal striations. The anterior edge of the shaft is also somewhat sharper than the posterior edge, and becomes very sharp as the shaft thins approaching the apex (Fig. 5A). The preserved part of the dorsal apex thins very abruptly (Fig. 5A, C). This may indicate an ossified suprascapula. Two tiny elongate depressions just below this abrupt thinning on the medial surface seem to be natural, and may end in tiny foramina.

The overall long and slender form of the scapula compares well with *Silesaurus* (*Dzik, 2003, figure 9*), *Sacisaurus* (*Langer & Ferigolo, 2013, figure 8i*), and the basal theropod *Tawa* (*Nesbitt et al., 2009b, figure 2B*). In most Late Triassic and Early Jurassic theropods, the element seems to be somewhat shorter with a much broader dorsal apex (*e.g. Rowe, 1989: figure 2; Colbert, 1989: figures 2-3; Carpenter, 1997: figure 5; Sereno, 1994; Tykowski, 2005: figure 59-62; Langer, Bittencourt & Schultz, 2011; Martinez et al., 2011*). However, in the absence of known silesaurid apomorphies, the Eagle Basin scapula can only be assigned to Dinosauriformes.

**Femur**

Several un-figured proximal femora (DMNH EPV. 27699, DMNH EPV.43126, and DMNH EPV.43588) are known from Main Elk Creek that are referable to Dinosauriformes based on the presence of an anterior trochanter but lack a trochanteric shelf; moreover, DMNH EPV.43126 possesses a posterolateral trochanter, which also diagnoses Dinosauriformes (*Langer & Benton, 2006; Nesbitt, 2011*). Preserved portions of these elements are identical to the silesaurid femora described below and likely belong to *Kwanasaurus*, but the proximal ends are too badly worn to preserve critical silesaurid apomorphies. As a result, they can only be assigned to Dinosauriformes.

**Tibia**

DMNH EPV.63875 (Fig. 6), a complete right tibia from Lost Bob East, DMNH EPV.56652 (Fig. 7A), a badly worn proximal tibia from Main Elk Creek, DMNH EPV.63872 (Fig. 7B-F), a proximal right tibia from Lost Bob, and DMNH EPV.67955 (Fig. 7G-K), a proximal left tibia from Lost Bob, can also be referred to Dinosauriformes. The combination of character states in these elements is consistent with silesaurids, although there aren't any identified tibia autapomorphies for silesaurids.

The posterior lateral and medial condyles at the proximal end (lc and mc in Figs.6-7) are adjacent in all specimens except for DMNH EPV.56652 (Fig. 7A), which is too badly worn to tell. Adjacent proximal condyles occur in silesaurids and theropods (*Langer & Benton, 2006; Nesbitt et al., 2009b; Nesbitt, 2011*). However, the proximal surfaces of DMNH EPV. 63875 and DMNH EPV.63872 are gently convex (Fig. 6C, E; 7D), and the cnemial crest is more or less straight (cc in Figs. 6A, 7B, G), as in non-dinosaurian dinosauromorphs. All specimens possess a distinct fibular crest (fc in Figs. 6E, 7A, F, K) as in most Triassic dinosauriforms except for *Tawa* (*Nesbitt et al., 2009b*). Moreover, unlike the condition in neotheropods, the cnemial crest does not project more proximally than the rest of the proximal end, and lacks a concavity separating the crest from the condyles (Fig. 6C, E, 7D, F, I, K). Unlike the basal theropod *Chindesaurus bryansmalli* (*Long & Murry, 1995; Nesbitt et al., 2009b; Marsh et al. 2016*), the lateral and medial condyles are about the same size (Fig. 6A, 7B).

The posteromedial surface of the proximal end of the tibiae has a distinct swelling adjacent to the medial condyle in DMNH EPV.63875 (sw in Fig. 6A, C-D) that is apparently absent in the smaller specimens. The fibular crest extends parallel to the long axis of all tibiae and terminates distally before reaching the midpoint of the element (Fig. 6E, 7A, F, K). A

distinct ridge is also present on the lateral side of the cnemial crest DMNH EPV.63875 and DMNH EPV.67955 (where cc is labeled in Figs. 6E, 7K).

The shafts of the tibiae are mediolaterally somewhat constricted and oval in cross section for about the proximal third, and then become subcircular in cross section by the midpoint of the shaft. Roughly the distal third of the posterolateral edge of the shaft of DMNH EPV.63875 is slightly constricted above the posterolateral flange at the distal end (Fig. 6D).

In DMNH EPV.63875, the distal end of the tibia bears a distinct slightly distally projecting and blade-like posterolateral process (plp in Fig. 6D-F) as in other dinosauriforms. This seems to be more similar to the pronounced crest-like posterolateral process of *Sacisaurus* (*Langer & Ferigolo, 2013, figure 18*) than to the smaller process of *Silesaurus* (*Dzik, 2003, figure 13*). There is a broad depression for the ascending process of the astragalus (as.ar in Fig. 6E-F), bounded anteriorly by a distinct thickening that is slightly wider than the posterolateral process, a character shared by silesaurids and saurischian dinosaurs (*Novas, 1996; Langer & Benton, 2006; Nesbitt, 2011*). Anterior to the depression for the ascending process, the anterior part of the distal end projects slightly anterior to the tibia shaft as a slightly pinched eminence (Fig. 6E-F).

These tibiae compare well overall to the element in *Silesaurus* (*Dzik, 2003: figure 13*) and *Sacisaurus* (*Langer & Ferigolo, 2013: figure 18*), and lack character states present in neotheropods such as dorsal expansion of the cnemial crest, posterolateral concavity at the distal end, and a proximodistally oriented ridge on the posterior side of the distal end (distinct from the posterolateral flange) (*Nesbitt, 2011*). The elements cannot currently be completely ruled out as non-neotheropod theropods, as the presence of these characters is variable in basal theropods such as *Tawa* and herrerasaurids (*Nesbitt et al., 2009b: p. 1532; Nesbitt, 2011*), and the tibiae of

364 *Eodromaeus murphi* and *Daemonosaurus chauliodus* are unknown (*Martinez et al., 2011*).
365 However, for reasons discussed above the elements are not referable to *Tawa* or *Chindesaurus*.
366
367 **Silesauridae** *Nesbitt et al., 2010*
368 **Definition (stem-based)**: The most inclusive clade for Silesauridae contains *Silesaurus*
369 *opolensis* Dzik, 2003 but not *Passer domesticus* Linnaeus, 1758, *Triceratops horridus* Marsh,
370 1889 and *Alligator mississippiensis* Daudin, 1802.
371 **Diagnosis.** See Appendix 3.
372
373 **Sulcimentisauria clade nov.**
374 **Definition (stem-based)**. The most inclusive clade that includes *Silesaurus opolensis Dzik 2003*
375 but not *Asilisaurus kongwe Nesbitt et al. 2010*.
376 **Diagnosis**. See Appendix 3.
377 **Etymology**. Latin *sulcus*- "grooved" + Latin *mentum* "chin" + Greek *sauros* "lizard." In
378 reference to the ventrally placed Meckelian groove on the dentary.
379
380 ***Kwanasaurus* gen. nov.**
381 **LSID.** urn:lsid:zoobank.org:act:E9514954-F9FD-4D79-A620-D705122D59D5
382 **Type species.** *Kwanasaurus williamparkeri.*
383 **Etymology**. Ute *kwana*- "eagle" + Greek *sauros* "lizard." The generic name honors the town and
384 county of Eagle in Colorado, located near the fossil localities that produced the type and referred
385 specimens, as well as the Ute people. The town and county of Eagle are named for the Eagle

River (Río Águila in Spanish), said to be translated from a local Ute name for the river or from the name of a Ute chief.

**Autapomorphic diagnosis**. *Kwanasaurus* is distinguished from other silesaurid taxa by the following autapomorphies: Main body and posterior process of maxilla extremely short and robust; ascending process of the maxilla extends at least half the anteroposterior length of the element, prominent posterolateral flange and complex jugal and lacrimal articulations on posterior end of posterior process of the maxilla, massive subtriangular, ventromedially oriented flange on medial surface of the maxilla; twelve maxillary teeth and fourteen dentary teeth; ilium with elongate and blade-like preacetabular process that extends beyond the pubic peduncle; concave ventral acetabular margin of ilium; medial condyle at distal end of femur very thin compared to lateral condyle and crista tibiofibularis; depression on distal end of the femur anterior to the crista tibiofibularis.

**Differential diagnosis**. *Kwanasaurus* shares the following combination of character states with various silesaurid taxa: Anterior edge of ascending process of maxilla rises steeply (as in *Sacisaurus*, edge slopes more gently in *Lewisuchus*); tooth positions extend nearly to the posterior end of the maxilla (as in *Lewisuchus*, the posteriormost end of the maxilla is edentulous in *Silesaurus* and *Sacisaurus*); dentary with lateral ridge (shared with *Diodorus* and *Eucoelophysis;* absent in *Silesaurus, Sacisaurus,* and *Technosaurus*); Meckelian groove located near ventral margin of dentary (shared with *Silesaurus*, *Sacisaurus*, *Diodorus*, *Technosaurus*, and *Eucoelophysis*; differs from *Asilisaurus* in which the grove is near the midline of the dentary); Meckelian groove extends through dentary symphysis (shared with *Silesaurus* and *Sacisaurus*, groove does not extend through symphysis in *Diodorus*); dentary teeth “leaf-shaped”, broad-based, coarsely denticulate, and not distally striated (as in *Diodorus*,

409 *Technosaurus*, and *Eucoelophysis*, differs from the more conical, finely denticulate, and
410 sometimes distally striated teeth of *Asilisaurus*, *Silesaurus* and *Sacisaurus,* as well as the
411 recurved and serrated teeth of *Lewisuchus*); most dentary teeth not anteriorly canted (shared with
412 *Silesaurus*, *Sacisaurus*, *Technosaurus*, and *Eucoelophysis*; differs from *Diodorus*, in which all
413 dentary teeth are anteriorly canted); humerus with distinct torsion between proximal and distal
414 ends (as in *Silesaurus*, differs from *Diodorus* in which the proximal and distal ends are more
415 parallel); iliac blade horizontal and 'saddle-shaped' (as in *Silesaurus* and *Eucoelophysis*; iliac
416 blade more vertically oriented in *Lutungutali* and *Ignotosaurus*); anterior trochanter of femur in
417 at least some individuals subtriangular and not notched (shared with smaller individuals of
418 *Silesaurus*; trochanter is notched in *Diodorus, Sacisaurus*, and larger individuals of *Silesaurus*);
419 trochanteric shelf absent (as in *Diodorus, Sacisaurus*, *Eucoelophysis*, and some individuals of
420 *Silesaurus*; shelf present in larger individuals of *Silesaurus*); fourth trochanter present (shared
421 with *Silesaurus*, *Diodorus* and *Sacisaurus*, trochanter absent in *Eucoelophysis*).
422
423 ***Kwanasaurus williamparkeri* sp. nov.**
424 **LSID.** urn:lsid:zoobank.org:act:25A4AE71-56B3-4797-B30D-1FA1D37E1F3F
425 **Etymology**. Honors friend and colleague Bill Parker, whose research has helped to greatly
426 clarify our understanding of Late Triassic dinosauromorph diversity in the western United States.
427 **Holotype**. DMNH EPV.65879 (Fig. 8A-H), a partial left maxilla.
428 **Type horizon and locality**. Locality DMNH 4340 (Burrow Cliff), "red siltstone member" of the
429 Chinle Formation (Upper Triassic, Norian and/or Rhaetian), northern Colorado, USA.
430 **Referred specimens**. (See Table 1 for localities) DMNH EPV.63650 (Fig. 8I-P), partial right
431 maxilla; DMNH EPV.125921 (Fig. 9A-H), partial left maxilla; DMNH EPV.125923 (Fig. 9I-P),

partial right maxilla; DMNH EPV.63136 (Fig. 11), almost complete left dentary; DMNH EPV.63135 (Fig. 12A-D), partial right dentary; DMNH EPV.63660 (Fig. 12J-L), anterior left dentary; DMNH EPV.65878 (Fig. 12G-I), partial right dentary; DMNH EPV.57599 (Fig. 12E-F), partial ?right dentary; DMNH EPV.43577 (Fig. 14A), isolated tooth; DMNH EPV.63142 (Fig.14B), isolated tooth; DMNH EPV.63143 (Fig. 14C), isolated tooth; DMNH EPV.63661 (Fig. 14E), isolated tooth; DMNH EPV. 63843 (Fig. 13D); DMNH EPV.125922 (Fig. 13F), isolated tooth; DMNH EPV.59302 (Fig. 15), nearly complete left humerus; DMNH EPV.48506 (Fig.16), complete left ilium; DMNH EPV.63653 (Fig. 17A-C), partial left ilium; DMNH EPV.52195 (Fig.17D-G), partial left ilium; DMNH EPV.34579 (Fig. 18), nearly complete left femur; DMNH EPV.54828 (Fig. 19A-E), proximal right femur; DMNH EPV.59311 (Fig. 21F-J), badly worn proximal right femur; DMNH EPV.44616 (Fig.19F-J), proximal right femur; DMNH EPV.56651 (Fig. 19K-O), proximal left femur; DMNH EPV.59301 (Fig. 21K-O), proximal left femur; DMNH EPV.63139 (Fig. 21A-E), proximal left femur; DMNH EPV.63874 (Fig. 20F-J), proximal left femur; DMNH EPV.67956 (Fig. 22), distal left femur; DMNH EPV.125924 (Fig. 20A-E), proximal right femur.

**Diagnosis**. As for genus, by monotypy.

**Description and discussion**.

Silesaurids (non-dinosaurian dinosauriforms) are the most abundant dinosauromorph elements in the Eagle Basin, although assigning any elements to a particular alpha taxon is problematic for several reasons:

1) Nearly all Eagle Basin specimens are isolated elements, reducing the number of potential autapomorphies that can be identified for any individual.

2) Few alpha taxon autapomorphies have been identified for members of Silesauridae (*Peecook et al., 2013; Langer and Ferigolo, 2013; Breeden et al., 2017*) with the exception of *Lewisuchus* (*Bittencourt et al., 2014*) and *Asilisaurus* (*Nesbitt et al., 2010*), the oldest and most basal undisputed silesaurid taxon.
3) Character state polarities within Silesauridae are currently largely unresolved so that the topology of Sulcimentisauria, the clade of all silesauirds more derived than *Asilisaurus*, is highly variable between analyses, and often a polytomy (*Nesbitt et al., 2010; Kammerer et al., 2012; Peecook et al., 2013; Sarigül, Agnolin & Chatterjee, 2018*). Moreover, character state polarities are, at least in some cases, subject to both ontogeny and intraspecific variation (*Piechowski, Tałanda & Dzik, 2014; Griffin and Nesbitt, 2016a, b*).

However, within the Eagle Basin collection, homologous elements with silesaurid apomorphies tend to share character states distinguishing these specimens from previously described silesaurid taxa. This is taken as circumstantial evidence that the Eagle Basin silesaurid material belongs to a single alpha taxon. Similar apomorphy-based logic has been applied to other silesaurid taxa where the holotype consists of a single element, and an overall picture of skeletal anatomy is cobbled together from isolated elements (*e.g. Nesbitt et al., 2010; Kammerer, Nesbitt & Shubin, 2012; Langer & Ferigolo, 2013, p. 355*). While far from ideal, this approach allows an at least a provisional combination of phylogenetically informative character states to be assembled that is subject to potential falsification with the discovery of associated material, subject to revision if more complete specimens are ever recovered.

**Maxilla**

Four incomplete silesaurid maxillae are known from the Eagle Basin Chinle Formation. The holotype is DMNH EPV.65879 (Fig. 8A-H), a left element from one of the largest individuals known from the collection with a preserved anteroposterior length of 56 mm. The other three specimens are much smaller with a preserved length of 30-35 mm long: right elements DMNH EPV.63650 (Figure 8I-P) and DMNH EPV.125921 (Fig. 9A-H), and left element DMNH EPV.125923 (Fig. 9I-P). All specimens can be assigned to Silesauridae due to the teeth being ankylosed into the sockets (*Nesbitt et al., 2010; Langer et al., 2013*), and they can all be assigned to *Kwanasaurus* based on the distinctive medial flange and their robust form compared to other silesaurids (see below). The external surface of the maxilla has been previously described in *Lewisuchus* (*Bittencourt et al., 2014*), *Silesaurus* (*Dzik, 2003*) and *Sacisaurus* (*Langer & Ferigolo, 2013*) (Fig. 10C-G), but the internal morphology of a silesaurid maxilla has only been figured by *Dzik (2003: Fig.5B)*, and is here described in detail for the first time (Figs. 8C-D, K-L, 9C-D, K-L; 10B, D, F). All elements preserve most of the tooth-bearing body of the maxilla. DMNH EPV.65879 and DMNH EPV.125921 lack the anteriormost tip of the element (Figs. 8A-H; 9A-F) and DMNH EPV.63650 and DMNH EPV.125923 lack the posterior tip (Figs. 8I-P; 9I-P). DMNH EPV.63650 preserves the base of the ascending process (Fig. 8A-F), which is completely missing in the other specimens; however, in DMNH EPV.125921 the process, although apparently lost, was reconstructed by pushing putty into the impression of the medial surface (Fig. 9A-F).

The main body and posterior process of the maxilla is a far dorsoventrally deeper, anteroventrally shorter, and more robust element than occurs in other silesaurid taxa (Figs. 8-10). In lateral view, the main tooth-bearing body of the maxilla is slightly dorsally emarginated by the antorbital fossa (see below) between about the fourth and sixth tooth positions (Figs. 8-9).

DMNH EPV.125921 is somewhat more gracile in appearance compared to the Eagle Basin specimens (Fig. 9A-F), but still more robust than other silesaurids (Fig. 10). In all specimens, there is a row of small subcircular to ovate foramina on the lateral surface of the maxilla immediately above the tooth row that extends the length of the tooth-bearing segment. The foramina do not have a one to one relationship with the alveoli (Figure 8A-B, I-J; 9A-B, I-J). In DMNH EPV.65879 and DMNH EPV.125923, additional scattered subcircular and elongate foramina of similar size occur above this lower row (Figs. 8A-B, 9I-J); this is not clearly evident in the other specimens.

In all specimens, the medial (lingual) surface of the main tooth-bearing body of the maxilla bears a row of larger foramina (rf in Figs. 8-9) that extend the length of the element just above the tooth sockets, and have a clear one to one relationship with the alveoli. These foramina are similar to those seen in some thyreophoran dinosaurs (*e.g. Edmund 1960; Colbert 1981*). All foramina are well-developed and smooth-walled, and might have been openings for nerve and vasculature to the alveolus instead of resorption pits, which are generally formed by the disappearance or remodeling of the tooth root and bone during the tooth replacement process. Consequently we use the term replacement foramina *sensu Edmund (1960)* for these openings instead of resorption pits. These foramina are particularly compressed and elongate above the first four to five tooth positions, and become more broadly ovate to circular more posteriorly. In DMNH EPV.65879, the first five elongate replacement foramina lie within a clearly defined groove (in Fig. 8C-D; largely concealed by medial flange), which shallows and ends at the sixth replacement foramen; this groove is absent in the smaller specimens, where the foramina are also relatively large. Foramina set within a groove occur in the same position in *Silesaurus* (Fig. 10F;

522 *Dzik, 2003, fig. 5A*), although the foramina do not seem to be much smaller than in any of the
523 *Kwanasaurus* specimens. Other numerous tiny foramina are scattered across the medial surface.
524 The anteriormost part of the lateral surface of the maxilla is slightly inset and angled
525 medially relative to the main body of the element above the first tooth position. This probably
526 represents the area overlapped laterally by the premaxilla (pm.ar in Figs. 8-9). The same
527 condition seems to be present in *Silesaurus* (*Dzik, 2003, fig. 5B*), and an anteriorly facing
528 concavity also occurs here in *Sacisaurus* (*Langer & Ferigolo, 2013*) (Fig. 10E, G). In
529 *Lewisuchus*, the "shallow notch" at the base of the ascending process of the maxilla (*Bittencourt*
530 *et al., 2014, p. 191*) may be homologous (labeled "pm.ar?" in Fig. 10C). This inset region
531 terminates anteriorly with a short pointed prong, the anteromedial process (amp in Figs. 8-10;
532 *Prieto-Marquez & Norell, 2011*), originating immediately anterior to the first tooth position,
533 which also occurs in *Silesaurus* (Fig. 10E*; Dzik, 2003, figure 5A*), *Lewisuchus* (Fig. 10C;
534 *Bittencourt et al., 2014* described this as the "maxillary cranial process"); and other archosaurs.
535 This region is either not well-preserved in *Sacisaurus*, or the process is extremely short in that
536 taxon (Fig. 10G; *Langer & Ferigolo, 2013, fig. 2*). The anteromedial process is best-preserved in
537 DMNH EPV.65879 and especially DMNH EPV.125923, and has a distinctly hooked shape in
538 dorsal view (Figs. 8E-F, 9O-P).
539 The medial surface of the anteriomedial process bears a sharp longitudinal crest (vo.ar in
540 Fig. 8-9), probably representing the vomerine flange (*e.g. Prieto-Marquez & Norell, 2011*). In
541 the three smaller specimens, the vomerine flange is very sharp, but in DMNH EPV.65879 it is
542 thicker with longitudinal striations along its ventral surface. In DMNH EPV.65879 and DMNH
543 EPV.125923 the process projects medially just anterior to the first tooth position (Fig. 8G-H, 9O-
544 P). The vomerine flange is also thicker in *Silesaurus* (Fig. 10F), but it is also present in

*Lewisuchus* (Fig. 10D) and *Sacisaurus* specimen MCN PV10091 (*Langer & Ferigolo, 2013, p. 355*, described a "short/plate-like palatal ramus" but did not figure it).

Only the very base of the ascending process of the maxilla remains in DMNH EPV.65879 (Fig. 8A-D) and DMNH EPV.125923 (Fig. 9P-N), but the ascending process is slightly more complete in DMNH EPV.63650 (Fig. 8I-L), although badly damaged, and at least the medial surface is reconstructed using putty pushed into the impression left by missing bone in DMNH EPV.125921 (Fig. 9C-F). The ascending process is extremely thin in DMNH EPV.63650, and this seems to have been the case in the other specimens as well judging by the width of the broken edge (brk in Figs. 8F, 9N). In all specimens, the ascending process originated at least as far anteriorly as the first tooth position, rising steeply posterodorsally from the anteromedial process or just posterior to it; the anterior edge of the ascending process also seems to rise steeply as in *Sacisaurus* (Fig. 10G; *Langer & Ferigolo, 2013*) and possibly *Silesaurus* (Fig. 10E-F; *Dzik, 2003, figure 6*) in contrast to the more gently posterodorsally sloping ascending process of *Lewisuchus* (Fig. 10C-D; *Bittencourt et al., 2014, figure 1*). The ascending process in DMNH EPV.63650 is somewhat dorsomedially inclined (Fig. 8M-N) though this is not evident in DMNH EPV.125921 (Fig. 9E-F). The posteroventral edge of the ascending process in DMNH EPV.63650 and DMNH EPV.125923 is intact, and slopes to join the dorsal edge of the main body of the maxilla above about the sixth tooth position (Figs. 8I-L; 9I-L). The ascending process seems to be much anteroposteriorly shorter in other silesaurids (Fig. 10).

Most specimens except for DMNH EPV.63650 preserve only a tiny remnant of the anterior edge of the antorbital fossa. However, DMNH EPV.63650 preserves what seems to be a nearly complete antorbital fossa (=the "recessed medial lamina of the dorsal process" *sensu*

568 *Prieto-Marquez & Norell, 2011*) that embays the posterior half or so of the lateral surface of the
569 ascending process (Fig. 8I-J). The fossa is subtriangular with slightly convex anterior and ventral
570 margins. The ventral margin extends between about the fourth and seventh tooth positions (also
571 seen in DMNH EPV.125923; Fig. 9I-J), while the anterior margin probably did not contact the
572 nasal. In DMNH EPV.65650 a distinct swollen area occurs at the ventral margin of the fossa
573 above the fourth tooth position. An irregular hole with clearly broken edges has removed most of
574 the surface of the fossa in this specimen, so it is unclear if there was a promaxillary fenestra as in
575 *Sacisaurus* (*Langer & Ferigolo, 2013*). The medial side of the posterior edge of the ascending
576 process is slightly thickened by a faint ridge in DMNH EPV.65650; in both that specimen and
577 the reconstructed DMNH EPV.125921 (Figs. 8K-L, 9C-D), the anterior part of the medial
578 surface bears a distinct concavity.
579 The most striking feature of the medial (lingual) side of the maxilla is an enormous
580 medial flange that is fully preserved in both DMNH EPV.65879 DMNH EPV.63650 (mef in Fig.
581 8C-D, K-L) and partially preserved in the other specimens (Fig. 9C-D, K-L). In all specimens,
582 the flange originates as a thick ridge that crests posterodorsally from the vomerine flange (Figs.
583 8C-D, K-L, 9C-D, K-L), and in the more complete specimens descends posteroventally to
584 become a sharper-edged, subtriangular flange that reaches its greatest breadth below the fifth and
585 sixth tooth positions. Posterior to this, the edge of the flange ascends posterodorsally to become a
586 smaller and even sharper-edged crest representing the palatine flange (see below). The medial
587 flange is clearly absent in *Silesaurus* (Fig. 10F; *Dzik, 2003, figure 5a*) and *Lewisuchus* (Fig. 10D;
588 *Bittencourt et al., 2014*), and the condition is unknown from other silesaurids, including
589 *Sacisaurus* for which the medial surface of the only known complete maxilla (MCN PV10050) is
590 concealed (*Langer & Ferigolo, 2013*). To our knowledge, nothing similar has been described in

any other Triassic dinosauromorphs, where the vomer and palatine articulations are usually fully separated rather than being joined by any kind of crest (*e.g. Dzik, 2003; Prieto-Marquez & Norell, 2011*). It is tempting to speculate that the medial flange in the Eagle Basin specimens is actually a separate element, perhaps the palatine fused to the maxilla, but it lacks any obvious medial articular surface for the pterygoid, and no trace of a continuous suture can be clearly discerned separating the flange from the maxilla in either specimen, even in the smaller (and likely less mature) specimens. Moreover, the probable sutural surface for the palatine can be discerned on its surface in the holotype (see below).

In DMNH.EPV 65879 there is a complex series of crests, grooves, ridges, and rugosities on the dorsal and medial surfaces of the posterior ramus of the maxilla probably representing the contacts for the jugal, lacrimal, and palatine (ju.la.ar in Fig. 8C-F). This region is far more complex in DMNH EPV.65879 than in *Lewisuchus*, *Silesaurus* (Fig. 10D, F), or the smaller *Kwanasaurus* specimens (Fig. 8K-N, 9C-F; concealed by matrix in DMNH EPV.125923; Fig. 9K-N). However, the morphology of this area is remarkably similar to the *Plateosaurus* specimen described by *Prieto-Marquez & Norell (2011, figures 4-5)*, and our interpretation is modeled after theirs. A prominent flange rises from the lateral side of the dorsal surface of the posterior ramus, convex on the lateral surface and concave on the medial surface; we refer to it as the posterolateral flange (plf in Fig. 8B, D; 10A-B). It is tempting to suggest that this crest represents part of the jugal or lacrimal, but it seems to clearly be part of the maxilla with no trace of a suture. In lateral view, this flange would have partly concealed the anterior end of the articulated jugal in lateral view. No similar flange occurs in the smaller Eagle Basin specimens (Figs. 8I-P, 9), so it is possible that this is a feature that develops with maturity.

In DMNH EPV.65879, two deep, longitudinal, dorsomedially-facing grooves separated by a ridge occur on the dorsal surface of the posterior end of the maxilla, above the posterior termination of the medial flange. These medial and lateral grooves probably represent the jugal and lacrimal articulations respectively (ju.la.ar in Fig. 8C-F). Both originate above the 9th tooth position, but the lateral groove extends to the posterior end of the maxilla, while the medial groove only extends as far as the 11th tooth position. Ventral to the medial (lacrimal?) groove, the medial surface of the posterior process is covered with pits and striations that may also be part of the lacrimal articulation. The posterior end of maxilla bears small tuberosities (Fig. 8A-B) suggesting a tight sutural contact with the jugal.

In DMNH EPV.65879 there is a distinct triangular embayment occurring slightly more anteriorly along the edge of the medial flange but just posterior to the apex of the flange (pa.ar in Figure 8C-D). This region probably represents the articulation with the palatine, in which case the palatine had a very broad contact with posterior edge of the medial flange of the maxilla. This sutural surface is not evident in any of the smaller specimens, although in DMNH EPV.123923 the region is not fully prepared.

In DMNH EPV.65879, the main tooth-bearing body of the maxilla seems to have a completely preserved tooth row with 12 tooth positions, with fully emergent teeth in the 1st, 2nd, and 4th alveoli (Figure 8A-D, G-H). This is similar to the maxillary tooth counts in *Silesaurus* (11; *Dzik, 2003*) and *Sacisaurus* (10; *Ferigolo & Langer, 2007*) but considerably less than in *Lewisuchus* (20; *Bittencourt et al., 2014*). The main body of the maxilla is missing past the ninth tooth position in DMNH EPV.63650 and not well-preserved in the other two specimens, but all seem to have had minimally nine teeth and probably more. The posteriormost alveoli in the maxilla are indicated by an arrow in Fig. 10; the alveoli extend almost to the posterior end of the

posterior ramus of the maxilla, which seems to be nearly complete DMNH EPV.65879; this is also the case in *Lewisuchus* (Fig. 10C-D; *Bittencourt et al., 2014*, *fig. 1*), but not in *Silesaurus* or *Sacisaurus*, where the posteriormost part of the maxilla seems to be edentulous (Fig. 10E-G; *Dzik, 2003*, *fig. 6*; *Langer & Ferigolo, 2013*).

In DMNH EPV.63650 and DMNH EPV.125923 there is a deep depression above the anteriormost teeth that contains a series of smaller subcircular depressions (rp in Fig. 9M-N; not visible in Fig. 8M-N due to the ascending process being preserved). In DMNH EPV.65879 this same region is contains a thickened area with circular areas of spongy bone occurring over the 2nd and 3rd tooth positions, and a poorly preserved pit seems to occur above the 1st tooth position (Fig. 8C-F). These depressed areas seem to be associated with the dorsal ends of the tooth roots; indeed, in DMNH EPV.125923 the root of the emerging third tooth crown projects from the dorsal surface of the medial flange (rt in Fig. 9I-N). The pattern of tooth replacement will be discussed in more detail below. In all specimens, the ventral side of the medial flange also defines an elongate depression with a series of deeper subcircular depressions occurring beneath the broadest part of the flange (best seen in Fig. 8G-H below where "mef" is labeled), which do not have a one to one relationship with the tooth positions.

The dorsal surface of the main body of the maxilla in DMNH EPV.65879 is covered with deep pits and grooves of uncertain nature (the dark patches near the region marked "brk" in Fig. 8F). Just anterior to the two grooves representing the jugal and lacrimal articulation is another deep groove, the posterior part of which seems to be surrounded by finished bone, but the anterior part and pits appear to be broken bone, and occur where the antorbital fossa of the ascending process occurs in DMNH EPV.63650 and DMNH EPV.125923. It is therefore suggested that these represent an originally closed canal and/or cavities that were covered by the

ascending process or exited its base as a foramen. A similarly positioned foramen seems to occur on the dorsal surface of the maxilla in *Silesaurus* (Fig. 10F; *Dzik, 2003, figure 5*), but cannot be clearly discerned in other Eagle Basin specimens.

**Dentary and angular**

Two nearly complete silesaurid dentaries are known from the Eagle Basin; DMNH EPV.63136 (a left; Fig. 11) and DMNH EPV.63135 (a right; Fig. 12A-D). DMNH EPV.63136 is the most complete silesaurid dentary described, as it seems to completely preserve both the anteriormost and posteriormost ends of the element, unlike all other described dentaries (Fig. 13; *Irmis et al., 2007; Nesbitt, Irmis & Parker, 2007; Nesbitt et al., 2010; Kammerer, Nesbitt & Shubin, 2012; Langer & Ferigolo, 2013*). DMNH EPV.63136 has a preserved anteroposterior length of 36 mm, and a maximum preserved dorsoventral height (not counting the tooth crowns) of 11 mm. DMNH EPV.63135 is missing an uncertain amount of the anterior and posterior ends, but based on comparison with the more complete specimen, the most anteriorly preserved tooth crown is probably the third tooth position; the specimen has a preserved anteroposterior length is 34 mm, and a maximum preserved dorsoventral height of 8 mm. Two other dentaries, DMNH EPV.57599 (a possible right; Fig. 12E-F), and DMNH EPV.65878 (a possible left; Fig. 12G-I), are missing an uncertain amount of the anterior and posterior ends, while DMNH EPV.63660 is a left anterior end (Fig. 12J-L). All of these specimens seem to represent individuals of comparable size or smaller than the more complete dentaries.

As with the maxillae, all specimens can be assigned to Silesauridae due to the teeth being ankylosed into the sockets (*Nesbitt et al., 2010; Langer et al., 2013*). These dentaries can also be assigned to Sulcimentisauria, the clade containing all known silesaurids exclusive of *Asilisaurus*

based on the following apomorphies: Meckelian groove lies near the ventral margin of the dentary (Mk in Figs. 11-12), and dentary teeth have constrictions below the crown (Appendix 1; *Nesbitt et al., 2010)*. Moreover, in DMNH EPV.63135 and DMNH EPV.63136 the dorsal edge of the dentary is clearly concave rather than convex, and the dentary teeth crowns are short and sub-triangular (Figs. 11, 12A-D) rather than peg-like, which also distinguishes these taxa from *Asilisaurus* (*Nesbitt et al., 2010*) and *Soumyasaurus* (*Sarigül, Agnolin & Chatterjee, 2018*). In DMNH EPV.63136 and DMNH EPV.63660, the only specimens to preserve the very tip of the dentary, the anterior tip is a sharp, edentulous point (Figs.11-12J-L), another silesaurid feature (*Nesbitt et al., 2010*).

The dentary of *Kwanasaurus* seems to be distinctly deeper than the relatively slender dentaries of *Eucoelophysis* (Fig. 13E-F), *Sacisaurus* (Fig. 13I-J), and *Soumyasaurus* (*Sarigül, Agnolin & Chatterjee, 2018: figure 5*). The ventral margins of DMNH EPV.63135, DMNH EPV.63136, and DMNH EPV.63660 are slightly convex (Fig. 11A-D, 12A-D, J-L); the other specimens are too incomplete to be certain if they share this feature. Viewed dorsally or ventrally, the two most complete dentaries also curve slightly anterolaterally, suggesting that this shape is natural; DMNH EPV.63136 is constricted at the edentulous tip and symphysis, with the rest of the mandible flaring posterolaterally (Fig. 11E-H).

The lateral surface of all the dentaries except DMNH EPV.63660 (which only possesses the anterior tip) bears a distinct lateral ridge roughly midway between the dorsal and ventral margins (lr in Figs. 11-12). In DMNH EPV.63136 the ridge originates approximately under the fourth alveolus, and terminates posteriorly at the anterior end of the mandibular fenestra, roughly below the 9$^{th}$ and 10$^{th}$ tooth positions (Fig. 12A-B). In DMNH EPV.63135 the ridge originates beneath the second preserved alveolus and is most prominent under the eighth tooth position

(Fig. 12A-B). In DMNH EPV.65878, the ridge is most prominent beneath the first three-preserved tooth positions, and then flattens out (Fig. 12G). Among other silesaurids, a distinct lateral ridge is reported only for *Diodorus* (Fig. 13M; *Kammerer, Nesbitt & Shubin, 2012)*, but also occurs in *Eucoelophysis* material from the Hayden Quarry (Fig. 13E; *J.W. Martz, pers. obs.* of GR 224).

A posteriorly facing foramen on the upper surface of the ridge occurs below the 9$^{th}$ tooth position in both DMNH EPV.63136, and DMNH EPV.63135 (fo in Figs. 11A-B, 12A-B). A similar posteriorly opening foramen is also known in aetosaurs (*Small, 2002*), and seems to also be present in *Diodorus* (Fig. 13M; *Kammerer, Nesbitt & Shubin, 2012, fig. 1A*). In DMNH EPV.57599 and DMNH EPV.63135, a canal conducted within the ridge was observed at the edges of the break in the element (in the latter specimen, it is no longer visible as the two halves of the dentary are glued together); the canal may connect to the posterior facing foramen. This canal also occurs within the ridge in *Eucoelophysis* (*J.W. Martz pers. obs.* of GR 224). Smaller nutrient foramina exit from the dorsal surface of the ridge in both of the more complete dentaries (Fig. 11A-B, 12A-B) as in *Diodorus* (Fig. 13M; *Kammerer, Nesbitt & Shubin, 2012)* and *Eucoelophysis* (Fig. 13E; *J.W. Martz, pers. obs.* of GR 224); in DMNH EPV.63136 and DMNH EPV.63135 even smaller foramina exit from the ventral side of the ridge and the underside of the edentulous tip.

In DMNH EPV.63136 and DMNH EP.63660, the anterior edentulous tip of the dentary bears a distinct groove on the lateral surface that extends from the tip of the element to enter the element beneath the second tooth position (gr in Figs. 11A-B, 12J). A similar groove occurs in *Silesaurus* and *Sacisaurus* (Fig. 13I, K) that *Dzik (2003)* describes it as a “vascular canal”, and that *Langer & Ferigolo (2013*) indicate originates in a “mental foramen” at the posterior end of

728 the groove, although this is difficult to evaluate in the *Kwanasaurus* specimens because matrix
729 has not been fully removed from the groove. In *Sacisaurus*, the groove differs from *Silesaurus*
730 and *Kwanasaurus* in that it rises to the dorsal margin (Fig. 13I; *Langer and Ferigolo, 2013*)
731 rather than extending longitudinally to the tip (Figs. 13A, K).

732 Fourteen tooth positions are present in the dentary DMNH EPV.63136 (Fig. 11), seven of
733 which contain fully erupted teeth (in positions 1, 3, 4, 6, 9, 11, and 12). This seems to represent
734 the entire tooth row, and falls within the general range of tooth counts seen in *Silesaurus* (12;
735 *Dzik, 2003*), *Sacisaurus* (15; *Ferigolo and Langer, 2013*), and *Soumyasaurus* (at least 15*;*
736 *Sarigül, Agnolin & Chatterjee, 2018*). At least 11 tooth positions are present in the less complete
737 DMNH EPV. 63135 (Fig. 12A-D), for which the tooth position numbering is inferred by
738 comparison with DMNH EPV.63136.

739 Replacement foramina identical to the replacement foramina of the maxillae occur
740 beneath each alveolus (rf in Fig. 11D, 12D, F, H). The medial surface the dentaries are slightly
741 inset just below the teeth as far back as the 8$^{th}$ alveolus, with a faint groove along the base of the
742 inset (where "rf" is labeled in Figs. 11-12); this is also seen in *Silesaurus* (Fig. 13L*; Dzik, 2003,*
743 *fig. 5E*), *Eucoelophysis* (Fig. 12F; *J.W. Martz, pers. obs.* of GR 224), and *Technosaurus* (Fig.
744 12H; *Martz et al., 2013, fig. 14G*). Anteriorly, the replacement foramina occur within the groove.
745 The inset and groove shallow to merge with the rest of the medial surface posteriorly beneath
746 about the ninth alveolus in DMNH EPV.63136 and DMNH EPV.63135. In DMNH EPV.63135
747 and DMNH EPV.63878, the foramina beneath emergent crowns are elongate ovals, while pits
748 under empty alveoli and crowns that are not fully emerged are larger and more circular (Fig.
749 12C-D, I). This difference in shape between foramina under fully erupted and unerupted crowns
750 is not evident in DMNH EPV.63136, where the replacement foramina generally become larger

posteriorly rather than beneath empty alveoli (Fig. 11C-D); this was the pattern also seen in DMNH EPV.65879 the holotype maxilla of *Kwanasaurus* (Fig. 8C-D).

In all specimens of *Kwanasaurus*, the dorsal margin of the dentary is strongly depressed above empty alveoli, and raised where it is fused to emergent crowns as a striated region below the crown (Fig. 11A-D; 12A-D). The depression of the alveolar margin is evident in other silesaurids, especially *Diodorus* (Fig. 13M-N; *Kammerer, Nesbitt & Shubin, 2012, fig. 1*), but more difficult to evaluate in *Silesaurus* (Fig. 13K-L; Dzik, 2003*, fig. 5*), *Technosaurus* (Fig. 13G-H; *Martz et al., 2013, fig. 14*), and *Eucoelophysis* (GR 224, Fig. 13E-F), where the teeth are more tightly packed and/or regions without teeth are damaged.

On the medial surface of all dentaries of *Kwanasaurus*, the Meckelian groove extends along the ventral edge (Fig. 11C-D, 12C-D, F, H, K), as in *Silesaurus, Sacisaurus, Diodorus. Eucoelophysis,* and *Technosaurus* (Fig 13E-N; e.g. *Dzik 2003, fig. 5E; Ferigolo & Langer, 2007, fig. 7I; Irmis et al., 2007, fig. 2L*; *Kammerer, Nesbitt & Shubin, 2012; Martz et al., 2013*, fig. 14G). This is not the case in *Asilisaurus*, where the groove is midway between the dorsal and ventral margins (Fig. 13C-D; *Nesbitt et al., 2010*).

The Meckelian groove extends to the anterior tip of the dentary in DMNH EPV.63136 and DMNH EPV.63660 (Fig. 11C-D; 12J-L) as in *Sacisaurus* and *Silesaurus* (Fig. 13J-L; *Dzik, 2003; Ferigolo & Langer, 2007)*, but unlike the condition in *Diodorus* where the groove terminates well short of the anterior end (Fig. 13N; *Kammerer, Nesbitt & Shubin, 2012*). In the most complete dentaries, the Meckelian groove is dorsoventrally widest posteriorly near the mandibular fenestra (Figs. 11C-D; 12C-D) and narrows anteriorly. In DMNH EPV.63136, the groove has a maximum height of 6 mm high, or about 55% of the height of the dentary exclusive of the teeth and the groove narrows to almost nothing beneath the third tooth position. However,

774 in DMNH EPV.63136 and DMNH EPV.63660, (Fig. 11C-D, 12K) the Meckelian groove
775 reappears between the third and first tooth positions, and again from an anteriorly opening
776 foramen beneath the first tooth position to extend to the edentulous tip. This foramen and groove
777 also occur in *Silesaurus* and *Sacisaurus* according to *Dzik (2003)* and *Ferigolo & Langer (2007)*
778 although it is difficult to make out in their figures, and is therefore not drawn in Fig. 13. In
779 DMNH EPV.63136, there is another thin groove on the edentulous tip above the Meckelian
780 groove (Fig. 11C-D).

781 Unlike any other known silesaurid dentary, in which the posteriormost part of the dentary
782 is usually damaged or missing (Fig. 13C-N; *Dzik, 2003; Ferigolo and Langer 2007; Nesbitt et*
783 *al., 2010; Kammerer, Nesbitt & Shubin, 2012; Martz et al., 2013*), DMNH EPV.63136 preserves
784 a very thin and fragile posteroventral process forming the ventral border of the mandibular
785 fenestra (below "maf" in Figs. 11A-D; 13A-B); the medial side of this process is concave and
786 formed the lateral border of the posterior part of the Meckelian groove. This makes DMNH
787 EPV.63136 the most complete silesaurid dentary known.

788 In the holotype, the sharply pointed anteriormost tip of the angular (an in Fig. 11A-D) is
789 preserved in contact with the posterior end of the posteroventral process. The posteroventral
790 process tapers posteriorly to a sharp point that overlies the anterior tip of the angular; comparing
791 the lateral and medial shapes of the contact between the elements suggests that the process of the
792 dentary slightly overlapped the tip of the angular laterally (Fig. 13A-B).

793 The posterior end of the tooth-bearing section of the dentary, which forms the
794 anterodorsal border of the mandibular fenestra, is also better preserved in DMNH EPV.63136
795 and DMNH EPV.63135 than in any previously described silesaurid specimen (Figs. 11, 13). The
796 dorsal surface of this process is a sharp edge behind the thirteenth and final dentary tooth. The

ventral surface of the process is embayed by a deep groove. A distinct notch occurs on the lateral surface of the process below or just behind the thirteenth tooth position that probably received the anterior tip of the surangular (sa.ar in Fig. 11A-B, E-H). The posterodorsal process seems to be somewhat deeper relative to the rest of the dentary in *Sacisaurus* specimen MCN PV10043 (Fig. 13I-J; *Langer & Ferigolo, 2013*, *fig. 4a*).

**Tooth morphology**

In addition to the emergent tooth crowns in the maxillae and dentaries just described (Figs. 8-13), there are six isolated teeth with the same crown morphology: DMNH EPV.43577 (Fig. 14A), DMNH EPV.63142 (Fig. 14B), DMNH EPV.63661 (Fig. 14C), DMNH EPV.63143 (Fig. 14D), DMNH EPV.63843 (Fig. 14E), and DMNH EPV.125922 (Fig. 14F). The referral of the isolated teeth to Silesauridae must be considered extremely tentative, based on their resemblance to those in the maxillae and dentaries rather than the presence of unique silesaurid dental autapomorphies.

Nearly all, maxillary, dentary, and isolated crowns are somewhat labially-lingually constricted (more at the tip than near the base) with a faint midline ridge and swollen base on both surfaces that is more prominent on the lingual side (the "cingulum" of *Langer & Ferigolo, 2013*; but see *Irmis et al., 2007*). The midline ridges bear a longitudinal groove in DMNH EPV.125922 (Fig. 14F, left images). Faint longitudinal striations occur on the lingual side of the crown in DMNH EPV.63143, but are absent on the labial side, and no striations can be discerned in other specimens; longitudinal striations are common on the crowns of other silesaurids (*Dzik, 2003; Nesbitt, Irmis & Parker, 2007; Nesbitt et al., 2010*). The crowns are usually asymmetrical in lingual or labial view, with the mesial (posterior) side of the base being more ventrally

positioned, but not recurved. The distal (anterior) carinae are often (but not always) slightly more convex than the mesial carniae so that the crowns are nearly recurved. The carinae possess coarse denticles at an acute angle to the mesial and distal edges.

Similar "phyllodont" or "folidont" (*Hendrickx, Mateus, & Araújo, 2015*) tooth crown morphology occurs in a variety of extinct diapsids that are herbivorous or interpreted as herbivorous (e.g. *Sues, 2000*). Folidont tooth crowns are expanded beyond the root and lanceolate rather than recurved (*Hendrickx, Mateus, & Araújo, 2015*). Folidont teeth also frequently possess a midline ridge extending from the base to the apex on the lingual and labial surfaces, and large denticles projecting at an angle to the tooth margin. In addition to *Kwanasaurus*, folidont teeth occur in *Sacisaurus* and *Eucoelophysis* (*Irmis et al., 2007, fig.2L; Langer &Ferigolo, 2013*) but distinct from the non-folidont condition in *Asilisaurus*, *Silesaurus*, and *Soumyasaurus* in which the crowns are more conical with smaller and less distinct denticles ("conidont" *sensu Hendrickx, Mateus, & Araújo, 2015*) (Fig. 13K-L; *Dzik, 2003, Nesbitt et al, 2010; Sarigül, Agnolin & Chatterjee, 2018*). The condition is harder to assess in the holotypes of *Technosaurus* (TTU P-9021) and *Diodorus* (MNHM-ARG 30). In *Technosaurus*, the crowns are damaged, making the presence of denticles or "accessory cusps" (*Hunt & Lucas, 1994*) difficult to evaluate, but the overall crown shape is similar to *Kwanasaurus* (Fig. 13G-H). In *Diodorus* the crowns also seem to be damaged and their form is therefore difficult to assess (Fig. 13M-N; *Kammerer, Nesbitt & Shubin, 2012*, *fig. 1*). Folidont teeth also occur in early ornithischians, early sauropodomorphs, some theropods (e.g. *Barrett, 2000; Araújo, Castanhiha, & Mateus, 2011; Hendrickx, Mateus, & Araújo, 2015*) and various enigmatic Late Triassic taxa that had been previously considered to be ornithischians (*Heckert, 2002; Parker et al., 2005; Irmis et al., 2007; Nesbitt, Irmis & Parker, 2007*).

Compared to the dentary teeth, the maxillary crowns of *Kwanasaurus* are relatively squat and robust-looking, and the anteriormost teeth in the larger maxilla DMNH EP.65879 and DMNH EPV.125923 are more labially-lingually swollen so that they almost circular rather than ovate in occlusal view (Fig. 8G-H; 9O-P), consistent with the overall robust form of the maxillae. Denticles cannot be discerned on the crowns of DMNH EPV.63650 or DMNH EPV.125923 (Fig. 8I-L, O-P; 9I-L, O-P). In comparison, the crowns of the teeth in dentaries DMNH EPV.63135, DMNH EPV.63660, DMNH EPV.65878 (Fig. 12I, L), and isolated teeth DMNH EPV.43577, DMNH EPV.63843, and DMNH EPV.125922 (Fig. 13A, D-F) are less swollen at the base and are more mesially-distally compressed, and are also relatively symmetrical in mesial, distal, or occlusal views.

In maxillae DMNH EPV.65879 DMNH EPV.63650, the crowns and empty alveoli become gradually smaller posteriorly (Fig. 8), indicting a posterior reduction in maxillary tooth size as in known silesaurid maxillae (Fig. 10C-G) for *Lewisuchus* (*Bittencourt et al., 2014*), *Silesaurus* (*Dzik, 2003*, fig. 5C), and *Sacisaurus* (*Langer & Ferigolo, 2013*). This is less certain in DMNH EPV.125923 and DMNH EPV.125921, where the posterior part of the tooth row is less well-preserved (Fig. 9). There is no clear canting or recurvature in maxillary teeth.

In contrast, in the most complete dentaries of *Kwanasaurus* (DMNH EPV.63136 and DMNH EPV.63135) the teeth clearly increase in the size into the middle of the jaw then decrease in the posteriormost alveoli (Figs. 11, 12A-D) as also occurs in all known silesaurid dentaries that are sufficiently complete to evaluate (Fig. 13), specifically *Diodorus*, *Silesaurus*, *Sacisaurus*, and *Technosaurus* (*Dzik, 2003, fig. 5E-F; Kammerer, Nesbitt & Shubin, 2012; Langer & Ferigolo, 2013*). In DMNH EPV.63660, the first tooth is slightly more conical than the following teeth, is slightly anteriorly canted and has a concave mesial edge making it slightly recurved

(Fig. 12J-L). This also occurs in the anterior teeth of *Sacisaurus* (Fig. 13I-J; MCN PV10050; *Langer & Ferigolo, 2013*, *figure 2*). The first tooth of DMNH EPV.63136 is damaged, but the third tooth is also anteriorly canted (but not recurved) due to the mesial edge being longer than the distal edge (Fig. 11A-D). The anteriormost dentary teeth are not known in *Eucoelophysis* or *Technosaurus*, so it is not known if they shared the condition.

None of the maxillary teeth of *Kwanasaurus* are sufficiently well-preserved to determine if denticle count changes with crown size, but in the dentaries and isolated crowns, larger crowns have more denticles; in dentary teeth, this means that there is a general anterior to posterior increase in denticle counts (Table S1). This relationship between crown size and denticle count also occurs in the isolated crowns. There appear to be at least four or five denticles (not all are preserved) along both the mesial and distal edges of DMNH EPV.63142, DMNH EPV.43577 and DMNH EPV.63661, but seven on each edge of DMNH EPV.63143, the largest of the isolated crowns (Fig. 14C).

The isolated crowns all preserve a single root, which appears to be nearly complete in all four specimens (Fig. 14). The relatively complete roots of DMNH EPV.63142, DMNH EPV.63661, and DMNH EPV.63143 are about twice the length of the crown. The roots taper away from the crown; they are thicker and subcircular or oval closer to the crown, where they are slightly constricted labially-lingually, and narrow to a thinner subcircular tip. In mesial and distal views the root curves slightly, probably lingually as this is the direction of crown inclination in DMNH EPV.63136 and DMNH EPV.63135.

**Tooth counts and replacement patterns**

Ankylosis of fully erupted socketed teeth to jaw ("ankylosed thecodont" or "ankylothecodont" *sensu Edmund, 1969*, p. 129 and *Chatterjee, 1974*, p. 230) occurs in the Eagle Basin specimens as in all silesaurids where tooth-bearing elements are preserved (*Dzik, 2003; Nesbitt et al., 2010; Irmis et al., 2007; Kammerer, et al., 2012, Langer & Ferigolo, 2013; Martz et al., 2013*), and is an autapomorphy of Silesauridae (*e.g. Nesbitt et al., 2010*). Tooth replacement in the Eagle Basin material occurs in a generally alternating sequence (Figs. 8-12, Table S1; Zahnreinhen waves of replacement *sensu Woerdeman, 1921*), but there are complications to this pattern, as will be discussed below.

Tooth replacement occurred on the lingual side of the fully erupted crown, as is typical of amniotes (*e.g. Edmund, 1969*); in the fourth tooth position of the largest maxilla DMNH EPV.65879 (Fig. 8C-D), the incoming replacement crown lies in an embayment on the lingual side of the fully emergent crown, indicating that dissolution of the medial side of the root accompanied the emergence of the replacement crown within the same socket ("iguanid" tooth replacement *sensu Edmund, 1960*, *p. 61-62*). The dorsal surface of the maxilla is damaged above the fourth tooth position, so it is not clear if the root of the replacement tooth was still intact. However, in DMNH EPV.125923 (Fig. 9I-P), the incoming replacement tooth still possesses a root projecting above the main body of the maxilla, and the prior crown is already gone. This suggests that maxillary tooth replacement occurred as follows:

1) The replacement tooth forms with the root projecting above the main body of the maxilla. As the tooth moves into position, the lingual side of the previously emplaced crown and the cement holding it to the alveolar margin is dissolved (as seen in DMNH EPV.65879).

2) The emplaced crown and whatever remains of the root is released while the replacement crown moves into position, the root still attached (as seen in DMNH EPV.125923).
3) With the replacement crown fully emplaced, at least the part of the root projecting above the main body of the maxilla is dissolved, leaving a spongy replacement pit, while the tooth is ankylosed into the jaw below the crown.

It is not clear if this pattern was identical in the dentary teeth; only DMNH EPV.63135 display incoming replacement teeth (simultaneously in tooth positions 7 and 9), and the roots, if present, are concealed inside the dentary (Fig. 12A-D). It can at least be said that they do not project below the Meckelian groove.

The number and pattern of emplaced teeth shows an interesting degree of variation among silesaurids. In *Kwanasaurus*, there is a clear alternating pattern of tooth replacement in both the maxilla and dentary in which there are no more than two adjacent fully erupted and ankylosed crowns (Figs. 8-13), DMNH EPV.63135 shows replacement teeth coming in simultaneously on either side of a fully emergent crown (Fig. 11A-D). An alternating pattern of replacement in which there are no more than two adjacent fully erupted crowns also occurs in some dentaries of *Sacisaurus* (Fig. 13I-J; *Langer & Ferigolo, 2013, figs. 3-4*), and apparently the less complete holotype dentaries of *Diodorus* (Fig. 13M-N; *Kammerer, Nesbitt & Shubin, 2012*) and *Asilisaurus* (*Nesbitt et al., 2010, fig. 1b*).

However, in another dentary of *Sacisaurus* (MCN PV10048; *Langer & Ferigolo, 2013, figs. 5*) there are three adjacent fully erupted crowns, and a maxilla assigned to that taxon has five sequential fully erupted crowns (Fig. 9G; *Langer & Ferigolo, 2013, fig. 5*). *Silesaurus* maxilla ZPAL Ab III/361/26 has four sequential fully erupted crowns (while dentary ZPAL Ab

933 III/437/1 has five (Fig. 12K-L; *Dzik, 2003, figs. 5A-B, E-F*). In the holotype dentary of
934 *Technosaurus* (TTU P-11282) there are 6 sequential fully erupted crowns (Fig. 12G-H;
935 *Chatterjee, 1984; Martz et al., 2013, fig. 14G*).
936 In summary, there are silesaurid tooth-bearing elements with rows of almost entirely fully
937 emergent teeth, others in which replacement has left blocks of three or more sequential teeth, and
938 some in which fully emplaced crowns mostly alternate between odd and even teeth tooth
939 positions. It is not clear if these patterns of variation are taxonomically significant, or if different
940 silesaurid specimens merely show the same pattern patterns of tooth replacement at different
941 stages; the latter seems most likely given that some but not all specimens of *Sacisaurus* show
942 alternating tooth replacement (*Langer & Ferigolo, 2013*). Tooth replacement patterns can be
943 complex (*Edmund, 1960; Whitlock & Richman, 2013*), and are easier to evaluate in pleurodont
944 dentitions where the lingual surfaces of the roots are exposed, showing the earlier stages of root
945 resorption (*Edmund, 1969, p. 136*).
946
947 **Humerus**
948 DMNH EPV.59302, a nearly complete left humerus (Fig. 15; measurements in Table 2A), is
949 remarkably similar to those of *Silesaurus* and *Diodorus* in being long, straight, very sender, and
950 simple in form (*Dzik, 2003: figure 9B; Kammerer, Nesbitt & Shubin, 2012: figure 2*). The
951 proximal end is not fully preserved, but the articular surface is not distinctly thickened (Fig.
952 15A), or as straight in anterior and posterior views (Fig. 15B, D) as in *Silesaurus* and *Diodorus*
953 (*Dzik, 2003, fig. 9B*; *Kammerer, Nesbitt & Shubin, 2012, fig 2A1, 2A3*). In anterior and posterior
954 views, the proximal end is only slightly expanded medially, whereas the lateral side bearing the
955 deltopectoral crest is straight ("dc" in Fig. 15B, D). The deltopectoral crest is incompletely

preserved, but seems to have been weakly developed, curved anteriorly, and did not extend distally more than 1/3rd of the length of the shaft (Fig. 15B), similar to *Silesaurus* and *Diodorus* (*Kammerer, Nesbitt & Shubin, 2012*) and in contrast with the more distally elongate deltopectoral crests of dinosaurs (*Langer & Benton, 2006*). The anterior face of the proximal end is slightly concave, narrowing distally to a groove that shallows before the midpoint of the humerus (Fig. 15B).

The midshaft is almost circular in cross section. The distal end is twisted so that the long axis is almost perpendicular to that of the proximal end (Fig. 15G); torsion also seems to occur to some extent in *Silesaurus* (*Dzik, 2003, fig. 9B*) but not in *Diodorus*, where the long axis of the proximal and distal ends are parallel (*Kammerer, Nesbitt & Shubin, 2012, p. 279*). The distal end is even less expanded relative to the shaft than the proximal end (Fig. 15E-G), with no trace of entepicondylar or ectepicondylar flanges or grooves as is typical for ornithodirans (*e.g. Nesbitt, 2011, character 234*). Both the anterolaterally and posteromedially facing surfaces of the distal end are concave between the condyles ("ect" and "ent" in Fig. 15), with the concavity extending somewhat proximally up the shaft. The concavity on the anterolateral surface is deeper, with a deep groove ("gr" in Fig. 15E); a similar groove also occurs here in *Diodorus* (*Kammerer, Nesbitt & Shubin, 2012, figure 2A3*).

As no unique humeri autapomorphies have been identified for Silesauridae, referral to the clade is likely but tentative and based on the strong resemblance of the element to that of *Silesaurus* (*Dzik, 2003: figure 9B*) and *Diodorus* (*Kammerer, Nesbitt & Shubin, 2012: figure 2*). Shuvosaurids also have extremely similar long and slender humeri with weakly developed deltopectoral crests (*e.g. Long & Murry, 1995, p. 160, figure 164; Nesbitt 2011, characters 236*), but *Effigia* (*Nesbitt, 2007: p. 45, figure 37*) and *Shuvosaurus* (TTU P-9001; *J.W. Martz, personal*

979 *obs; Long and Murry 1995*, *fig. 164B*) have large bulbous tubers on the posterior side of the
980 proximal end that are lacking in silesaurids.
981
982 **Ilium**
983 DMNH EPV. 48506, a left ilium (Fig. 16; measurements in Table A2), bears a combination of
984 characters that suggest that it is probably a silesaurid, although with some differences from
985 previously described taxa (*Dzik, 2003; Nesbitt et al., 2010*). DMNH EPV.63650, a slightly less
986 complete ilium missing most of the iliac blade and end of the postacetabular process (Fig. 17A-
987 C) is nearly identical in size and shape. DMNH EPV.52195, a partial iliac blade with the
988 postacetabular process preserved (Fig. 17D-G) shares key similarities with DMNH EPV.48506,
989 and may also be silesaurid.
990 In all specimens, the iliac blade ("ilb" in Fig. 16A-F; 17A-C, F) is thin and almost
991 horizontally inclined so that it slopes ventrolaterally. This unusual orientation of the iliac blade
992 gives the ilium a saddle-like appearance in lateral view similar to *Silesaurus* (*Dzik 2003*),
993 *Eucoelophysis* (*Irmis et al., 2007: figure 2M*), and *Ignotosaurus* (*Martinez et al., 2012*). The
994 region is not preserved in *Sacisaurus* (MCN PV 10100; *Langer & Ferigolo, 2013: figure 10*).
995 The Middle Triassic silesaurids *Asilisaurus* and *Lutungutali*, which are basal to most members of
996 Sulcimentisauria (*Peecook et al., 2013; see below*) differ from *Kwanasaurus*, *Silesaurus*,
997 *Eucoelophysis*, and *Ignotosaurus* in having a more vertically oriented tall iliac blade (*Peecook et*
998 *al., 2013: figures 2-3, 6*) more like what is seen in other archosauriforms (*e.g. Nesbitt, 2011, fig.*
999 *34*), suggesting that this is the plesiomorphic condition for Silesauridae.
1000 In lateral view, the flattened preacetabular process of both DMNH EPV.48506 and
1001 DMNH EPV.63653 is elongate and anterodorsally oriented ("pra" in Fig. 16A-D, 17A-B) as in

*Silesaurus* (*Peecook et al., 2013: figure 6F*) *Eucoelophysis* (*Irmis et al., 2007, fig. 2M; J.W. Martz, pers. obs. of GR 225*), and *Ignotosaurus* (*Martinez et al., 2012*) in contrast to the extremely thick and blunt preacetabular process in *Lutungutali* (*Peecook et al., 2013*); the process is not known for *Asilisaurus* or *Sacisaurus*. In DMNH EPV.48506, the anterior tip of the preacetabular process tapers medially to a point in dorsal view (Fig. 16E-F). Just posterior to the tapering tip, the lateral edge of the preacetabular process in both DMNH specimens is a sharp and grooved crest in the same position as the "tuberosity" in *Silesaurus* and *Ignotosaurus* (*Dzik, 2003; Martinez et al., 2012*). This sharp crest flattens and thickens to merge with the lateral surface of the ilium without quite contacting the supracetabular crest.

The preacetabular process in DMNH EPV.48506 is so elongate that it extends anterior to the acetabulum (Fig. 16) as is generally seen only in neotheropods and ornithischians (*Langer & Benton, 2006: 68-1; Nesbitt, 2011: character 269-1*). In DMNH VP.63653, the process is not complete, but is also elongate and blade-like (Fig. 17A-B). This differs from the slightly shorter preacetabular processes of *Silesaurus* (*Dzik, 2003: figure 11; Peecook et al., figure 6F-G*), *Ignotosaurus* (*Martinez et al., 2012*) and especially from the extremely short and blunt process in *Lutungutali* (*Peecook et al., 2013*). In *Eucoelophysis* specimen GR 225 (*Irmis et al., 2007: figure 2M*), the process is incomplete. A preacetabular process that does not extend beyond the pubic peduncle is allegedly plesiomorphic for dinosauromorphs (*Nesbitt, 2011; 269-0*). Although *Ferigolo & Langer (2007)* claim this process is also short in *Sacisaurus* (MCN PV10100), it is mostly missing in that specimen (*Langer & Ferigolo, 2013: figure 10*), and the ilium of *Diodorus* is undescribed. The highly elongate preacetabular process of *Kwanasaurus* is considered to be an autapomorphy.

The postacetabular process of DMNH EPV.48506, DMNH EPV.63653 and DMNH EPV.52195 ("poa" in Figs. 16A-D, G; 17A, D, F) is large, slightly longer than the preacetabular process and extending well posterior to the acetabulum. It bears a large, ventrolaterally oriented brevis shelf sheltering a distinct brevis fossa (Figs. 16A-B, G-H; 17A, C) as occurs in other members of Sulcimentisauria: *Silesaurus* (*Dzik, 2003*), *Eucoelophysis* (GR 225; *Irmis et al., 2007, figure 2M*), *Lutungutali* (*Peecook et al., 2013*), *Ignotosaurus* (*Martinez et al., 2012*), and *Sacisaurus* (*Langer & Ferigolo, 2013*), although incomplete preservation and preparation MCN PV 10100 make comparisons difficult. A distinct brevis shelf and brevis fossa ("bs" and "bf" in Figs. 16-17) unites dinosaurs and some non-dinosaurian dinosauromorphs (*e.g. Langer & Benton, 2006; Nesbitt, 2011*), although both are weakly developed or absent in *Asilisaurus* (*Nesbitt et al., 2010*) and herrerasaurids (*Langer & Benton, 2006*). Very faint longitudinal striations occur along the lateral edge of the brevis shelf in all three DMNH specimens, but do not form the more rugose surface present in *Silesaurus* (*Dzik, 2003: figure 11*), *Ignotosaurus* (*Martinez et al., 2012*) and *Lutungutali* (*Peecook et al., 2013*). The sharp ventrolateral edge of the brevis shelf merges with the a low rounded ridge that extends to the edge of the acetabulum (Fig. 16A-B, G-H; 17A, C), as in other silesaurids (*Dzik, 2003; Ferigolo & Langer, 2007, Fig. 2E; Irmis et al., 2007, fig. 2M; Langer & Ferigolo, 2013, figure 10a*) and most other dinosauromorphs except theropods (*Langer & Benton, 2006*).

A small triangular process protrudes from the midpoint of the thin posteroventral edge of the postacetabular process of both DMNH EPV.48506 and DMNH EPV.63655, (Figs. 16A-B, 17A-B) which probably marked the posteroventral extent of the last (?third) sacral rib (Fig. 16C-D; see below). A small similarly positioned projection is illustrated in *Silesaurus* (*Dzik 2003, Fig.2*), *Ignotosaurus* (*Martinez et al., 2012: figure 3*), and *Marasuchus lilloensis* (*Sereno &*

*Arcucci, 1994b, fig. 6*); this region is not well-preserved in DMNH EPV.52195, *Sacisaurus* (MCN PV10100) or *Eucoelophysis* (GR 225; *J.W. Martz, pers. obs.*). In DMNH EPV.48506 and DMNH EPV.63653, a small foramen occurs near the edge of the brevis fossa, just anteroventral to the triangular process.

The acetabulum in both DMNH EPV.48506 and DMNH EPV.63653 ("ac" in Figs. 16A-B, G-H; 17A, C) is deep with a well-developed and sharp-edged supracetabular crest ("suc" in Figs. 16-17), so that the acetabulum faces ventrally. As in *Lutungutali* (*Peecook et al., 2013*), there is no trace of an antitrochanteric fossa as occurs in *Silesaurus (Dzik, 2003)*. In DMNH EPV.48506, the ventral edge of the ilium and acetabulum (the "ventral flange" of *Martinez et al., 2013*) is thin, ventrally concave, and seems to be a natural edge rather than a break (Fig. 16A-D). In DMNH EPV.63653, the ventral rim of the acetabulum is clearly damaged, but the bone is extremely thin, suggesting that it had the same condition (Fig. 17A-B). This suggests partial perforation of the acetabulum between the ilium and ischium/pubis as in *Ornithosuchus longidens* (*Walker, 1964*) and herrerasaurids (*Langer & Benton, 2006*). *Nesbitt et al. (2010)* considered a straight ventral margin of the acetabulum to be a silesaurid synapomorphy. If so, *Kwanasaurus* is the only known non-dinosaurian dinosauriform with a semiperforate acetabulum, which differs from other silesaurids in which the ventral margin of the acetabulum is convex (*Nesbitt et al., 2010; Nesbitt, 2011*).

The pubic and ischiac peduncles are both preserved in DMNH EPV.48506 and DMNH EPV.63653 (Figs 16, 17A-C). The pubic peduncle ("pup" Fig. 16-17) is larger and bluntly truncated where it contacted the pubis. The pubic articulation is divided into an anteroventral facing surface and a more rugose ventrally facing surface (best seen in Fig. 16G-H). The lateral margin of the pubic peduncle thins posterodorsally to become the supracetabular crest, and the

medial margin tapers ventromedially to merge with the sharp ventral edge of the acetabulum. The ischial peduncle ("isp" in Fig. 16A-B, G-H) is much smaller than the pubic peduncle and faces ventrolaterally.

On the medial side of the ilium in DMNH EPV.48506, the subhorizontal iliac blade forms a thin crest overhanging the rest of the medial surface ("ilb" in Fig. 16C-D), extending between the anterior tip of the precetabular process to the posterior tip of the postacetabular process. The blade this is not well-preserved in DMNH EPV.52195 and DMNH EPV.63653 (Fig. 17B, E).

The regions of sacral rib attachment can be discerned in both DMNH EPV.48506 (Fig. 16D) and DMNH EPV.63653 (Fig. 17B), although clear divisions between the attachments of different ribs are not clear, making an exact count impossible. The following interpretation of the sacral rib attachment sites is aided by those made for other archosaurs (*Novas, 1994, fig. 5B; Dzik, 2003, fig. 11B; Nesbitt, 2005, fig. 23C; Nesbitt, 2011, p. 117*). The first primordial sacral rib probably attached in a slight depression on the anterior part of the medial surface of the ilium, just below the preacetabular process ("sac 1.ar" in Figs. 16D, 17B), while the second and possibly a third (primordial second?) sacral rib attached in a larger and more posterior depression ("sac 2.ar" and "sac 3.ar") bounded dorsally by a short sharp-edge crest extending from the posterior margin of the postacetabular process, and posteroventrally by the small triangular projection on the thin posteroventral edge of the postacetabular process. These two depressions are connected over the acetabulum, and the entire region of sacral rib attachment is very faintly rugose. The rib attachment sites in *Ignotosaurus* appear to be very similar (*Peecook et al., 2013, Fig. 3F*), although those authors only inferred the presence of two sacral ribs. Two or three ribs

attach in *Silesaurus* (*Dzik, 2003; Langer & Benton, 2006, p. 328; Nesbitt, 2011, p. 117*) but the precise attachments are undescribed for other silesaurids for which the ilium is known.

**Femur**

Femora are by far the most common silesaurid elements from the Eagle Basin localities (Figs. 18-22; measurements in Table A2). The most complete is a large left femur, DMNH EPV.34579 from the Derby Junction locality (Fig. 18), but several proximal femora can also be assigned to Silesauridae: DMNH EPV.54828 (Fig. 19A-E) and DMNH EPV.59311 (Fig. 21F-J) from Shuvosaur Surprise, DMNH EPV.44616 (Fig. 19F-J), DMNH EPV.56651 (Fig.19K-O), DMNH EPV.59301 (Fig. 21K-O) from Main Elk Creek, DMNH EPV.63139 (Fig. 21A-E) from Lost Bob, and DMNH EPV.63874 (Fig. 20F-J) and DMNH EPV.125924 (Fig. 20A-E) from Lost Bob East.

All of these specimen preserve at least two of the following silesaurid autapomorphies of the proximal end of the femur recognized in *Asilisaurus*, *Silesaurus*, *Eucoelophysis*, *Sacisaurus*, and *Diodorus* (*Dzik, 2003; Ferigolo & Langer, 2007; Nesbitt et al., 2010; Nesbitt, 2011; Kammerer, Nesbitt & Shubin, 2012; Langer & Ferigolo, 2013*): the femoral head possesses a longitudinal groove in proximal view ("gr" in Figs. 19, 21).

1) A flattened medial articular surface between the anteromedial and anterolateral tubers ("amt" and "alt" in Figs. 19, 20A-B, 21)
2) A distinct notch ventral to the head ("vn" in Figs. 18-21).
3) As in all silesaurids except for *Asilisaurus* (*Nesbitt et al., 2010; Nesbitt, 2011: 313-1*), the proximal ends of these femora are also subtriangular in proximal view due to the absence of a well-developed posteromedial tuber (although a slight

swelling is present at the same area in all Eagle Basin specimens) and a fossa trochanteris (=posterolateral depression, =facies articularis antitrochanterica).

Four other badly worn unfigured proximal femora (DMNH EPV. 27699, DMNH EPV. 43126, and DMNH EPV.43588 from Main Elk Creek, and DMNH EPV.44616 from Main Elk Creek), are also probably silesaurid based on the general similarity shape of the head, dorsolateral trochanter, and lesser trochanter (discussed below), although unequivocal silesaurid autapomorphies cannot be identified; the presence of distinct dorsolateral and lesser trochanters allows the femora to be assigned at least to Dinosauriformes (*e.g. Langer & Benton, 2006; Nesbitt, 2011*). Three distal femora, DMNH EPV.34028 from Main Elk Creek, DMNH EPV.59310 from Shuvosaur Surprise, and DMNH EPV.67956 (Fig. 22; found in association with previously described scapula with the same number but too small to belong to the same individual) also cannot be assigned to Silesauridae based on apomorphies, but share key similarities to the other specimens (see below).

Nearly all specimens preserving the proximal end possess a distinct ridge-like dorsolateral trochanter (*sensu Langer & Benton, 2006*) on the proximal end of the femur ("dt" in Figs. 18-21), except for DMNH EPV.27699 and DMNH EPV.59311, where this region is damaged. The dorsolateral trochanter is best preserved in DMNH EPV.44616 (Fig. 19F-G, J), DMNH EPV.59301 (Fig. 21K-L, O), and DMNH EPV.63139 (Fig. 21A-B). Although at least slightly damaged in the other specimens, the form seems to be consistent. The dorsolateral trochanter projects laterally from the shaft, sometimes curling slightly anterolaterally. Proximally, the trochanter thins and merges with the head. When well-preserved, the posterolateral surface of the trochanter is somewhat flattened, bearing faint longitudinal grooves

and ridges. The posterior margin of the proximal part of the femur is distinctly pinched into a rounded crest extending distally from the dorsolateral trochanter.

Nearly all specimens preserve a distinct anterior trochanter (=lesser or cranial trochanter) on the anterolateral surface of the femur, just distal to the head ("at" on Figs. 18-21). The lesser trochanter is an anteroposteriorly compressed crest extending parallel to the long axis of the femur. DMNH EPV.44616 is the only specimen with a perfectly preserved anterior trochanter (Figs. 19H, J), which is asymmetrically subtriangular in anterior and posterior views, slightly curled anterolaterally, and distinctly lacks a cleft between the trochanter and the main body of the femur; it is somewhat similar to the "longitudinal blade" forming part of the anterior trochanter of *Silesaurus* (*Dzik, 2003, fig. 13*). DMNH EPV.34579 (Fig. 18D), DMNH EPV.54828 (Fig. 19C), and DMNH EPV.125924 (Fig. 20C) possess a cleft between the trochanter and the main body of the femur, but it is not clear if this is natural or due to damage. The presence of an anterior (=lesser) trochanter is restricted to dinosauriforms and larger individuals of *Dromomeron gregorii* and *D. gigas* (*e.g. Novas, 1992, 1996; Sereno & Arcucci, 1994b; Langer & Benton, 2006; Nesbitt et al., 2009a; Nesbitt, 2011; Martinez et al., 2015*), while a cleft between the trochanter and the main body of the femur is known primarily in most theropods and some ornithischians (*Novas, 1996; Langer & Benton, 2006*) although it also occurs in the silesaurids *Eucoelophysis, Sacisaurus* and *Diodorus* (*Sullivan & Lucas, 1999, fig. 6; Ezcurra, 2006; Ferigolo & Langer, 2007; Kammerer, Nesbitt & Shubin, 2012*).

There is no trochanteric shelf (=transverse tuber sensu *Dzik, 2003*) in the majority of the Eagle Basin specimens except for DMNH EPV.125924, where a distinct scar interpreted as a weakly-developed shelf extends ventrolaterally from the anterior trochanter ("ts" in Fig. 20B-E), resembling the trochanteric shelf in larger specimens of *Dromomeron gregorii* (*Nesbitt et al.,*

*2009a: figure 2A-B*). In DMNH EPV.125924, the trochanteric shelf ends with a posterolateral swelling with the distal end of the lesser trochanter that is present in other specimens lacking the shelf ("sw" in Figs. 18-20), and occurs in the same position as the end of the trochanteric shelf in *Dromomeron romeri* (*Nesbitt et al., 2009a: figure 2*). The swelling is therefore interpreted as part of the attachment for the M. iliotrochantericus caudalis.

The trochanteric shelf is absent in known specimens of *Sacisaurus, Eucoelophysis* and *Diodorus* (*Ferigolo & Langer, 2007; Ezcurra, 2006; Nesbitt et al., 2010; Kammerer, Nesbitt & Shubin, 2012; Langer & Ferigolo, 2013*), although the trochanteric shelf is present in *Asilisaurus* (*Nesbitt et al., 2010*), and some individuals of *Silesaurus* (*Dzik, 2003; Piechowski, Tałanda & Dzik, 2014*). The trochanteric shelf has been suggested to develop ontogenetically in at least some dinosauromorphs and highly subject to individual variation (*Nesbitt, 2011; Griffin and Nesbitt, 2016a; Piechowski, Tałanda & Dzik, 2014*). It should be noted however that some specimens lacking the shelf (most notably the largest and most complete specimen, DMNH EPV.34579) are similar in size to some of the larger femora of *Silesaurus* possessing the shelf (*Dzik, 2003: figure 13A; Piechowski, Tałanda & Dzik, 2014*).

A fourth trochanter ("ft" in Figs. 18-21) is distinctly present in DMNH EPV.34579, DMNH EPV.63139, DMNH EPV.63874, and the worn specimens DMNH EPV.43126, DMNH EPV.43588, although none preserve it completely. The proximal end of the fourth trochanter rises smoothly from the posteromedial side of the femur as a pinched crest, distal to the distal end of the anterior trochanter on the opposite side of the femur. The distal end of the fourth trochanter is not preserved in any Eagle Basin specimens, so it is not known if the trochanter was proximodistally symmetrical. The trochanter is also a low crest in other specimens of *Dromomeron romeri* as well as *D. gregorii* (*Nesbitt et al., 2009*), and very different from the

massive crest present in *Ixalerpeton polesinensis* (*Cabreira et al., 2016: figure S1D-E*). At least in DMNH EPV.63874 (Fig. 20G-H) and DMNH EPV.63139 (Fig. 21B-C), where the region is well-preserved, a shallow depression occurs just anterior to the fourth trochanter on the medial side of the femur as in *Diodorus* (*Kammerer, Nesbitt & Shubin, 2012*) and *Sacisaurus* (*Langer & Ferigolo, 2013*).

The only femur with known silesaurid apomorphies for which the distal end of the femur is preserved is DMNH EPV.34579 (Fig. 18). The distal end is slightly expanded relative to the shaft. The sulcus dividing the medial and lateral condyles on the posterior side of the femur (Fig. 18B) extends about 1/3$^{rd}$ of the length of the shaft (Fig. 18F), a silesaurid synapomorphy (*Nesbitt et al., 2010*). There is also a slight sulcus on the anterior side of the distal end (Fig. 18C-D), causing the medial side of the distal end to protrude slightly anteriorly to the shaft. In distal view (Fig. 18B), the angle between the lateral condyle and the crista tibiofibularis (=fibular condyle) is obtuse, as in most archosaurs except for paracrocodylomorphs (*Nesbitt, 2011*).

The medial condyle is a surprisingly sharp-edged flange, very similar to the crista tibiofibularis in distal view, but smaller than both the crista tiobiofibularis and lateral condyle (Fig. 18B-F). This appears to distinguish *Kwanasaurus* from *Silesaurus*, *Diodorus*, *Sacisaurus*, and *Eucoelophysis*, in which the medial condyle is quite broad and blunt in distal view (*Sullivan & Lucas, 1999, fig. 5; Dzik, 2003; Kammerer, Nesbitt & Shubin, 2012: fig. 3E*). Indeed, this character state is shared uniquely between *Kwanasaurus* and lagerpetids (*Nesbitt et al., 2010, character 225*). There is a deep depression on the distal surface of the femur just behind the crista tibiofibularis (Fig. 17B); a depression also occurs on the distal end of the femur in *Diodorus*, but seems to occur between the medial condyle and crista tibiofibularis (*Kammerer, Nesbitt & Shubin, 2012, fig. 3E*).

Distal femora DMNH EPV.67956 (Fig. 22), DMNH EPV.34028, and DMNH EPV.59310 (the latter two specimens are unfigured), do not possess known silesaurid apomorphies, and moreover the latter two specimens are somewhat worn. As a result, we are reluctant to formally assign them to *Kwanasaurus*. However, all three seem to share interesting similarities to DMNH EPV.34579: the medial condyle is at least slightly more slender and sharper-edged compared to both the lateral condyle and crista tibiofibularis, and a deep depression occurs on the distal surface behind the crista tibiofibularis (Fig. 22A). In DMNH EPV.67956, the sulcus between the medial condyle and crista tibiofibularis is a particularly deep groove (Fig. 22A, E).

## PHYLOGENETIC ANALYSIS

### Methods

*Nesbitt's (2011)* phylogenetic analysis of Archosauriformes and *Nesbitt et al.'s (2010)* more focused phylogenetic analysis of Silesauridae have served as the basis for most subsequent analyses of silesaurids. The phylogenetic analyses of *Kammerer, Nesbitt & Shubin (2012)*, *Peecook et al. (2013)* and *Martinez et al. (2012)*, which described *Diodorus*, *Lutungutali* and *Ignotosaurus* respectively, all began with the data matrix of *Nesbitt et al. (2010)*. The analyses of *Langer & Ferigolo (2013)*, *Bittencourt et al. (2014)* and *Agnolin & Rozadilla (2017)* were both based on modified versions of the data matrix of *Nesbitt (2011)*.

We have opted to utilize the data matrix of *Peecook et al. (2013)*, acquiring the Nexus file for from Morphobank. The matrix of *Peecook et al. (2013)* is slightly modified from the matrix of *Nesbitt et al. (2010)*, with the addition of one character making a total of 291, and some character re-numberings to match the numberings given by *Nesbitt et al. (2010)* (see Appendix 2 for details). We edited the Nexus file in Mesquite (v. 3.51) by added the codings of

*Kwanasaurus williamparkeri* from the present study, the codings of *Diodorus scytobrachion* from *Kammerer*, *Nesbitt & Shubin (2012)*, the codings of *Ignotosaurus fragilis* provided by *Martinez et al. (2012)*, and codings for the humerus of *Dromomeron romeri* based on the material described here. The codings of *Lewisuchus admixus/Pseudolagosuchus major* were combined. This brought the total number of taxa in the analysis to 37.

As nearly all silesaurid elements from the Eagle Basin are individual elements, so that the codings for *Kwanasaurus* are a composite of multiple specimens (Appendix 2). Moreover, the dinosauriform scapula and tibiae described above, which are potentially silesaurid but lack known autapomorphies for the clade, are also included in the composite. Although this compositing is not ideal, it has been used by other researchers (*Kammerer, Nesbitt & Shubin, 2012; Langer & Ferigolo, 2013*) and is difficult to avoid given that silesaurids are often recovered as individual elements (*Irmis et al., 2007; Kammerer, Nesbitt & Shubin, 2012, p. 278; Langer & Ferigolo, 2013, p. 355; Martinez et al., 2012*), with only some taxa being known from associated elements (*Dzik, 2003; Nesbitt et al., 2010; Peecook et al., 2013; Bittencourt et al., 2014*).

We conducted our analysis using PAUP 4.0a163 for Macintosh OS. Following *Nesbitt et al. (2010)* and *Peecook et al. (2013)*, all characters were equally weighted and characters 23, 78, 89, 98, 116, 142, 159, 169, 175, 177, 195, 200, 227, 250, and 281 were ordered. *Erythrosuchus africanus* and *Euparkeria capensis* were chosen as paraphyletic outgroups. Trees were searched for using the parsimony criterion implemented under the heuristic search option on Wagner trees using TBR (tree bisection–reconnection) branch-swapping with 1,000 random addition sequences holding 10 trees per replicate, continuing subsequent TBR swapping on all stored minimum length trees.

## Results

In the following discussion, clade definitions were taken from *Langer et al. (2013)* and sources cited therein, except for the new clade name Sulcimentisauria introduced here. Our analysis recovered 30 most parsimonious trees (MPTs) with a best score tree lengths of 758 (C.I = 0.46, R.I. = 0.705). Synapomorphies for well-supported clades are given in Appendix 3.

Neither our strict consensus tree nor our identical Adams consensus trees (Fig. 23) do much to revolutionize current understandings of silesaurid phylogeny. As with most previous analyses (*Nesbitt et al., 2010; Nesbitt, 2011; Kammerer et al., 2012; Martinez et al., 2012; Peecook et al., 2013*), Silesauridae is sister taxon to Dinosauria, and the combined *Lewisuchus admixus/Pseudolagosuchus major* and *Asilisaurus kongwe* were found to be consecutive outgroups to all other silesaurids. *Pisanosaurus mertii*, which was found to be another basal silesaurid by *Agnolin & Rozadilla (2017)*, was recovered as an ornithischian.

Sulcimentisauria is proposed as our name for all silesaurids more derived than *Asilisaurus* (see Systematic Paleontology). Within Sulcimentisauria, *Eucoelophysis baldwini* and *Diodorus scytobrachion* are consecutive sister taxa to other Sulcimentisaurians. A clade comprising *Lutungutali sitwensis* and *Ignotosaurus fragilis* forms a polytomy with other Sulcimentisaurians (Figure 23). None of the phylogenetic relationships within Sulcimentisauria are particularly well-supported, although the clade itself remains robust (Appendix 3).

## DISCUSSION

Within the last decade, it has become clear that the Late Triassic dinosaur assemblage of western North America was of low diversity, being represented only by basal theropods and

basal neotheropods that co-existed with non-dinosaurian dinosauromorphs (lagerpetids and silesaurids) (*Nesbitt, Irmis & Parker, 2007, Nesbitt et al., 2009a, b; Irmis et al., 2007; Sues et al., 2011; Marsh et al., 2016*). While the western North American Late Triassic dinosauromorph fauna has been previously described from the Colorado Plateau and western Texas (*Ezcurra, 2006; Nesbitt, Irmis & Parker, 2007; Irmis et al., 2007; Nesbitt & Chatterjee, 2008; Martz et al., 2013*), the Eagle Basin dinosauromorph fauna described here for the first time in detail demonstrates that similar patterns of dinosauromorph diversity existed north of the Ancestral Uncompahgre Highlands. Indeed, the Eagle Basin fauna is the northernmost Triassic dinosauromorph fauna known from North America (Fig. 25) with the possible exception of basal neotheropod material from the Nugget Sandstone in Utah, which might be Upper Triassic or Lower Jurassic (*Britt et al., 2010; Britt et al., 2015*). However, unlike the Utah material, the Eagle Basin collection includes lagerpetids and silesaurids, which is therefore the northern-most non-dinosaurian dinosauromorph material in North America. Coelophysoid neotheropods are also known from the Eagle Basin, and will be described in a future publication. Although non-neotheropod theropods such as *Tawa* (*Nesbitt et al., 2009b)*, *Daemonosaurus* (*Sues et al., 2011*) and *Chindesaurus* (*Long & Murry, 1995; Marsh et al., 2016*) have not been identified in the northern Colorado assemblage, much material from the Eagle Basin localities remains to be prepared.

**Size and morphological variation within *Kwanasaurus***

A tentative composite skeleton reconstruction for *Kwanasaurus williamparkeri* is presented in Fig. 24. Composited from multiple elements of different sizes, the reconstruction is based on the highly ambiguous assumption that *Kwanasaurus* was proportioned like *Silesaurus*,

with the scale bars representing the smallest and largest femora in the quarry. This size variation is best illustrated by the femora, the most commonly encountered element (Table A2). The largest preserved femur (DMNH EPV.34579; Fig. 18) is about 18 cm long, while the smallest (DMNH EPV.63139; Fig. 19A-E) is estimated by comparison to have been perhaps 6 cm long.

Assuming that this size variation is largely ontogenetic, qualitative examination of the material shows few obvious morphological changes with ontogeny, although most elements are at least partially damaged and so few approach being complete that little can be said with confidence. It is worth noting that development of the muscle attachments does not seem to be subject to strong variation as occurs in *Asilisaurus* and theropods (*Griffin and Nesbitt, 2016a, b*). In particular, the lesser trochanter in *Kwanasaurus* is a simple, longitudinally oriented process with no trochanteric shelf except for DMNH EPV.125924, where the trochanteric shelf is present but weakly developed.

Interesting differences do occur between the large holotype maxilla (DMNH EPV.65879; Fig. 8A-H) and the smaller referred specimens (DMNH EPV.63650, DMNH EPV.125921, and DMNH EPV.125923; Fig. 8I-P, 9). All maxillae are relatively robust elements compared to other silesaurids, and possess fused dentition and the enormous medial flange characterizing the taxon. However, the smaller specimens do not possess the prominent sutural surfaces for the jugal, lacrimal, and palatine seen in the larger holotype, so these may have developed with increased maturity.

**The distinctiveness of *Kwanasaurus* from other North American silesaurids**

*Kwanasaurus williamparkeri* contributes to our understanding of North America silesaurid diversity. It is the fourth silesaurid alpha taxon named from North America following

*Eucoelophysis baldwini* (*Sullivan & Lucas, 1999; Ezcurra, 2006; Nesbitt, Irmis & Parker, 2007; Breeden et al., 2017*), *Technosaurus smalli* (*Chatterjee, 1984; Nesbitt, Irmis & Parker, 2007; Martz et al., 2013*) and *Soumyasaurus aenigmaticus* (*Sarigül, Agnolin & Chatterjee, 2018*). Assuming that all elements discussed here truly belong to the same taxon, *Kwanasaurus* is currently the most thoroughly described North American silesaurid.

*Kwanasaurus* seems to be distinct from *Eucoelophysis baldwini*. The two taxa share leaf-shaped denticulate teeth and a ventrally placed Meckelian groove, but these occur in other sulcimentisaurians. Perhaps more significantly, both taxa have a pronounced lateral ridge on the dentary, a feature shared with *Diodorus*. However, *Kwanasaurus* possesses character states absent in *Eucoelophysis*: a highly elongate and bladelike preacetabular process of the ilium, a relatively small and slender medial distal condyle of the femur compared to lateral condyle and crista tibiofibularis, and a depression on distal end of the femur anterior to the crista tibiofibularis. Moreover, *Eucoelophysis* autapomorphically lacks a fourth trochanter, which is present in *Kwanasaurus* (*Breeden et al., 2017*).

The taxonomic distinctiveness of *Kwanasaurus* from the holotype and only known specimen of *Technosaurus smalli* is more ambiguous as the latter specimen is currently accepted to include only the dentary and premaxilla (*Nesbitt, Irmis & Parker, 2007; Martz et al., 2013*), which are both poorly preserved; other elements assigned to the taxon by *Chatterjee (1984)* have been re-identified as shuvosaurid and theropod (*Irmis et al., 2007; Nesbitt, Irmis & Parker, 2007*). As the premaxilla is not known in *Kwanasaurus*, this permits only the dentaries to be compared. *Technosaurus* seems to lack the lateral ridge on the dentary shared by *Kwanasaurus*, *Eucoelophysis*, and *Diodorus*, and the dentary teeth of *Technosaurus*, though damaged, appear to

be somewhat more robust than those of *Kwanasaurus*. We therefore tentatively consider *Kwanasaurus* and *Technosaurus* to also be distinct taxa.

*Soumyasaurus aenigmaticus* is known from a single incomplete dentary (*Sarigül, Agnolin & Chatterjee, 2018*). The dentary of *Soumyasaurus* is extremely slender compared to that of *Kwanasaurus*, the anterior part is anteroventrally oriented as in *Asilisaurus* whereas that of *Kwanasaurus* is anterodorsally oriented, and it seems to lack a lateral ridge present in *Kwanasaurus* (*Sarigül, Agnolin & Chatterjee, 2018:figure 5*). Moreover, the tooth crowns of *Soumyasaurus* are small and conical, whereas the crowns of *Kwanasaurus* are broad and denticulate.

**North American silesaurid biochronology**

The age of *Kwanasaurus* relative to the other three western North American taxa is unclear. *Technosaurus* and *Soumyasaurus* are known from the Post Quarry vertebrate assemblage in the lower Cooper Canyon Formation of the Dockum Group in Texas (*Chatterjee, 1984; Martz et al., 2013; Sarigül, Agnolin & Chatterjee, 2018*), which on the basis of lithostratigraphic correlation and the overall nature of the assemblage, probably falls within the later part of the Adamanian estimated holochronozone, with a plausible late Lacian or early Alaunian age between 220-215 Ma (*Martz et al., 2013; Martz & Parker, 2017*). The Hayden Quarry, which lies in the Mesa Montosa Member or lower Petrified Forest of the Chinle Formation (*Lucas et al., 2003; Irmis et al., 2007*), contains silesaurid material assigned to *Eucoelophysis* (*Irmis et al., 2007; Breeden et al., 2017*) that falls within the early part of the Revueltian estimated holochronozone (*Martz & Parker, 2017*), making it slightly younger than the Post Quarry. The Hayden Quarry is very well-constrained geochronologically by a

radiometric date of 211.9 ± 0.7 Ma (*Irmis et al., 2011*), making it late Alaunian in age. The postulated Revueltian age for *Kwanasaurus* suggests that it is at least closer in age to *Eucoelophysis* than to *Technosaurus* and *Soumyasaurus*.

**Silesaurid phylogeny and distribution**

Silesaurids were herbivorous non-dinosaurian dinosauriforms that lived during the Middle and Late Triassic (Ladinian-Norian) and had a cosmopolitan distribution across both the northern and southern regions of Pangea (*Nesbitt et al., 2010; Langer et al., 2013*). They are represented by at least 11 putatively acknowledged alpha taxa, including the four from North American already discussed (Fig. 25).

Given the poor support for relationships within Sulcimentisauria we do not take the consensus topologies within the clade too seriously, although Sulcimentisauria itself is well-supported clade (Appendix 3). Moreover, the broad picture of silesaurid evolution is somewhat geochronologically consistant. *Lewisuchus* and *Pseudolagosuchus* are not only the basal-most silesaurids, but also the oldest known, occurring in the Ladinian (Middle Triassic) Chanares Formation of Argentina (*Bittencourt et al., 2014*). *Asilisaurus kongwe* the sister taxon to Sulcimentisauria in both strict consensus and Adams consensus trees, is only slightly younger, being known from the Anisian (Middle Triassic) of Tanzania (*Nesbitt et al., 2010; Griffin et al., 2016a*). With the exception of *Lutungutali sitwensis*, which is known from the Anisian (Middle Triassic) Ntawere Formation of Zambia (*Peecook et al., 2013*), all other sulcimentisaurians (*Eucoelophysis baldwini*, *Ignotosaurus fragilis*, *Technosaurus smalli*, *Kwanasaurus williamparkeri, Sacisaurus aguodensis*, *Silesaurus opolensis*, and *Diodorus scytobrachion*) are Late Triassic in age (*Dzik, 2003; Irmis et al., 2007; Martz et al., 2013; Langer & Ferigolo,*

*2013; Martinez et al., 2012*). In summary, phylogenetic analyses suggest an Early or Middle Triassic origin for Silesauridae in southern Gondwana, with Sulcimentisauria originating in the Middle Triassic in Gondwana but being a primarily Late Triassic clade that expanded into the northern part of Pangea (Fig. 25B)

**Silesaurid paleoecology**

The origin of herbivorous dinosaurs occurred during the Carnian stage of the Late Triassic and became dominant herbivores during the Norian in the higher latitudes (*Langer et al., 2010*). However, in the lower-mid latitude Norian Chinle/ Dockum beds of the western USA herbivorous dinosaurs were absent (*Nesbitt, Irmis & Parker, 2007*). Instead, other amniotes have been identified as possibly occupying herbivorous or omnivorous niches, including a variety of small archosauromorphs (*Parker et al., 2005; Nesbitt, Irmis & Parker, 2007; Nesbitt et al., 2017, 2017*), shuvosaurids (*Nesbitt, 2007*), aetosaurs (*Desojo et al., 2013*), and dicynodonts (*Camp & Welles, 1956*). Silesaurs can now be considered major herbivores of the Late Triassic in both high latitude 'wet belts' globally and the lower latitude 'dry belts' of the Chinle/Dockum and in other parts of the world (*Langer et al., 2013*). While their remains are scattered throughout the Chinle/Dockum beds, they are generally rare (*Martz et al., 2013; Parker, Irmis & Nesbitt, 2006; Ezcurra, 2006; Nesbitt & Chatterjee, 2008*), except for the Hayden Quarry in New Mexico (*Irmis et al., 2007; Breeden et al., 2017*) and the Eagle Basin (this study) where their remains are locally abundant.

An overview of silesaurid dental diversity suggests that their widespread distribution across Pangea may have been driven, at least in part by their dietary adaptability. *Lewisuchus admixtus* retained the probably plesiomorphic slender jaws and ziphodont dentition of other early

dinosauromorphs and theropods, while *Asilisaurus kongwe*, *Silesaurus opolensis, and* *Soumyasaurus aenigmaticus* had relatively peg-like, almost conical teeth with weakly developed serrations. In contrast, other members of Sulcimentisauria possessed the short and broad folidont teeth (*sensu Hendrickx, Mateus, & Araújo, 2015*) with massive denticles, similar to those of other herbivorous reptiles (*Reisz and Sues, 2000; Barrett, 2000*). The overall picture of silesaurid dental evolution suggests a shift from faunivorous to increasingly herbivorous species throughout the Triassic as ziphodont-toothed taxa were succeeded by taxa with conical teeth in the Middle Triassic, and eventually by sulcimentisaurian taxa with strongly denticulate teeth that radiated across Gondwana in the Late Triassic. These stages may mirror the stages of herbivorous dietary specialization in sauropodomorphs that also occurred during the Late Triassic (*Barrett, Butler & Nesbitt, 2011, p. 386*).

*Kwanasaurus* is suggested here to represent the most extreme adaptations for folivory yet known within Silesauridae. In addition to possessing leaf-shaped denticulate teeth, the maxilla is an extremely short and robust element compared to the more slender maxillae of other silesaurids (Fig. 10), with thick, almost durophagous folidont teeth, and extremely prominent sutural surfaces for contact with the palatine, jugal, and lacrimal on a massive flange unlike anything seen in other silesaurid taxa. The dentary does not seem to have been as massive, but is at least more robust than the extremely slender elements in *Eucoelophysis*, *Sacisaurus,* and *Soumyasaurus* (Fig. 13). These adaptations suggest that *Kwanasaurus* had a relatively powerful bite in which the maxilla was reinforced by strong contacts with other skull elements. The taxon may therefore have been consuming tougher food than most other silesaurids, consistent with the tendency of herbivorous lizards to evolve more compact and powerful skulls to deal with tough, fibrous plant material (*e.g. Metzger & Herrel, 2005*).

1436

1437 **Institutional Abbreviations**

1438 DMNH EPV., Denver Museum of Nature and Science, Denver, Colorado, USA

1439 GR, Ghost Ranch Ruth Hall Museum of Paleontology, Ghost Ranch, New Mexico, USA

1440 MCN PV, Museu de Ciências Naturais, Fundação Zoobotanânica do Rio Grande do Sul, Porto

1441 Alegre, Brazil.

1442 MHNM-ARG, Museum d'Histoire Naturelle de Marrakech (Argana Basin Collection),

1443 Marrakech, Morocco

1444 TMM, Texas Memorial Museum, Austin, Texas, USA

1445 TTU P, Museum of Texas Tech University Paleontology, Lubbock, Texas, USA

1446 ZPAL, Institute of Paleobiology of the Polish Academy of Sciences in Warsaw, Poland.

1447

1448 **Anatomical Abbreviations**

1449 **ac** = acetabulum; **afe** = antorbital fenestra; **afo** = antorbital fossa; **ag** = articular glenoid; **alt** =

1450 anterolateral tuber; **amp** = anteromedial process; **amt** = anteromedial tuber; **an** = angular; **an.ar**

1451 = articulation with the angular; **as.ar** = articular surface for the ascending process of the

1452 astragalus; **asc** = apex of scapula; **asm** = ascending process of the maxilla; **at** = anterior

1453 trochanter; **bf** = brevis fossa; **bs** = brevis shelf; **brk** = broken bone surface; **cc** = cnemial crest;

1454 **cnc** = concavity; **cnv** = convexity; **co.ar** = articulation with the coracoid; **dc** = deltopectoral

1455 crest; **dt** = dorsolateral trochanter; **ec** = ectotuberosity; **ect** = ectepicondyle; **en** = entotuberosity;

1456 **ent** = entepicondye; **ecf** = ectepicondylar flange; **faa** = facies articularis antitrochantera; **fc** =

1457 fibular crest; **fo** = foramen; **ft** = fourth trochanter; **gr** = groove; **ilb** = iliac blade; **isp** = ischial

1458 peduncle; **ju.la.ar** = jugal and lacrimal articulation; **lc** = lateral condyle; **lr** = lateral ridge; **mc** =

medial condyle; **maf** = mandibular fenestra; **mef** = medial flange; **Mk** = Meckelian groove; **mt** = medial tuberosity; **pa.ar** = palatine articulation; **pit** = pit; **pra** = preacetabular process; **poa** = postacetabular process; **plf** = posterolateral flange; **plp** = posterolateral process; **pm.ar** = premaxilla articulation; **pmt** = posteromedial tuber; **pup** = pubic peduncle; **rf** = replacement foramina; **rp** = replacement pits; **rt** = root; **sa.ar** = articular surface for the surangular; **sac #.ar** = articulation for sacral #; **suc** = supracetabular crest; **sul** = sulcus; **sw** = swelling; **sy** = symphysis; **tb** = crista tibiofibularis; **tc** = thin crest; **ve** = ventral emargination; **vn** = ventral notch; **vo.ar** = vomerine flange

## ACKNOWLEDGEMENTS

We thank Bill Parker and Sterling Nesbitt for useful discussions. Randy Irmis, Bill Mueller, and Sterling Nesbitt provided us with photos of *Technosaurus*, *Eucoelophysis*, *Silesaurus*, and *Asilisaurus*. Special thanks to numerous DMNH volunteers who have assisted in the field excavations and preparation of much of the material presented here. Denver Museum of Nature and Science provided access to specimens in their collection. Ben Creisler's linguistic research and advice was invaluable in formulating the taxon names *Kwanasaurus* and Sulcimentisauria. Susan Drymala was invaluable in guiding us through the use of PAUP and Mesquite.

## ADDITIONAL INFORMATION AND DECLARATIONS

### Funding

Financial assistance for field support for this project was provided by the Denver Museum of Nature and Science and Robert and Cyndi Douglass. The funders had no role in study design, data collection, analysis, decision to publish, or preparation of the manuscript.

**Competing Interests**

The authors declare that there are no competing interests.

**Author Contributions**

- Jeffrey W. Martz conceived and designed the experiments, performed the experiments, analyzed the data, contributed reagents/materials/analysis tools, prepared figures, and/or tables, authored or reviewed drafts of the paper, approved the final draft.
- Bryan J. Small conceived and designed the experiments, performed the experiments, analyzed the data, contributed reagents/materials/ analysis tools, authored or reviewed drafts of the paper, approved final draft.

**Field Study Permissions**

Field permits provided and approved by the United States Bureau of Land Management (permit numbers C-49819 and C-49819d).

**Data Availability**

The following information was supplied regarding data availability:

The original data matrix *Peecook et al. (2013)* is available as a Nexus file at Morphobank; our modified data matrix is supplied as a Supplemental Dataset File.

The specimens described in this manuscript are housed in the vertebrate paleontology collections at the Denver Museum of Nature and Science. Catalog numbers appear in Referred Specimen sections and Table 1).

**Supplemental Information**

Supplemental information for this article can be found online at ??????

**REFERENCES**

**Agnolin FL, Rozadilla S. 2017.** Phylogenetic reassessment of *Pisanosaurus mertii* Casamiquela, 1967, a basal dinosauriform from the Late Triassic of Argentina. *Journal of Systematic Palaeontology*, DOI 10.1080/14772019.2017.1352623.

**Araújo R, Castanhinha R, Mateus O. 2011.** Evolutionary major trends of ornithopod dinosaur teeth. In: Calvo JD, Porfiri JD, González BJ, & Dos Santos D, eds. *Dinosaurios y Paleontología desde América Latina. EDIUNC, Editorial de la Universidad Nacional de Cuyo, Mendoza, Argentina*, 25–31.

**Arcucci AB. 1986.** Nuevos materiales y reinterpretacion de *Lagerpeton chanarensis* Romer (Thecodontia, Lagerpetonidae nov.) del Triásico medio de La Rioja, Argentina. *Ameghiniana* **23**:233–242.

**Bachmann GH, Kozur HW. 2004.** The Germanic Triassic: correlations with the international chronostratigraphic scale, numerical ages and Milankovich cyclicity. *Hallesches Jahrbuch für Geowissenschaften, B* **26**:17–62.

1525 **Barrett P, 2000**. Prosauropod dinosaurs and iguanas: speculations on the diets of extinct reptiles.
1526 In: Sues, H-D, ed. *Evolution of Herbivory in Terrestrial Vertebrates, Cambridge*
1527 *University Press*, 42–78.
1528 **Barrett PM, Butler RJ, Nesbitt SJ. 2011.** The role of herbivory and omnivory in early dinosaur
1529 evolution. *Earth and Environmental Science Transactions of the Royal Society of*
1530 *Edinburgh* **101**:383–396. DOI 10.1017/S1755691011020111.
1531 **Bell CJ, Gauthier JA, Bever GS. 2010.** Covert biases, circularity, and apomorphies: A critical
1532 look at the North American Quaternary Herpetofaunal Stability Hypothesis. *Quaternary*
1533 *International* **217**:30–36. DOI 10.1016/j.quaint.2009.08.009.
1534 **Benton MJ. 1985.** Classification and phylogeny of the diapsid reptiles. *Zoological Journal of the*
1535 *Linnean Society* **84**:97–164. DOI 10.1111/j.1096-3642.1985.tb01796.x.
1536 **Bever GS. 2005.** Variation in the ilium of North American *Bufo* (Lissamphibia: Anura) and its
1537 implication for species-level identification of fragmentary anuran fossils. *Journal of*
1538 *Vertebrate Paleontology* **25**:548–560.
1539 DOI 10.1617/0272-4634(2005)025[0548:VITION]2.0.CO;2.
1540 **Bittencourt JS, Arcucci AB, Mariscano CA, Langer MC. 2014.** Osteology of the Middle
1541 Triassic archosaur *Lewisuchus admixtus* Romer (Chañares Formation, Argentina), and its
1542 inclusivity, and relationships amongst early dinosauromorphs. *Journal of Systematic*
1543 *Palaeontology,* DOI 10.1080/14772019.2013.878758.
1544 **Blakey RC, Gubitosa R. 1983.** Late Triassic paleogeography and depositional history of the
1545 Chinle Formation, southern Utah and northern Arizona. In: Reynolds MW, Dolly ED,
1546 eds. *Mesozoic Paleogeography of West-Central United States, Rocky Mountain Section,*
1547 *S.E.P.M.*, 57–75.

1548 **Bonaparte JF. 1975.** Nuevos materials de *Lagosuchus talampayensis* Romer (Thecodontia-
1549 Pseudosuchia) y su significado en el origen de los Saurischia. Chañarense Inferior,
1550 Triasico Medio de Argentina. *Acta Geologica Lilloana* **13(1)**:5–90.
1551 **Breeden BT, Irmis R, Nesbitt SJ, Smith ND, Turner AH. 2017.** New silesaurid (Archosauria:
1552 Dinosauriformes) specimens from the Upper Triassic Chinle Formation of New Mexico
1553 and phylogenetic relationships of *Eucoelophysis baldwini*. *Journal of Vertebrate*
1554 *Paleontology*, Programs and Abstracts, 2017, 86.
1555 **Britt BB, Chure D, Engelmann G, Scheetz R, Hansen R. 2010.** Multi-taxic theropod bonebeds
1556 in an interdunal setting of the Early Jurassic eolian Nugget Sandstone, Utah. *Journal of*
1557 *Vertebrate Paleontology*, Programs and Abstracts, 2010, 65A.
1558 **Britt BB, Chure D, Engelmann G, Dalla Vecchia F, Scheetz RD, Meek S, Thelin C,**
1559 **Chambers M. 2015.** A new, large, non-pterodactyloid pterosaur from a Late Triassic
1560 interdunal desert environment within the eolian Nugget Sandstone of northeastern Utah,
1561 USA indicates early pterosaurs were ecologically diverse and geographically widespread.
1562 *Journal of Vertebrate Paleontology*, Programs and Abstracts, 2015, 97A.
1563 **Cabreira SF, Kellner AWA, Dias-da-Silva S, Silva LR, Bronzati M, Marsola JCA, Müller**
1564 **RT, Bittencourt JS, Batista BJ, Raugust T, Carrilho R, Brodt A, Langer MC. 2016.**
1565 A unique Late Triassic dinosauromorph assemblage reveals dinosaur ancestral anatomy
1566 and diet. *Current Biology* **26**:1–6. DOI 10.1016/j.cub.2016.09.040.
1567 **Camp CL, Welles SP. 1956.** Triassic dicynodont reptiles. Part I. The North American genus
1568 *Placerias*. *Memoirs of the University of California* **13**:255–341.

1569 **Carpenter K. 1997.** A giant coelophysoid (Ceratosauria) theropod from the Upper Triassic of
1570 New Mexico, USA. *Neues Jahrbuch für Geologie und Paläontologie Abhandlungen*
1571 **205(2)**:189–208.
1572 **Chatterjee S. 1974.** A rhynchosaur from the Upper Triassic Maleri Formation of India.
1573 *Philosophical Transactions of the Royal Society of London. Series B, Biological Sciences*
1574 **267**:209–261.
1575 **Chatterjee S. 1984.** A new ornithischian dinosaur from the Triassic of North America.
1576 *Naturwissenschaften* **71**: 630–631.
1577 **Colbert EH. 1981.** A primitive ornithischian dinosaur from the Kayenta Formation of Arizona.
1578 *Museum of Northern Arizona Bulletin* **53**:1–61.
1579 **Colbert EH. 1989.** The Triassic dinosaur *Coelophysis*. *Museum of Northern Arizona Bulletin*
1580 **57**:1–160.
1581 **Desojo JB, Heckert AB, Martz JW, Parker WG, Schoch RR, Small BJ, Sulej T. 2013.**
1582 Aetosauria: a clade of armored pseudosuchians from the Upper Triassic continental beds.
1583 In: Nesbitt SJ, Desojo JB, Irmis RB, eds. *Anatomy, Phylogeny, and Palaeobiology of*
1584 *Early Archosaurs and their Kin,* Geological Society, London, Special Publications **379**,
1585 203–239. DOI 10.1144/SP379.17.
1586 **Daudin FM. 1802.** Histoire Naturelle Générale et Particuliére des Reptiles. Volume 2. Dufart,
1587 Paris.
1588 **Dubiel RF. 1992.** Sedimentology and depositional history of the Upper Triassic Chinle
1589 Formation in the Uinta, Piceance, and Eagle Basins, northwestern Colorado and
1590 northeastern Utah. *U.S. Geological Survey Bulletin* **1787**: 25p.

1591 **Dubiel RF. 1994.** Triassic deposystems, paleogeography, and paleoclimate of the western
1592 interior. In: Caputo MV, Peterson JA, Franczyk KJ, eds. *Mesozoic Systems of the Rocky*
1593 *Mountain Region, USA*. SEPM. 133–168.
1594 **Dubiel RF, Skipp G. 1989.** Stratigraphic and sedimentologic studies of the Upper Triassic
1595 Chinle Formation, western Colorado. *U.S. Geological Survey Open-File Report* **89-2**:26
1596 p.
1597 **Dzik J. 2003.** A beaked herbivorous archosaur with dinosaur affinities from the early Late
1598 Triassic of Poland. *Journal of Vertebrate Paleontology* **23**:556–574.
1599 DOI 10.1671/A1097.
1600 **Edmund AG. 1960.** Tooth replacement phenomena in the lower vertebrates. *Royal Ontario*
1601 *Museum, Life Sciences Division*, *contribution* **52**:1–190.
1602 **Edmund AG. 1969.** Dentition. In: Gans C, Bellairs DA, Parsons TS, eds. *Biology of the*
1603 *Reptilia, vol. 1.* Academic Press, London, 117–200.
1604 **Ezcurra MD. 2006.** A review of the systematic position of the dinosauriform archosaur
1605 *Eucoelophysis baldwini* Sullivan & Lucas, 1999 from the Upper Triassic of New Mexico,
1606 USA. *Geodiversitas* **28(4)**:649–684.
1607 **Ferigolo J, Langer MC. 2007.** A Late Triassic dinosauriform from south Brazil and the origin
1608 of the ornithischian predentary bone. *Historical Biology* **19**:23–33.
1609 DOI 10.1080/08912960600845767.
1610 **Garcia MS, Müller RT, Da-Rosa AAS, Dias-da-Silva S. 2018**. The oldest known co-
1611 occurrence of dinosaurs and their closest relatives: A new lagerpetid from a Carnian
1612 (Upper Triassic) bed of Brazil with implications for dinosauromorph biostratigraphy,

1613 early diversification and biogeography. *Journal of South American Earth Sciences*
1614 **91**:302–319. DOI 10.1016/j.jsames.2019.02.005.
1615 **Griffin CT, Nesbitt SJ. 2016a.** The femoral ontogeny and long bone histology of the Middle
1616 Triassic (?late Anisian) dinosauriform *Asilisaurus kongwe* and implications for the
1617 growth of early dinosaurs. *Journal of Vertebrate Paleontology* **36(3)**:e1111224
1618 DOI 10.1080/02724634.2016.1111224.
1619 **Griffin CT, Nesbitt SJ. 2016b.** Anomalously high postnatal development is ancestral for
1620 dinosaurs but lost in birds. *Proceedings of the National Academy of Sciences* **113(51)**:
1621 14757–14762. DOI 10.1073/pnas.1613813113.
1622 **Heckert AB. 2002.** A revision of Upper Triassic ornithischian dinosaur *Revueltosaurus*, with a
1623 description of a new species. In: Heckert, AB, Lucas SG, eds. *Upper Triassic*
1624 *Stratigraphy and Paleontology,* New Mexico Museum of Natural History and Science
1625 Bulletin **21**:253–268.
1626 **Heckert AB, Lucas SG. 2000.** Taxonomy, phylogeny, biostratigraphy, biochronology,
1627 paleobiogeography, and evolution of the Late Triassic Aetosauria (Archosauria:
1628 Crurotarsi). *Zentralblatt für Geologie und Paläontologie* Teil I 1998, Heft **11-12**:1539–
1629 1587.
1630 **Heckert AB, Lucas SG, Hunt AP, Spielmann JA. 2007.** Late Triassic aetosaur biochronology
1631 revisited. In: Lucas SG, Spielmann JA, eds. *The Global Triassic*. New Mexico Museum
1632 of Natural History and Science **41**, 49–50.
1633 **Hendrickx C, Mateus O, and Araújo R. 2015.** A proposed terminology of theropod teeth
1634 (Dinosauria, Saurischia). *Journal of Vertebrate Paleontology* **35(5)**: e982797-1-18.
1635 DOI 10.1080/02724634.2015.982797.

1636 **Hunt AP, Lucas SG. 1994.** Ornithischian dinosaurs from the Upper Triassic of the United
1637 States. In: Fraser NC, Sues H-D, eds. *In the shadow of the Dinosaurs: early Mesozoic*
1638 *tetrapods*. Cambridge University Press, Cambridge, 225–241.
1639 **Irmis RB, Nesbitt SJ, Padian K, Smith ND, Turner AH, Woody D, Downs A. 2007.** A Late
1640 Triassic dinosauromorph assemblage from New Mexico and the rise of dinosaurs.
1641 *Science* **317**:358–361. DOI 10.1126/science.1143325.
1642 **Irmis RB, Mundil R, Martz JW, Parker WG. 2011.** High-resolution U-Pb ages from the
1643 Upper Triassic Chinle Formation (New Mexico, USA) supports a diachronous rise of
1644 dinosaurs. *Earth and Planetary Science Letters* **309**:258–267.
1645 DOI 10.1016/j.epsl.2011.07.015.
1646 **Kammerer CF, Nesbitt SJ, Shubin NH. 2012.** The first basal dinosauriform (Silesauridae)
1647 from the Late Triassic of Morocco. *Acta Palaeontologica Polonica* **57(2)**:277–284.
1648 DOI 10.4202/app.2011.0015.
1649 **Langer MC, Benton MJ. 2006.** Early dinosaurs: A phylogenetic study. *Journal of Systematic*
1650 *Palaeontology* **4(4)**:309–358. DOI 10.1017/S1477201906001970.
1651 **Langer MC, Ferigolo J. 2013.** The Late Triassic dinosauromorph *Sacisaurus agudoensis*
1652 (Caturrita Formation; Rio Grande do Sul, Brazil): anatomy and affinities. In: Nesbitt SJ,
1653 Desojo JB, Irmis, RB, eds. *Anatomy Phylogeny, and Palaeobiology of Early Archosaurs*
1654 *and their Kin*: Geological Society, London, Special Publications **379**.
1655 DOI 10.1144/SP379.16.
1656 **Langer MC, Ezcurra MD, Bittencourt JS, Novas FE. 2010.** The origin and early evolution of
1657 dinosaurs. *Biological Reviews* **85**:55–110. DOI 10.1111/j.1469-185X.2009.00094.x.

**Langer MC, Bittencourt JS, Schultz CL. 2011.** A reassessment of the basal dinosaur *Guaibasaurus candelariensis*, from the Late Triassic Caturrita Formation of south Brazil. *Earth and Environmental Science Transactions of the Royal Society of Edinburgh* **101**:301–332. DOI 10.1017/S175569101102007X.**Langer MC, Nesbitt SJ, Bittencourt JS, Irmis RB. 2013.** Non-dinosaurian Dinosauromorpha. In: Nesbitt SJ, Desojo JB, Irmis RB, eds. *Anatomy, Phylogeny and Palaeobiology of early Archosaurs and their Kin*. Geological Society of London, Special Publications **379**, DOI 10.1144/SP379.9.

**Linnaeus C. 1758.** *Systema Naturae per regna tria naturae, secundum classes, ordines, genera, species, cum chararteribus, differentiis, synonymis, locis*. Tomus 1. Editio decima, reformata. Laurentius Salvius, Stockholm. 824 pp.

**Long RA, Murry PA. 1995.** Late Triassic (Carnian and Norian) tetrapods from the southwestern United States. *Bulletin of the New Mexico Museum of Natural History and Science* **4**:1–254.

**Lucas SG. 1993.** The Chinle Group: Revised stratigraphy and biochronology of Upper Triassic nonmarine strata in the western United States. In: Morales M, ed. *Aspects of Mesozoic Geology and Paleontology of the Colorado Plateau*. Museum of Northern Arizona Bulletin **59**:27–50.

**Lucas SG. 1998.** Global Triassic tetrapod biostratigraphy and biochronology. *Palaeogeography, Palaeoclimatology, Palaeoecology* **143**:347–384.

**Lucas SG, Hunt AP, Long RA. 1992.** The oldest dinosaurs. Naturwissenschaften **79**:171–172.

**Lucas SG, Hunt AP, Spielmann, JA. 2006**. *Rioarribasuchus*, a new name for an aetosaur from the Upper Triassic of north-central New Mexico. In: Harris JD, Lucas SG, Spielmann JA, Lockley MG, Milner ARC, Kirkland, JI, eds. *The Triassic-Jurassic Terrestrial*

*Transition, New Mexico Museum of Natural History and Science Bulletin*. 37. Albuquerque: New Mexico Museum of Natural History and Science, 581–582.

**Lucas SG, Zeigler KE, Heckert AB, Hunt AB. 2003.** Upper Triassic stratigraphy and biostratigraphy, Chama Basin, north-central New Mexico. *New Mexico Museum of Natural History and Science Bulletin* **24**:15–39.

**Marsh A. 2018.** A new record of *Dromomeron romeri* Irmis et al., 2007 (Lagerpetidae) from the Chinle Formation of Arizona, U.S.A. PaleoBios **45**:1–8.

**Marsh AD, Parker WG, Langer MC, Nesbitt SJ. 2016.** An anatomical and phylogenetic revision of *Chindesaurus bryansmalli* from Petrified Forest National Park and its implication for the Late Triassic dinosaurian record of North America. *Journal of Vertebrate Paleontology*, Program and Abstracts, 2016, 184.

**Marsh OC. 1889.** Notice of gigantic horned Dinosauria from the Cretaceous. *American Journal of Science* **38(3)**:173–175.

**Martinez RN, Sereno PC, Alcober OA, Colombi CE, Renne PR, Montañez IP, Currie BS. 2011.** A basal dinosaur from the dawn of the dinosaur era in southwestern Pangaea. *Science* **331**:206–210. DOI 10.1126/science.1198467.

**Martinez RN, Apaldetti C, Alcober OA, Colombi CE, Sereno PC, Fernandez E, Santi Malnis P, Correa GA, Abelin D. 2012.** Vertebrate succession in the Ischigualasto Formation. *Journal of Vertebrate Paleontology* **32**:sup 1, 10-30. DOI 10.1080/02724634.20134.818546.

**Martinez RN, Apaldetti C, Correa GA, Abelín D. 2015.** A Norian lagerpetid dinosauromorph from the Quebrada del Barro Formation, northwestern Argentina. *Ameghiniana* **53**:1–13. DOI 10.5710.AMGH.21.06.2015.2894.

1704 **Martz JW. 2008.** Lithostratigraphy, chemostratigraphy, and vertebrate biostratigraphy of the
1705 Dockum Group (Upper Triassic), of southern Garza County, west Texas. Ph.D.
1706 Dissertation Texas Tech University, Lubbock, TX. 504p.
1707 **Martz JW, Small BJ. 2016.** A new silesaurid (Dinosauriformes) allied to *Diodorus* from the
1708 Chinle Formation of northern Colorado, and its significance to Late Triassic
1709 dinosauromorph paleobiogeography. *Journal of Vertebrate Paleontology*, Program and
1710 Abstracts 2016, 184.
1711 **Martz JW, Parker WG. 2017.** Revised formulation of the Late Triassic land vertebrate
1712 "faunachrons" of western North America: recommendations for codifying nascent
1713 systems of vertebrate biochronology. In: Zeigler KE, Parker WG, eds. *Terrestrial*
1714 *Depositional Systems*. Elsevier, 39–125. DOI 10.1016/B978-0-12-803243-5.00002-9.
1715 **Martz JW, Mueller B, Small BJ. 2003.** Two new aetosaurs (Archosauria, Stagonolepididae)
1716 from the Upper Triassic of Texas and Colorado, and problems in aetosaur identification
1717 and taxonomy. *Journal of Vertebrate Paleontology* **23(3)**:76A.
1718 **Martz JW, Mueller B, Nesbitt SJ, Stocker MR, Parker WG, Atanassov M, Fraser N,**
1719 **Weinbaum J, Lehane JR. 2013**. A taxonomic and biostratigraphic re-evaluation of the
1720 Post Quarry vertebrate assemblage from the Cooper Canyon Formation (Dockum Group,
1721 Upper Triassic) of southern Garza County, western Texas. *Earth and Environmental*
1722 *Science Transactions of the Royal Society of Edinburgh* **103(3-4)**:339–364.
1723 DOI 10.1017/S1013000376.
1724 **Martz JW, Kirkland JI, Milner ARC, Parker WG, Santucci VL. 2017**. Upper Triassic
1725 lithostratigraphy, depositional systems, and vertebrate paleontology across southern Utah.
1726 *Geology of the Intermountain West* **4**:99–180.

1727 **Metzger KA, Herrel A. 2005**. Correlations between lizard cranial shape and diet: a quantitative,
1728 phylogenetically informed analysis. *Biological Journal of the Linnean Society* **86(4)**:433–
1729 466.
1730 **Müller RT, Langer MC, Dias-da-Silva S. 2018.** Ingroup relationships of Lagerpetidae
1731 (Avemetatarsalia: Dinosauromorpha): a further phylogenetic investigation on the
1732 understanding of dinosaur relatives. *Zootaxa* **4392(1)**:149–158.
1733 DOI 10.11646/zootaxa.4392.1.7.
1734 **Nesbitt SJ. 2005.** Osteology of the Middle Triassic pseudosuchian archosaur *Arizonasaurus*
1735 *babbitti*. *Historical Biology* **17**:19–47. DOI 10.1080/08912960500476499.
1736 **Nesbitt S. 2007**. The anatomy of *Effigia okeeffeae* (Archosauria, Suchia), theropod-like
1737 convergence, and the distribution of related taxa. *Bulletin of the American Museum of*
1738 *Natural History* **302**:1–84. DOI 10.1206/0003-0090(2007)302[1:TAOEOA]2.0.CO:2.
1739 **Nesbitt SJ. 2011**. The early evolution of archosaurs: relationships and the origin of a major
1740 clade. *Bulletin of the American Museum of Natural History* **352**:1–292.
1741 DOI 10.1206/352.1.
1742 **Nesbitt SJ, Stocker MR. 2008**. The vertebrate assemblage of the Late Triassic Canjilon Quarry
1743 (northern New Mexico, USA), and the importance of apomorphy-based assemblage
1744 comparisons. *Journal of Vertebrate Paleontology* **28(4)**:1063–1072.
1745 DOI 10.1671/0272-4634-28.4.1063.
1746 **Nesbitt SJ, Chatterjee S. 2008**. Late Triassic dinosauriforms from the Post Quarry and
1747 surrounding areas, west Texas, U.S.A. *Neues Jahrbuch für Geologie und Paläontologie*
1748 *Abhandlungen* **249(2)**:143–156. DOI 10.1127/0077-7749/2008/0249-0143.

1749 **Nesbitt SJ, Irmis RB, Parker W.G. 2007**. A critical reevaluation of the Late Triassic dinosaur
1750 taxa of North America. *Journal of Systematic Palaeontology* **5(2)**:209–243.
1751 DOI 10.1017/S1477201907002040.
1752 **Nesbitt SJ, Irmis RB, Parker WG, Smith ND, Turner A.H, Rowe T**. **2009a**. Hindlimb
1753 osteology and distribution of basal dinosauromorphs from the Late Triassic of North
1754 America. *Journal of Vertebrate Paleontology* **29(2)**:498–516.
1755 DOI 10.1617/039.029.0218.
1756 **Nesbitt SJ, Smith ND, Irmis RB, Turner AH, Downs A, Norell MA. 2009b**. A complete
1757 skeleton of a Late Triassic saurischian and the early evolution of dinosaurs. *Science*
1758 **326**:1530–1533. DOI 10.1126/science.1180350.
1759 **Nesbitt SJ, Sidor CA, Irmis RB, Angielczyk KD, Smith RMH, Tsuji LA. 2010**. Ecologically
1760 distinct dinosaurian sister group shows early diversification of Ornithodira. *Nature* **464**
1761 **(4)**:95–98. DOI 10.1038/nature08718.
1762 **Nesbitt SJ, Stocker MR, Ezcurra M, Fraser NC, Heckert AB, Marsh A, Parker, W,**
1763 **Mueller B, Pritchard AC. 2017**. The “strange reptiles” of the Triassic: the morphology,
1764 ecology, and taxonomic diversity of the clade Allokotosauria illuminated by the
1765 discovery of an early diverging member. *Journal of Vertebrate Paleontology*, Programs
1766 and Abstracts, 2017, 168.
1767 **Novas FE. 1992**. Phylogenetic relationships of the basal dinosaurs, the Herrerasauridae.
1768 *Palaeontology* **35(1)**:51–62.
1769 **Novas FE. 1994**. New information on the systematic and postcranial skeleton of *Herrerasaurus*
1770 *ischigualastensis* (Theropoda: Herrerasauridae) from the Ischigaulasto Formation (Upper
1771 Triassic) of Argentina. *Journal of Vertebrate Paleontology* **13**:400–423.

DOI 10.1080/02724634.1994.10011523.

**Novas FE. 1996**. Dinosaur monophyly. *Journal of Vertebrate Paleontology* **16(4)**:723–741. DOI 10.1080/02724634.1996.10011361.

**Padian K, May CL. 1993**. The earliest dinosaurs. *New Mexico Museum of Natural History and Science Bulletin* **3**:379–381.

**Pardo JD, Small BJ, Huttenlocker AK. 2017**. Stem caecilian from the Triassic of Colorado sheds light on the origins of Lissamphibia. *Proceedings of the National Academy of Sciences* 2017 **114(27)**: E5389-E5395. DOI 10.1073/pnas.1706752114.

**Parker WG, Irmis RB, Nesbitt SJ, Martz JW, Browne LS. 2005**. The Late Triassic pseudosuchian *Revueltosaurus callenderi* and its implications for the diversity of early ornithischian dinosaurs. *Proceedings of the Royal Society of London, Biological Science* **272**:963–969. DOI 10.1098/rspb.2004.3047.

**Parker WG, Irmis RB, Nesbitt SJ. 2006**. Review of the Late Triassic dinosaur record from Petrified Forest National Park, Arizona. In: Parker WG, Irmis RB, eds. *A Century of Research at Petrified Forest National Park:* G*eology and Paleontology.* Museum of Northern Arizona Bulletin **62**, 160–161.

**Peecook BR, Sidor SA, Nesbitt SJ, Smith RMH, Steyer JS, Angielczyk KD. 2013**. A new silesaurid from the upper Ntawere Formation of Zambia (Middle Triassic) demonstrates the rapid diversification of Silesauridae (Avametatarsalia, Dinosauriformes). *Journal of Vertebrate Paleontology* **33(5)**:1127–1137. DOI 10.1080/02724634.2013.755991.

**Piechowski R, Tałanda M, Dzik J. 2014**. Skeletal variation and ontogeny of the Late Triassic dinosauriform *Silesaurus opolensis*. *Journal of Vertebrate Paleontology* **34(6)**:1383–1393. DOI 10.1080/0272434.2014.873045.

1795 **Poole FG, Stewart JH. 1964**. Chinle Formation and Glen Canyon Sandstone in northeastern
1796 Utah and northwestern Colorado. *United States Geological Survey Professional Paper*
1797 **501-D**:D30–D39.
1798 **Prieto-Marquez A, Norell MA. 2011**. Redescription of a nearly complete skull of *Plateosaurus*
1799 (Dinosauria: Sauropodomorpha) from the Late Triassic of Trossingen (Germany).
1800 *American Museum Novitates* **3727**:1–58. DOI 10.1206/3727.2.
1801 **Reisz RR, Sues H-D. 2000**. Herbivory in late Paleozoic and Triassic terrestrial vertebrates. In:
1802 Sues H-D, ed. *Evolution of Herbivory in Terrestrial Vertebrates, Cambridge University*
1803 *Press,* 9–41.
1804 **Rowe T. 1989**. A new species of the theropod dinosaur *Syntarsus* from the Early Jurassic
1805 Kayenta Formation of Arizona. *Journal of Vertebrate Paleontology* **9(2)**:125–136.
1806 DOI 10.1080/02724634.1989.10011745.
1807 **Sarigül V. 2016**. New basal dinosauromorph records from the Dockum group of Texas, USA.
1808 *Palaeontologia Electronica* **19.2.21A**:1–16.
1809 **Sarigül V, Agnolin F, Chatterjee S. 2018**. Description of a multitaxic bone assemblage from
1810 the Upper Triassic Post Quarry of Texas (Dockum Group), including a new small basal
1811 dinosauriform taxon. *Historia Natural* **8**:5–24.
1812 **Sereno PC. 1991**. Basal archosaurs: phylogenetic relationships and functional implications.
1813 *Society of Vertebrate Paleontology Memoir***2**:1–53. DOI 10.2307/3889336.
1814 **Sereno PC. 1994**. The pectoral girdle and forelimb of the basal theropod *Herrerasaurus*
1815 *ischigualastensis*. *Journal of Vertebrate Paleontology* **13**:425–450.
1816 DOI 10.1080/02724634.1994.10011524.

**Sereno PC, Arcucci AB. 1994a**. Dinosaurian precursors from the Middle Triassic of Argentina: *Lagerpeton chanarensis*. *Journal of Vertebrate Paleontology* **13**:385–399. DOI 10.1080/02724634.1994.10011522.

**Sereno PC, Arcucci AB. 1994b**. Dinosaurian precursors from the Middle Triassic of Argentina: *Marasuchus lilloensis*, Gen. Nov. *Journal of Vertebrate Paleontology* **14(1)**:53–73. DOI 10.1080/02724634.1994.10011538.

**Small BJ. 1997**. A new procolophonid from the Upper Triassic of Texas, with a description of tooth replacement and implantation. *Journal of Vertebrate Paleontology* **17(4)**:674–678. DOI 10.1080/02724634.1997.10011016.

**Small BJ. 2001**. Geology and paleontology of the Main Elk Creek Locality (Late Triassic: Norian), Colorado. *Journal of Vertebrate Paleontology* **21**:102A.

**Small BJ. 2002**. Cranial anatomy of *Desmatosuchus haplocerus* (Reptilia: Archosauria: Stagonolepididae). *Zoological Journal of the Linnean Society* **136**:97–111.

**Small B. 2009**. A Late Triassic dinosauromorph assemblage from the Eagle Basin (Chinle Formation), Colorado, U.S.A. *Journal of Vertebrate Paleontology* **29(3)**:182A.

**Small BJ, Sedlmayr JC. 1995**. Late Triassic tetrapods from Colorado. *Journal of Vertebrate Paleontology* **15**:54A.

**Small BJ, Martz JW. 2013**. A new basal aetosaur from the Upper Triassic Chinle Formation of the Eagle Basin, Colorado, USA. In: Nesbitt SJ, Desojo JB, Irmis RB, eds. *Anatomy, Phylogeny and Palaeobiology of Early Archosaurs and their Kin*. Geological Society of London, Special Publications **379**:393–412. DOI 10.1144/SP379.18.

1838 **Stewart JH, Poole FG, Wilson RF. 1972**. Stratigraphy and origin of the Upper Triassic Chinle
1839 Formation and related strata in the Colorado Plateau region. *U.S. Geological Survey*
1840 *Professional Paper* **690**:336p.
1841 **Sues H-D. 2000**. Herbivory in terrestrial vertebrates: an introduction. In: Sues, H-D, ed.
1842 *Evolution of Herbivory in Terrestrial Vertebrates, Cambridge University Press*, 1–8.
1843 **Sues H-D, Nesbitt SJ, Berman DS, Henrici AC. 2011**. A late surviving basal theropod
1844 dinosaur from the latest Triassic of North America. *Proceedings of the Royal Society B.*
1845 DOI 10.1098/rspb.2011.0411.
1846 **Sullivan RM, Lucas SG. 1999**. *Eucoelophysis baldwini*, a new theropod dinosaur from the
1847 Upper Triassic of New Mexico, and the status of the original types of *Coelophysis*.
1848 *Journal of Vertebrate Paleontology* **19(1)**:81–90.
1849 DOI 10.1080/02724634.1999.10011124.
1850 **Tykowski RS. 2005**. Anatomy, ontogeny, and phylogeny of coelophysoid theropods. Ph.D.
1851 Dissertation, University of Texas, Austin. 553p.
1852 **Walker AD. 1964**. Triassic reptiles from the Elgin area: *Ornithosuchus* and the origin of
1853 carnosaurs. *Philosophical Transactions of the Royal Society of London, B* **248**:53–134.
1854 **Welles SP. 1984**. *Dilophosaurus wetherilli* (Dinosauria, Theropoda) osteology and comparisons.
1855 *Palaeontographica* **185A**:85–180.
1856 **Whitlock JA, Richman JM. 2013**. Biology of tooth replacement in amniotes. *International*
1857 *Journal of Oral Science* **5**:66–70.
1858 **Wild R. 1989**. *Aetosaurus* (Reptilia: Thecodontia) from the Upper Triassic (Norian) of Cene
1859 near Bergamo, Italy, with a revision of the genus. *Revista del Museo Civico di Scienze*
1860 *Naturali 'Enrico Caffi'* **14**:1–24.

**Woerdeman MW. 1921**. Beitrage zur Entwicklungsgeschichte von Zähnen und Gebiss der Reptilien. *Beitrage IV: Ueber die Anlage des Ersatzgebiss. Arch. Mikr. Anat.,* Abt. 1, vol. **95**:265–395.

1864 **Figure 1: Chinle Formation exposures in the Eagle Basin of northern Colorado**. (A) Map of
1865 Colorado showing approximate location of localities. (B) Stratigraphic section of the
1866 Chinle Formation showing approximate stratigraphic interval of dinosauromorph
1867 localities (modified from Derby Junction section of Dubiel, 1992:fig. 4). (C) Exposures
1868 of the red siltstone member along the Colorado River north of I-70 at 13S 033415
1869 4412881 NAD 27 showing the approximate division between the coarser facies similar to
1870 the Petrified Forest Member and the finer-grained facies similar to the Owl Rock
1871 Member. (D) Bone preserved in fine-grained silty to very fine-grained sandstone. (E)
1872 Intrabasinal conglomerate beds that have produced the bulk of the specimens.
1873
1874 **Figure 2: *Dromomeron romeri* voucher specimen (DMNH EPV.54826), proximal left femur,**
1875 **stereopairs and interpretive drawings.** (A) Proximal view. (B) Anterolateral view. (C)
1876 Anteromedial view. (D) Posteromedial view. (E) Posterolateral view. See text for
1877 abbreviations. Scale bar = 2 cm.
1878
1879 **Figure 3: *Dromomeron romeri* (DMNH EPV. 63873), proximal right femur, labeled**
1880 **steropairs. (**A) Anterolateral view. (B) Anteromedial view. (C) Posteromedial view. (D)
1881 Posterolateral view. See text for abbreviations. Scale bar = 1 cm.
1882
1883 **Figure 4: *Dromomeron romeri* (DMNH EPV.29956), right humerus, labeled stereopairs.** (A)
1884 proximal view. (B) Anterior view. (C) Medial view. (D) Posterior view. (E) Lateral view.
1885 (F) Proximal view showing angle of torsion between long axes of proximal and distal

ends, gray lines represent the long axes of the proximal and distal ends. See text for abbreviations. Scale bar = 2 cm.

**Figure 5: Dinosauriformes (DMNH EPV.67956), right scapula, labeled stereopairs.** (A) Anterior view. (B) Medial view. (C) Posterior view. (D) Lateral view. (E) Ventral view. Missing areas outlined with dots. See text for abbreviations. Scale bar = 2 cm.

**Figure 6: Dinosauriformes (DMNH EPV.63875), right tibia, labeled stereopairs.** (A) Proximal view. (B) Anterior view. (C) Medial view. (D) Posterior view. (E) Lateral view. (F) Distal view. See text for abbreviations. Scale bar = 2 cm.

**Figure 7: Dinosauriformes tibiae. (**A) DMNH EPV.56652, worn proximal tibia in lateral view. DMNH EPV.67955, proximal end of right tibia in (B) proximal view, (C) anterior view, (D) medial view, (E) posterior view, (F) lateral view. DMNH EPV.67955, proximal left tibia stereopairs in (G) proximal view, (H) anterior view, (I) medial view, (J) posterior view, (K) lateral view. See text for abbreviations. Scale bar = 2 cm.

**Figure 8: *Kwanasaurus williamparkeri* maxillae.** (A) Holotype (DMNH EPV.65879) left maxilla stereopairs of lateral view, (B) interpretive drawing of same, (C) stereopairs of medial view, (D) interpretive drawing of same, (E) stereopairs of dorsal view, (F) interpretive drawing of same, (G) stereopairs of ventral view, (H) interpretive drawing of same. (I) DMNH EPV.63650, right maxilla stereopairs of lateral view, (J) interpretive drawing of same, (K) stereopairs of medial view, (L) interpretive drawing of same, (M)

1909 stereopairs of dorsal view, (N) interpretive drawing of same, (O) stereopairs of ventral
1910 view, (P) interpretive drawing of same. Hatching indicates broken bone surface, dotted
1911 lines indicate broken bone edge. Dark gray areas filled with matrix. See text for
1912 abbreviations. Scale bars = 2 cm.
1913
1914 **Figure 9: *Kwanasaurus williamparkeri* maxillae.** (A) DMNH EPV.125921, left maxilla
1915 stereopairs of lateral view, (B) interpretive drawing of same, (C) stereopairs of medial
1916 view, (D) interpretive drawing of same, (E) stereopairs of dorsal view, (F) interpretive
1917 drawing of same, (G) stereopairs of ventral view, (H) interpretive drawing of same. (I)
1918 DMNH EPV.125923, right maxilla stereopairs of lateral view, (J) interpretive drawing of
1919 same, (K) stereopairs of medial view, (L) interpretive drawing of same, (M) stereopairs
1920 of dorsal view, (N) interpretive drawing of same, (O) stereopairs of ventral view, (P)
1921 interpretive drawing of same. Hatching indicates broken bone surface or putty
1922 reconstruction, dotted lines indicate broken bone edge. Dark gray areas filled with matrix.
1923 See text for abbreviations. Scale bar = 1 cm.
1924
1925 **Figure 10: Silesaurid left maxillae**. (A) *Kwanasaurus williamparkeri* (composite reconstruction
1926 based on DMNH EPV.65879 and DMNH EPV.63650) in lateral view, (B) same in
1927 medial view. (C) *Lewisuchus admixtus* (PULR 01 redrawn from Bittencourt et al., 2014,
1928 fig. 1) in lateral view reversed, (D) same in medial view. (E) *Silesaurus opolensis* (ZPAL
1929 Ab III/361/26) in lateral view reversed, (F) same in medial view. (G) *Sacisaurus*
1930 *agudoensis* (MCN PV 10050 reversed) in lateral view. Scale bar for A-F = 1 cm; scale

bar for G = 0.5 cm. Dashed lines indicate broken edges. Arrows indicate posterior end of tooth row based on published information and figures.

**Figure 11: *Kwanasaurus williamparkeri* DMNH EPV.63136 left dentary.** (A) Stereopairs of lateral view. (B) Interpretive drawing of same. (C) Stereopairs of medial view. (D) Interpretive drawing of same. (E) Stereopairs of dorsal view. (F) Interpretive drawing of same. (G) Stereopairs of ventral view. (H) Interpretive drawing of same. Hatching indicates broken bone surface, dotted lines indicate broken bone edge. Dark gray areas filled with matrix. See text for abbreviations. Scale bars = 2 cm.

**Figure 12: *Kwanasaurus williamparkeri* dentaries.** (A) DMNH 63135 right dentary stereopairs of lateral view, (B) interpretive drawing of same, (C) stereopairs of medial view, (D) interpretive drawing of same. (E) DMNH EPV.57599 right? dentary in lateral view, (F) same in medial view. (G) DMNH EPV.65878 left? dentary, lateral view, (H) same in medial view, (I) same in dorsal view. (J) DMNH EPV.63660 left dentary in lateral view, (K) same in medial view, (L) same in dorsal view. See text for abbreviations. Scale bar = 1 cm.

**Figure 13: Silesaurid left dentaries.** (A) *Kwanasaurus williamparkeri* (based primarily on DMNH EPV.63136) in lateral view, (B) same in medial view. (C) *Asilisaurus kongwe* (NMT R89) in lateral view, (D) same in medial view. (E) *Eucoelophysis baldwini* (GR 224) in lateral view, (F) same in medial view. (G) *Technosaurus smalli* (TTU P-9021, reversed) in lateral view, (H) same in medial view (also reversed). (I) *Sacisaurus*

1954 *agudoensis* (composite based on MCN PV10042 and MCN PV10043) in lateral view, (J)
1955 same in medial view. (K) *Silesaurus opolensis* (ZPAL AbIII/361/26) in lateral view, (L)
1956 same in medial view. (M) *Diodorus scytobrachion* (MNHM-ARG 30) in lateral view
1957 (reversed), (N) same in medial view (also reversed). Dashed lines indicate broken edges.
1958 Unshaded regions indicate the surface of the specimen is not exposed. All scale bars = 1
1959 cm.
1960
1961 **Figure 14: Isolated folidont teeth probably belonging to *Kwanasaurus williamparkeri*.** (A)
1962 DMNH EPV.43577 in (left to right) labial, lingual, edge-on, and occlusal views. (B)
1963 DMNH EPV.63142 in (left to right) labial, lingual, edge-on, and occlusal views. (C)
1964 DMNH EPV.63143 in (left to right) labial, lingual, edge-on, and occlusal views. (D)
1965 DMNH EPV.63843 in (left to right) labial, lingual, edge-on, and occlusal views. (E)
1966 DMNH EPV.63661 in (left to right) labial, edge-on, and occlusal views. (F) DMNH
1967 EPV.125922 in (left to right) labial, lingual, edge-on, and occlusal views.
1968
1969 **Figure 15: *Kwanasaurus williamparkeri* left humerus (DMNH EPV.59302) stereopairs.** (A)
1970 Proximal view (anterior side facing up). (B) Anterior view. (C) Medial view. (D)
1971 Posterior view. (E) Lateral view. (F) Distal view (anterior side facing up). (G) Drawing
1972 of overlapping proximal and distal ends showing degree of torsion. See text for
1973 abbreviations. Scale bar = 2 cm.
1974
1975 **Figure 16: *Kwansaurus williamparkeri* left ilium (DMNH EPV.48506).** (A) Stereopairs of
1976 lateral view. (B) Interpretive drawing of same. (C) Stereopairs of medial view. (D)

Interpretive drawing of same. (E) Stereopairs of dorsal view. (F) Interpretive drawing of same. (G) Stereopairs of ventral view. (H) Interpretive drawing of same. See text for abbreviations. Dotted lines indicate breaks, dashed lines outline sacral rib attachments. Scale bar = 2 cm.

**Figure 17*: Kwanasaurus williamparkeri* ilia.** (A) DMNH EPV.63653, mostly complete left ilium in lateral view, (B) medial view, (C) ventral view. (D) DMNH EPV.52195, stereopairs of partial left ilium in lateral view, (E) medial view, (F) dorsal view, (G) ventral view. See text for abbreviations. Scale bar = 2 cm.

**Figure 18: *Kwanasaurus williamparkeri* left femur (DMNH EPV.34579) stereopairs.** (A) Proximal view. (B) Distal view. (C) Anterolateral view. (D) Anteromedial view. (E) Posteromedial view. (F) Posterolateral view. See text for abbreviations. Scale bar = 2 cm.

**Figure 19: *Kwanasaurus williamparkeri* proximal femora, larger specimens.** (A) DMNH EPV.54828, right femur stereopairs, proximal view, (B) anterolateral view, (C) anteromedial view, (D) posteromedial view, (E) posterolateral view. (F) DMNH EPV.44616, right femur stereopairs, proximal view, (G) anterolateral view, (H) anteromedial view, (I) posteromedial view, (J) posterolateral view. (K) DMNH EPV.56651, left femur in proximal view, (L) anterolateral view, (M) anteromedial view, (N) posteromedial view, (O) posterolateral view. See text for abbreviations. Scale bar = 2 cm.

**Figure 20: *Kwanasaurus williamparkeri* proximal femora, larger specimens.** (A) DMNH EPV.125924, right femur stereopairs in proximal view, (B) anterolateral view, (C) anteromedial view, (D) posteromedial view, (E) posterolateral view. (F) DMNH EPV.63874, left femur stereopairs in proximal view, (G) anterolateral view, (H) anteromedial view, (I) posterolateral view, (J) posterolateral view. See text for abbreviations. Scale bar = 2 cm.

**Figure 21: *Kwanasaurus williamparkeri* proximal femora, smaller specimens.** (A) DMNH EPV.63139 left femur stereopairs in proximal view, (B) anterolateral view, (C) anteromaedial view, (D) posteromedial view, (E) posterolateral view. (F) DMNH EPV.59311 left femur in proximal view, (G) anterolateral view, (H) anteromedial view, (I) posteromedial view, (J) posterolateral view. (K) DMNH EPV.59301 left femur in proximal view, (L) anterolateral view, (M) anteromedial view, (N) posteromedial view, (O) posterolateral view. See text for abbreviations. Scale bar = 2 cm.

**Figure 22: *Kwanasaurus williamparkeri* distal femur DMNH EPV.67956.** (A) Distal view. (B) Lateral view. (C) Anterior view. (D) Medial view. (E) Posterior view. Scale bar = 2 cm.

**Figure 23: Phylogenetic analysis of Silesauridae, identical strict consensus and Adams consensus trees.**

**Figure 24: Skeletal reconstruction of *Kwanasaurus williamparkeri*.** Skeletal elements are based on individuals of varied sizes, all scaled under the assumption that *Kwanasaurus* is proportioned similarly to *Silesaurus*. Scale bars = 10 cm, given for probable largest specimen (DMNH EPV. 34579) and one of the smallest specimens (DMNH EPV.63139).

**Figure 25: Global and temporal distribution of non-dinosaurian dinosauromorphs.** (A) Lagerpetid distribution. (B) Silesaurid distribution.

**Figure S1. Measurements of appendicular elements detailed in Appendix 1.** (A) *Dromomeron romeri* proximal femur in proximal view, (B) posteromedial view, (C) posterolateral view. (D) *Dromomeron romeri* humerus in proximal view, (E) anterior view, (F) medial view, (G) distal view. (H) Dinosauriformes scapula in lateral view, (I) posterior view, (J) ventral view. (K) Dinosauriformes tibia in proximal view, (L) lateral view, (M) posterior view, (N) distal view. (O) Silesauridae humerus in proximal view, (P) anterior view, (Q) medial view, ® distal view. (S) Silesauridae femur in proximal view, (T) anteromedial view, (U) anteromedial view, (V) distal view.

**Table 1: Dinosauromorph specimens from the Chinle Formation of the Eagle Basin of Colorado at the Denver Museum of Nature and Science.** Voucher specimens are indicated in boldface; the voucher specimen for *Kwanasaurus williamparkeri* (DMNH EPV.65879) serves as voucher specimen for both Dinosauriformes and Silesauridae.

**Table S1: Measurements of appendicular elements of dinosauromorphs from the Chinle Formation of the Eagle Basin of Colorado at the Denver Museum of Nature and Science.** Measurements are all in millimeters, shown graphically in Fig. S1, and described in Appendix 1.

**Table S2: Silesaurid measurements and denticle counts for emergent tooth crowns, given by numbered tooth position.** See also Figs. 8-13. Mesial-distal width taken across broadest point, labial-lingual width across the basal swelling of the crown, and crown height taken from base of swelling to apex. All measurements are in millimeters. The number of denticles are also given for anterior and posterior edges. Uncertain counts are indicated with question marks. If the crown is incomplete or an incompletely exposed replacement tooth, > indicates the minimum (measured) size of the crown. Abbreviations: rpl = replacement tooth.

## Table 1(on next page)

Table_1_Basal_Dinosauromorph_Specimens

| TAXON | SPECIMEN # | ELEMENT | LOCALITY |
|---|---|---|---|
| *Dromomeron romeri* | **DMNH EPV.54826 (voucher)** | Proximal left femur | DMNH 1306 (Main Elk Creek) |
| | DMNH EPV.29956 | Complete right humerus | DMNH 1306 (Main Elk Creek) |
| | DMNH EPV.63873 | Proximal right femur | DMNH 1306 (Main Elk Creek) |
| Dinosauriformes | DMNH EPV.67956 | Partial right scapula | DMNH 3980 (Lost Bob) |
| | DMNH EPV.27699 | Worn proximal left femur | DMNH 1306 (Main Elk Creek) |
| | DMNH EPV.43126 | Worn proximal left femur | DMNH 1306 (Main Elk Creek) |
| | DMNH EPV.43588 | Worn proximal left femur | DMNH 1306 (Main Elk Creek) |
| | DMNH EPV.44616 | Worn proximal left femur | DMNH 1306 (Main Elk Creek) |
| | DMNH EPV.63875 | Complete right tibia | DMNH 4629 (Lost Bob East) |
| | DMNH EPV.63872 | Proximal right tibia | DMNH 3980 (Lost Bob) |
| | DMNH EPV.56652 | Worn proximal tibia | DMNH 1306 (Main Elk Creek) |
| | DMNH EPV.67955 | Proximal left tibia | DMNH 3980 (Lost Bob) |
| *Kwanasaurus parkeri* | **DMNH EPV.65879 (holotype)** | Partial left maxilla | DMNH 4340 (Burrow Cliff) |
| | DMNH EPV.63650 | Partial right maxilla | DMNH 3980 (Lost Bob) |
| | DMNH EPV.125921 | Partial left maxilla | DMNH 4629 (Lost Bob East) |
| | DMNH EPV.125923 | Partial right maxilla | DMNH 4629 (Lost Bob East) |
| | DMNH EPV.63136 | Nearly complete left dentary | DMNH 3980 (Lost Bob) |
| | DMNH EPV.63135 | Partial right dentary | DMNH 3980 (Lost Bob) |
| | DMNH EPV.63660 | Left anterior dentary | DMNH 3980 (Lost Bob) |
| | DMNH EPV.65878 | Partial left dentary | DMNH 4629 (Lost Bob East) |
| | DMNH EPV.57599 | Partial right? dentary | DMNH 1306 (Main Elk Creek) South 6 |
| | DMNH EPV.43577 | Tooth | DMNH 1306 (Main Elk Creek) South 2 |
| | DMNH EPV.63142 | Tooth | DMNH 3980 (Lost Bob) |

| | | | |
|---|---|---|---|
| | DMNH EPV.63143 | Tooth | DMNH 3980 (Lost Bob) |
| | DMNH EPV.63661 | Tooth | DMNH 3980 (Lost Bob) |
| | DMNH EPV.125922 | Tooth | DMNH 4629 (Lost Bob East) |
| | DMNH EPV.59302 | Nearly complete left humerus | DMNH 1306 (Main Elk Creek) South 7 |
| | DMNH EPV.48506 | Complete left ilium | DMNH 1306 (Main Elk Creek) |
| | DMNH EPV.63653 | Nearly complete left ilium | DMNH 3980 (Lost Bob) |
| | DMNH EPV.52195 | Partial ilium | DMNH 1306 (Main Elk Creek) South |
| | DMNH EPV.34579 | Nearly complete femur | DMNH 692 (Derby Junction) |
| | DMNH EPV.54828 | Proximal right femur | DMNH 3492 (Shuvosaur Surprise) |
| | DMNH EPV.59311 | Proximal right femur | DMNH 3492 (Shuvosaur Surprise) |
| | DMNH EPV.44616 | Proximal right femur | DMNH 1306 (Main Elk Creek) North 2 |
| | DMNH EPV.56651 | Proximal left femur | DMNH 1306 (Main Elk Creek) |
| | DMNH EPV.59301 | Proximal left femur | DMNH 1306 (Main Elk Creek) South |
| | DMNH EPV.63139 | Proximal left femur | DMNH 3980 (Lost Bob) |
| | DMNH EPV.63874 | Proximal left femur | DMNH 4629 (Lost Bob East) |
| | DMNH EPV.125924 | Proximal right femur | DMNH 4629 (Lost Bob East) |
| Silesauridae? | DMNH EPV.34028 | Distal right femur | DMNH 1306 (Main Elk Creek) |
| | DMNH EPV.59310 | Distal right femur | DMNH 3492 (Shuvosaur Surprise) |

1

# Figure 1

Figure_1_Map_and_Section

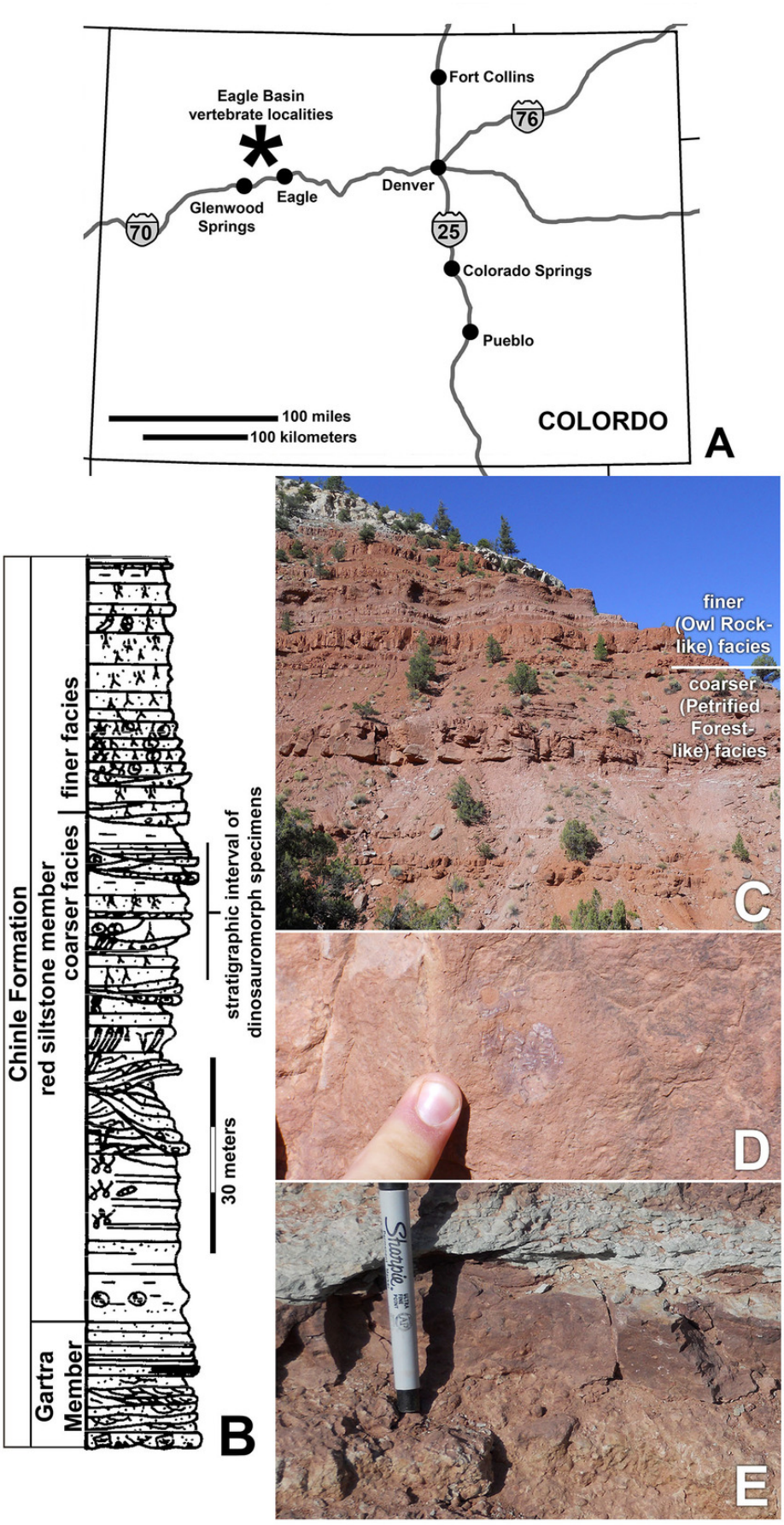
Fort Collins
Eagle Basin
vertebrate localities
76
Denver
Eagle
Glenwood
Springs
70
25
Colorado Springs
Pueblo
100 miles
100 kilometers
COLORDO
A
finer
(Owl Rock-
like) facies
coarser
(Petrified
Forest-
like) facies
C
Chinle Formation
red siltstone member
finer facies
coarser facies
Gartra
Member
stratigraphic interval of
dinosauromorph specimens
30 meters
B
D
Sharpie
E

# Figure 2

Figure_2_Dromomeron_54826_(voucher_femur)

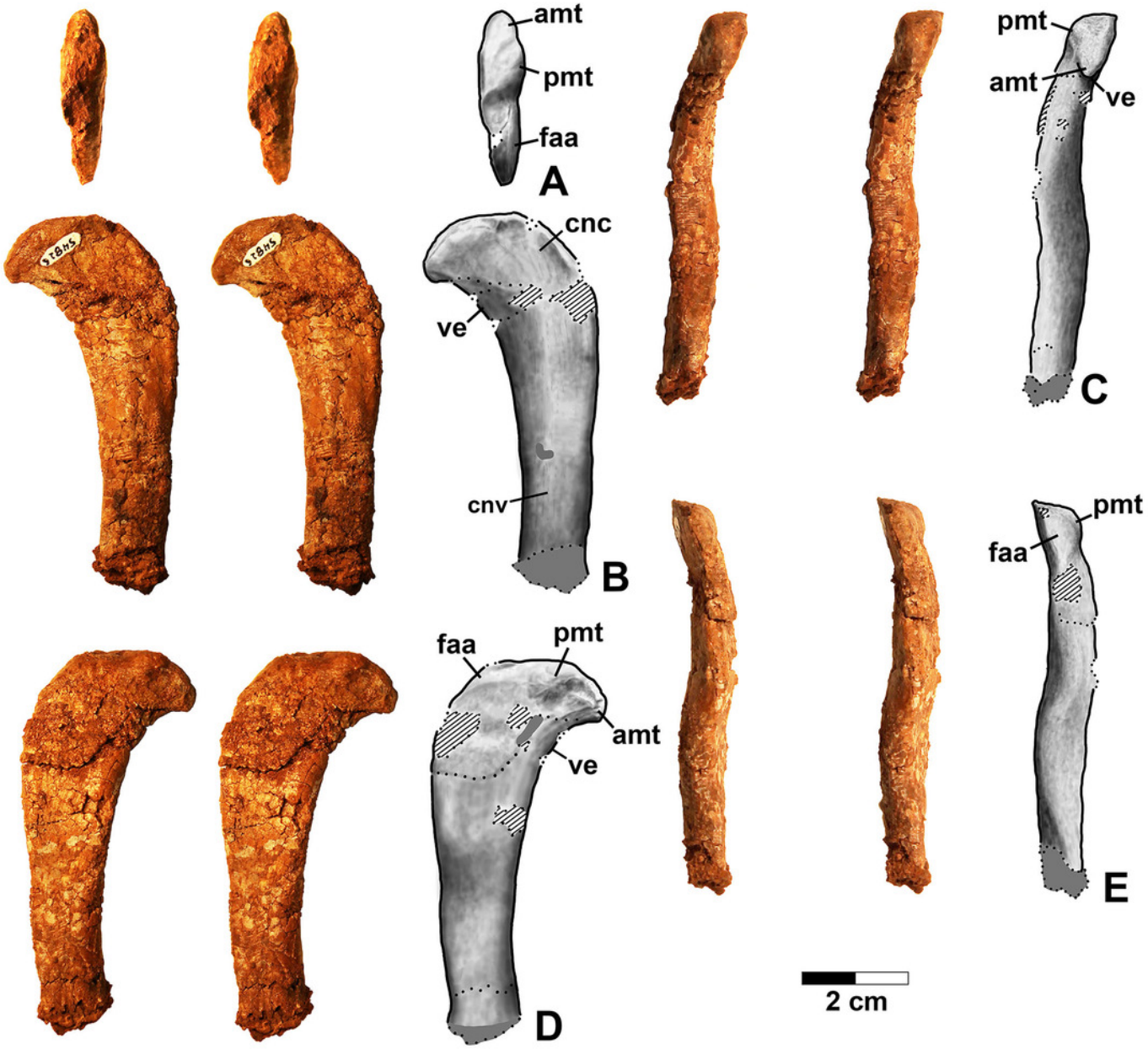

# Figure 3

Figure_3_Dromomeron_63073_(femur)

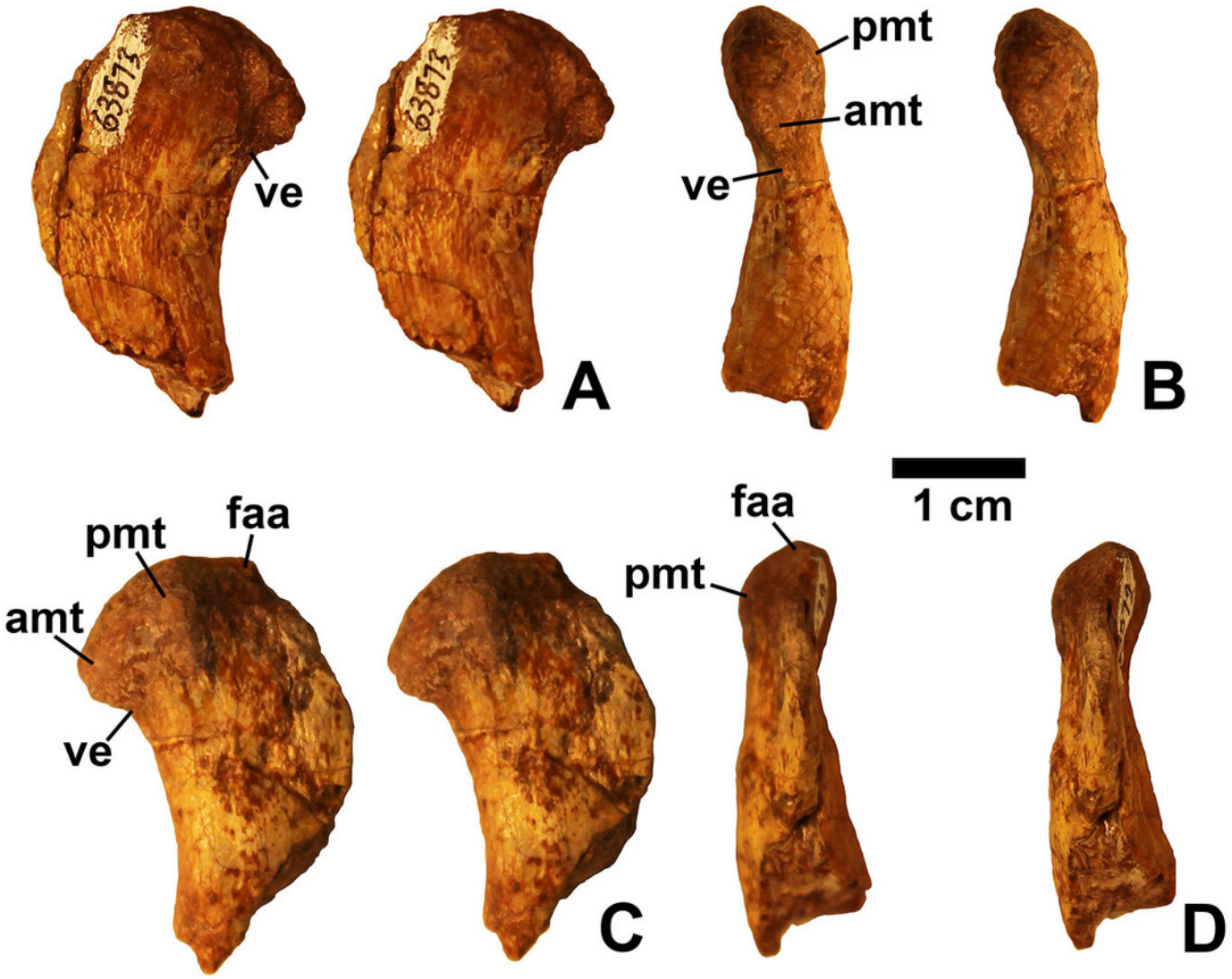

# Figure 4

Figure_4_Dromomeron_29956_(humerus)

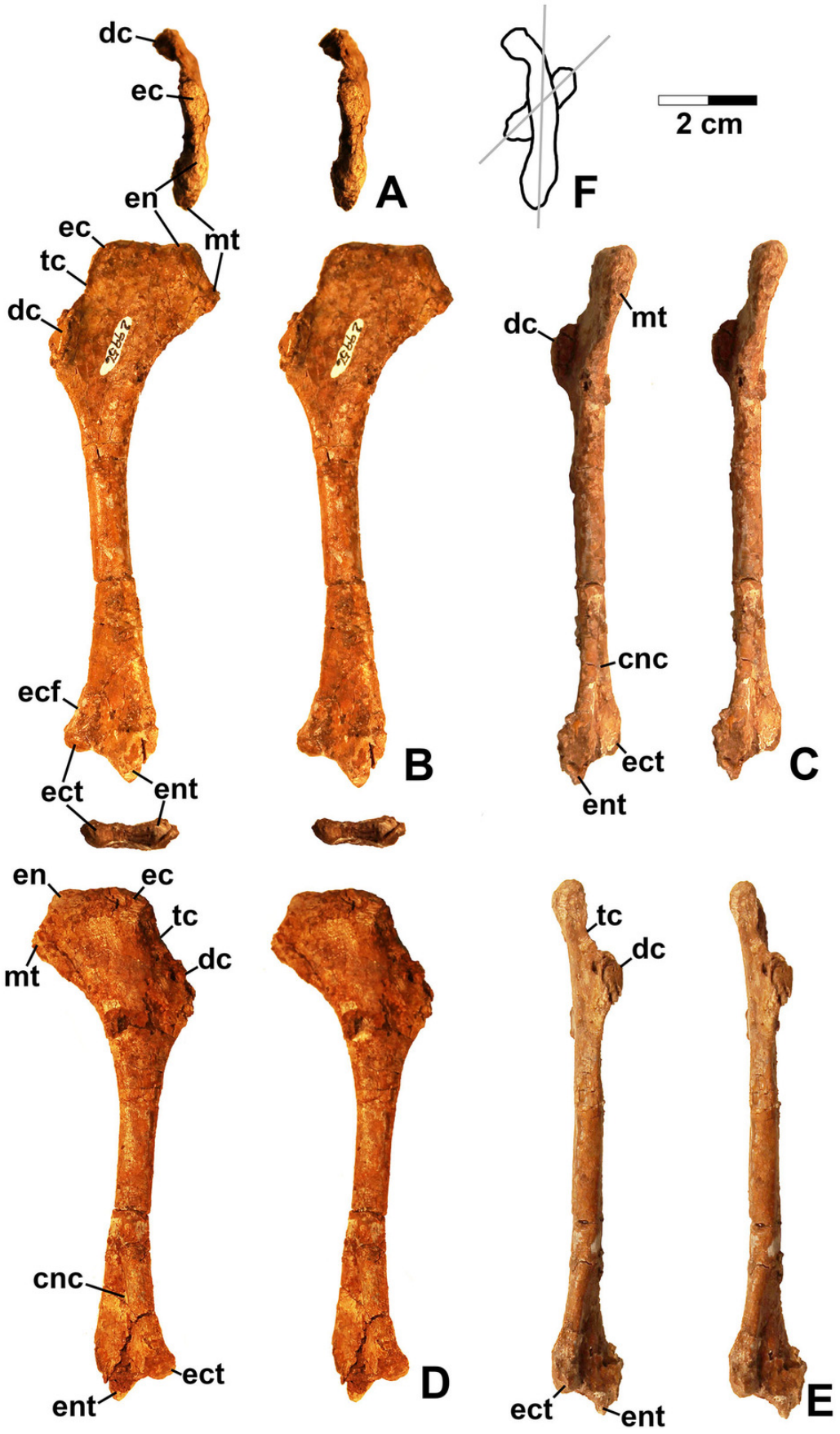
dc
ec
en
mt
ec
tc
dc
ecf
ect
ent
A
B
F
2 cm
dc
mt
cnc
ect
ent
C
en
ec
tc
mt
dc
cnc
ect
ent
D
tc
dc
ect
ent
E

# Figure 5

Figure_5_Dinosauriformes_67956_(scapula)

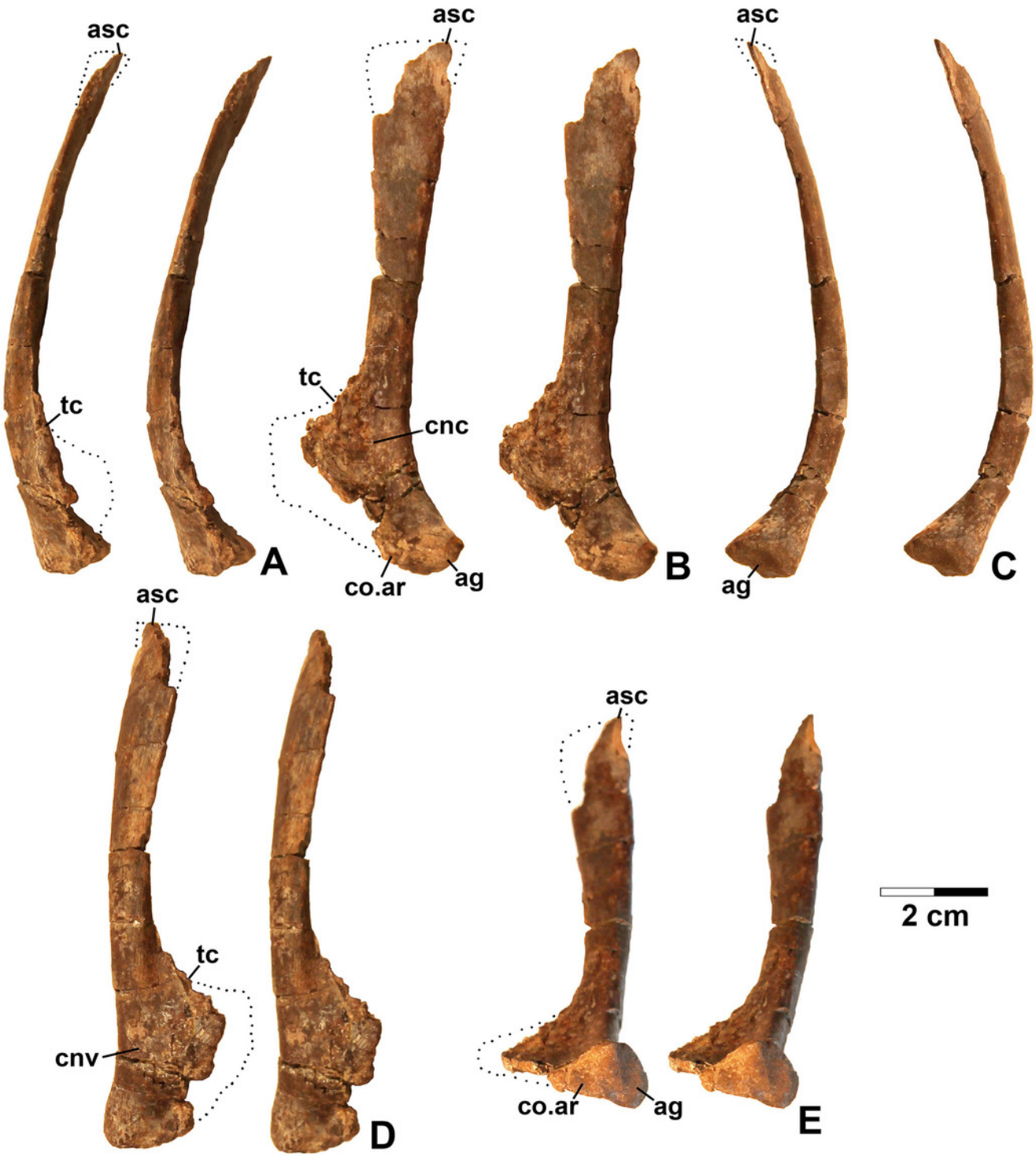
asc
tc
A
asc
tc
cnc
co.ar
ag
B
asc
ag
C
asc
tc
cnv
D
asc
co.ar
ag
E
2 cm

# Figure 6

Figure_6_Dinosauriformes_63875_(tibia)

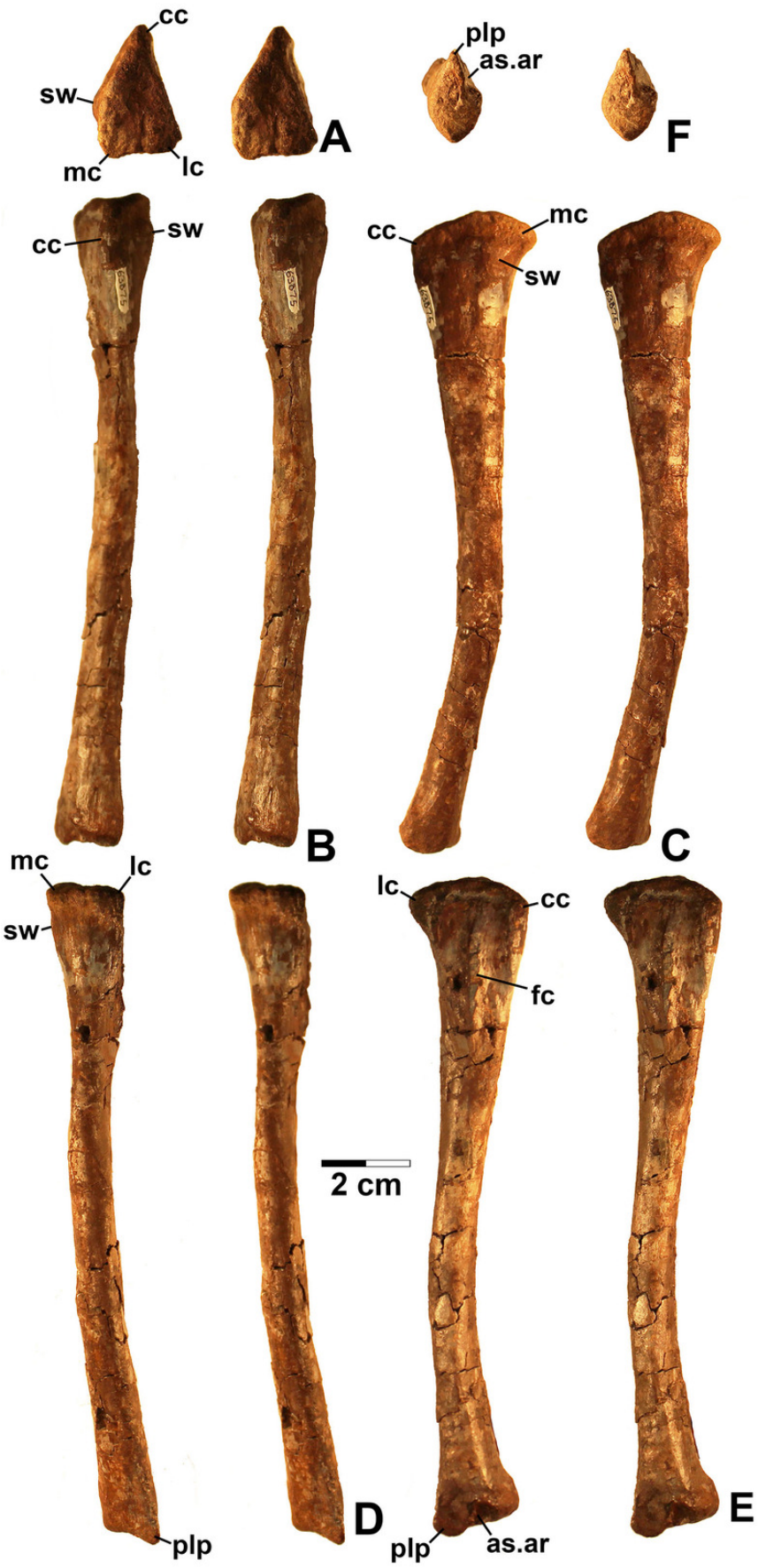
cc
sw
mc
lc
A
plp
as.ar
F
cc
sw
B
cc
mc
sw
C
mc
lc
sw
plp
D
lc
cc
fc
plp
as.ar
E
2 cm

# Figure 7

Figure_7_Dinosauriformes_63872,_67955,_56....ibiae)

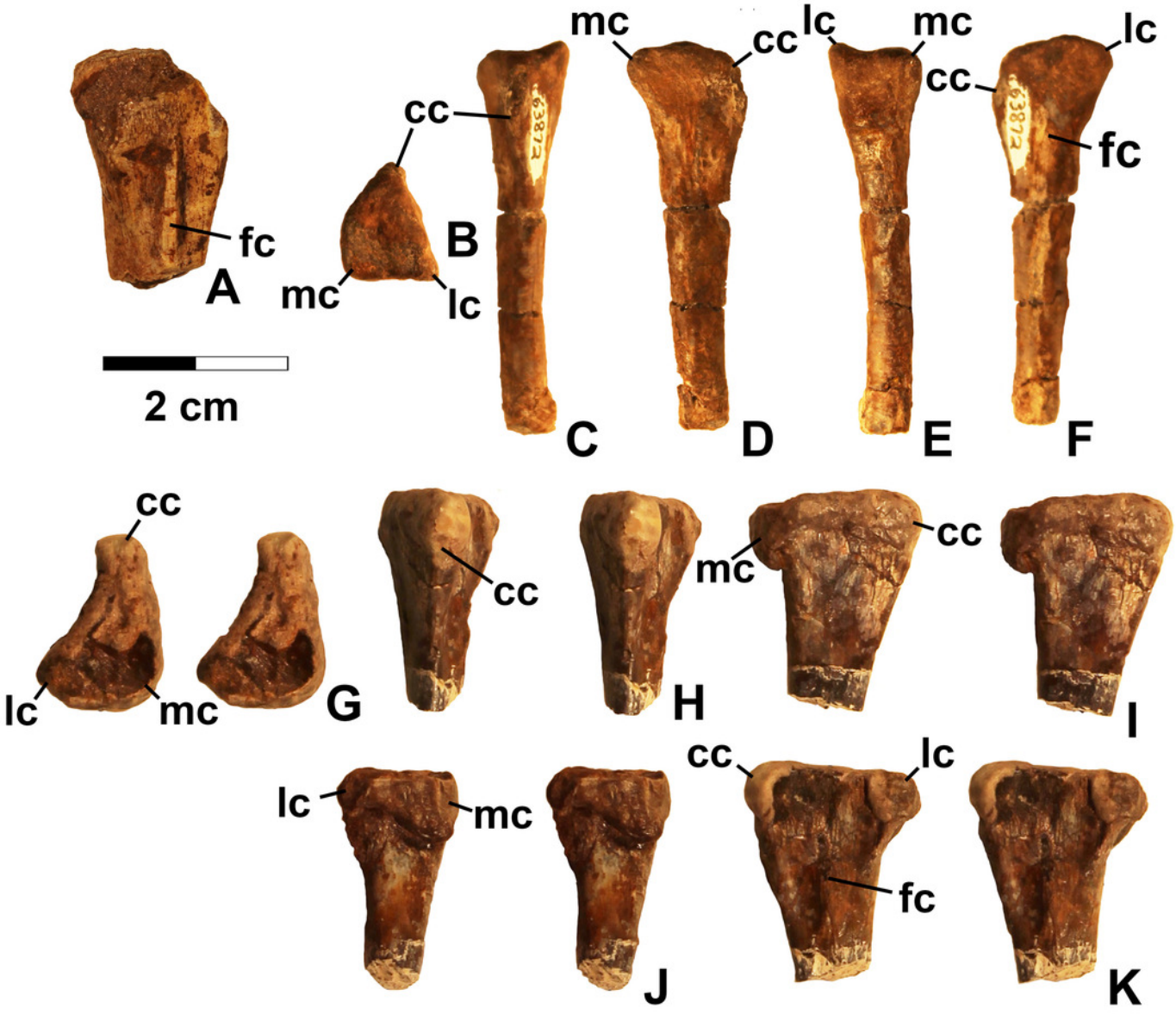

# Figure 8

Figure_8_Silesauridae_65879_(maxilla)

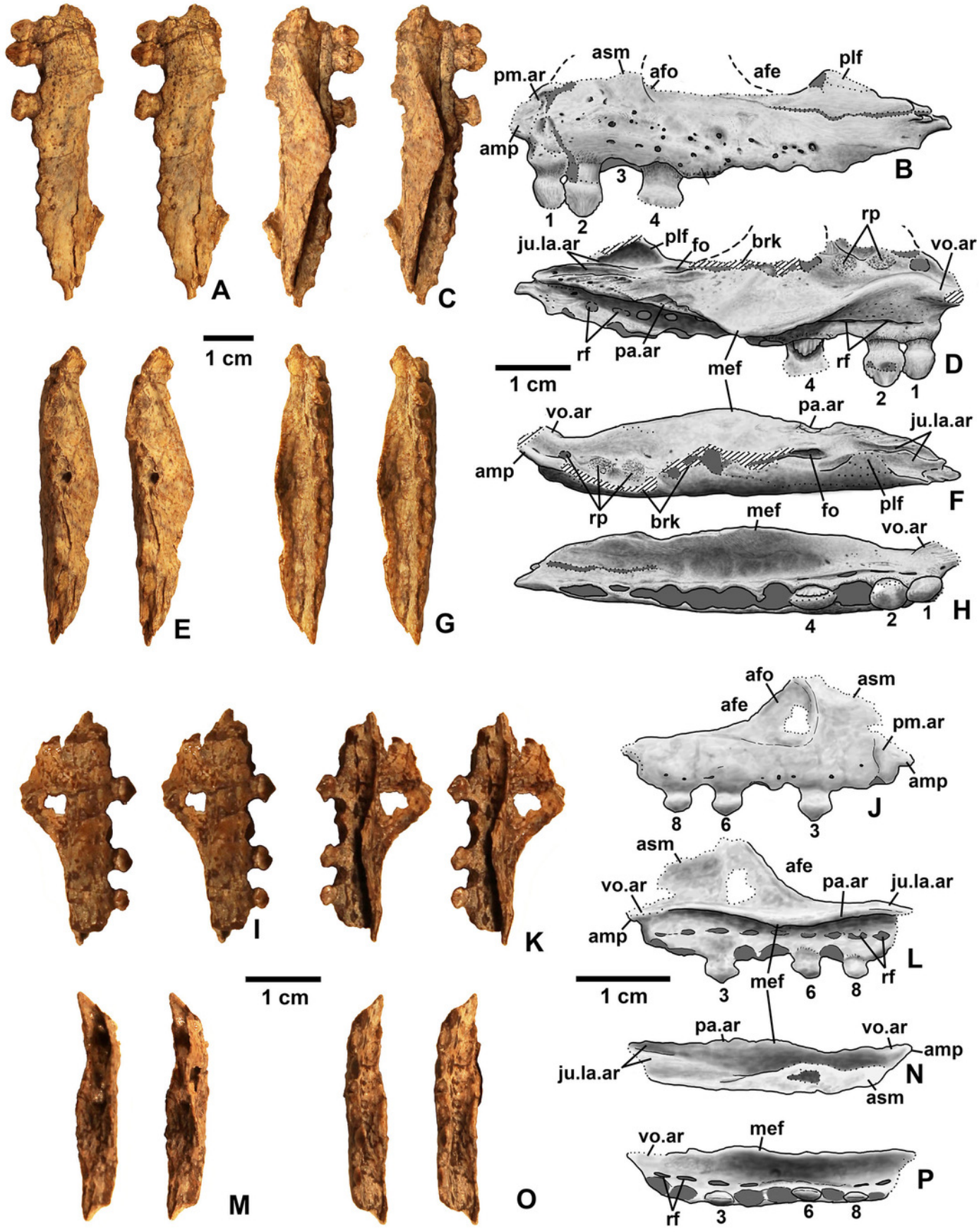
A
C
1 cm
E
G
asm
pm.ar
afo
afe
plf
amp
B
1
2
3
4
rp
ju.la.ar
plf
fo
brk
vo.ar
rf
pa.ar
mef
D
1 cm
vo.ar
pa.ar
ju.la.ar
amp
rp
brk
mef
fo
plf
F
vo.ar
H
I
K
1 cm
M
O
afo
asm
afe
pm.ar
amp
J
8
6
3
asm
afe
vo.ar
pa.ar
ju.la.ar
amp
L
1 cm
mef
rf
pa.ar
vo.ar
amp
ju.la.ar
N
asm
vo.ar
mef
P
rf

# Figure 9

Figure_9_Kwanasaurus_maxillae

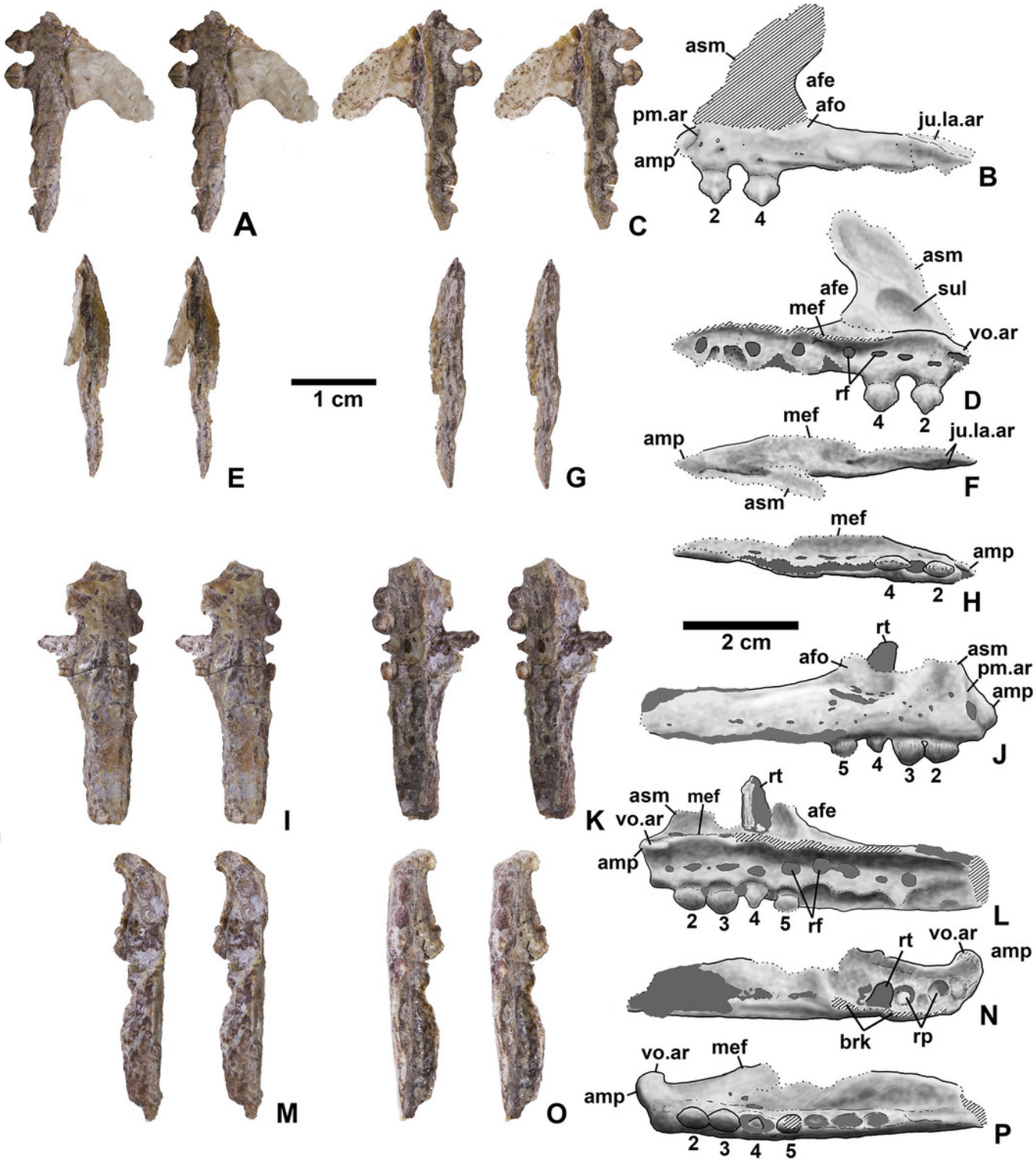
A
B
asm
afe
afo
pm.ar
ju.la.ar
amp
2
4
C
D
asm
sul
afe
mef
vo.ar
rf
4
2
E
1 cm
G
F
mef
amp
ju.la.ar
asm
H
mef
amp
4
2
I
2 cm
J
rt
afo
asm
pm.ar
amp
5
4
3
2
K
asm
mef
rt
vo.ar
afe
amp
L
2
3
4
5
rf
M
N
rt
vo.ar
amp
brk
rp
O
P
vo.ar
mef
amp
2
3
4
5

# Figure 10

Figure_10_Silesaurid_maxillae

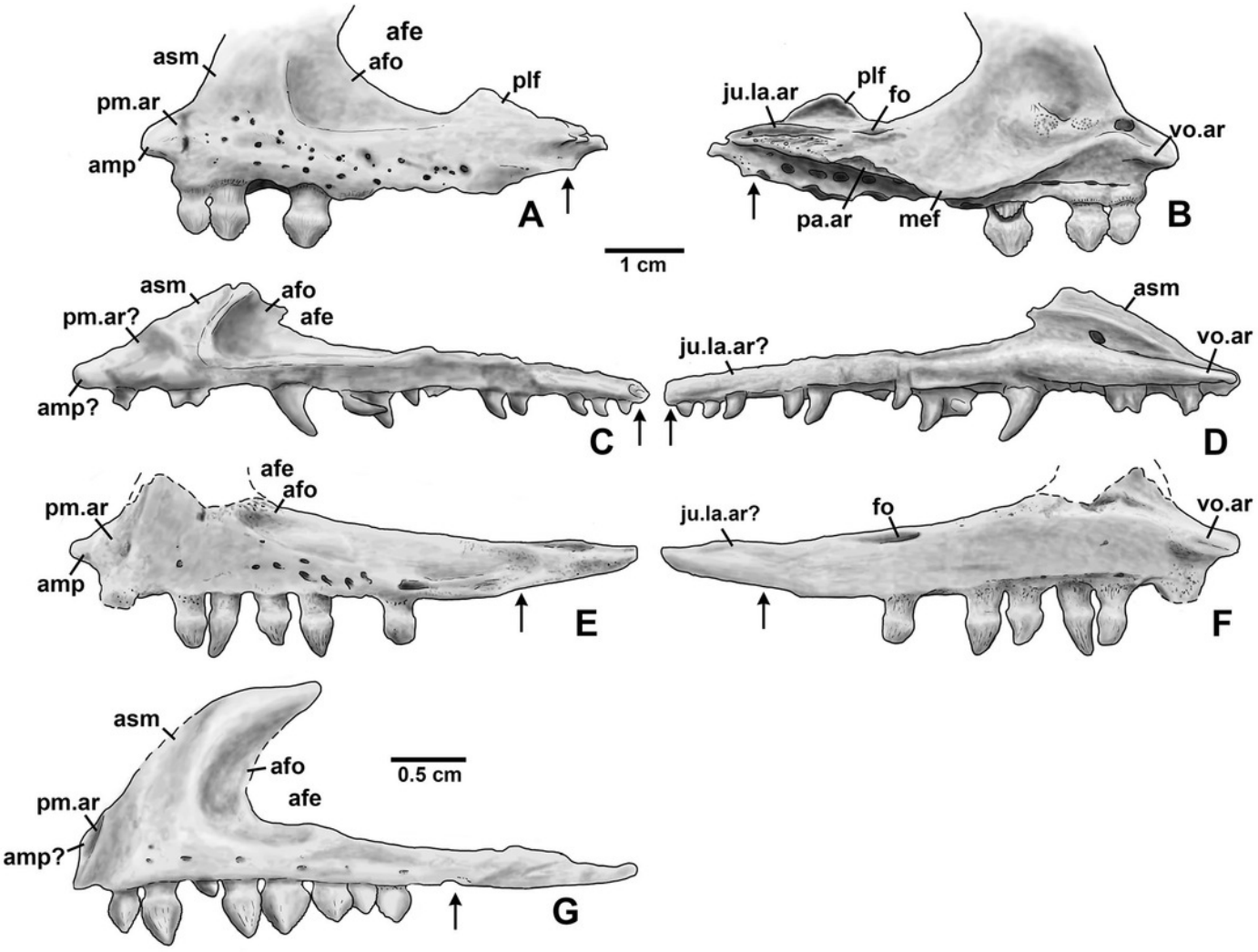

# Figure 11

Figure_11_Kwanasaurus_63136_(dentary)

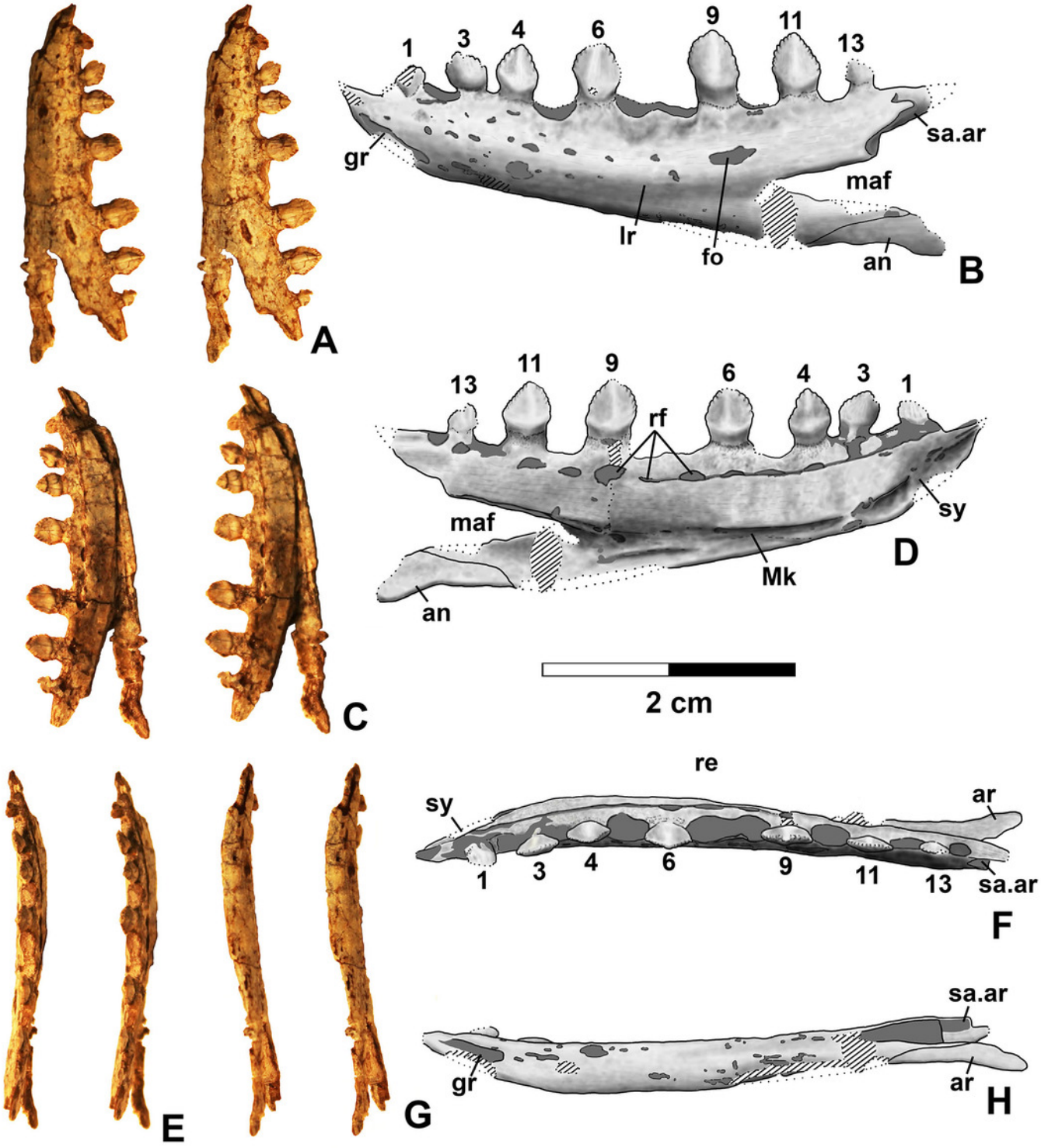
A
1
3
4
6
9
11
13
gr
sa.ar
maf
lr
fo
an
B
13
11
9
6
4
3
1
rf
sy
maf
Mk
an
D
2 cm
C
E
G
re
sy
ar
1
3
4
6
9
11
13
sa.ar
F
sa.ar
gr
ar
H

# Figure 12

Figure_12_Kwanasaurus_63135_(dentary)

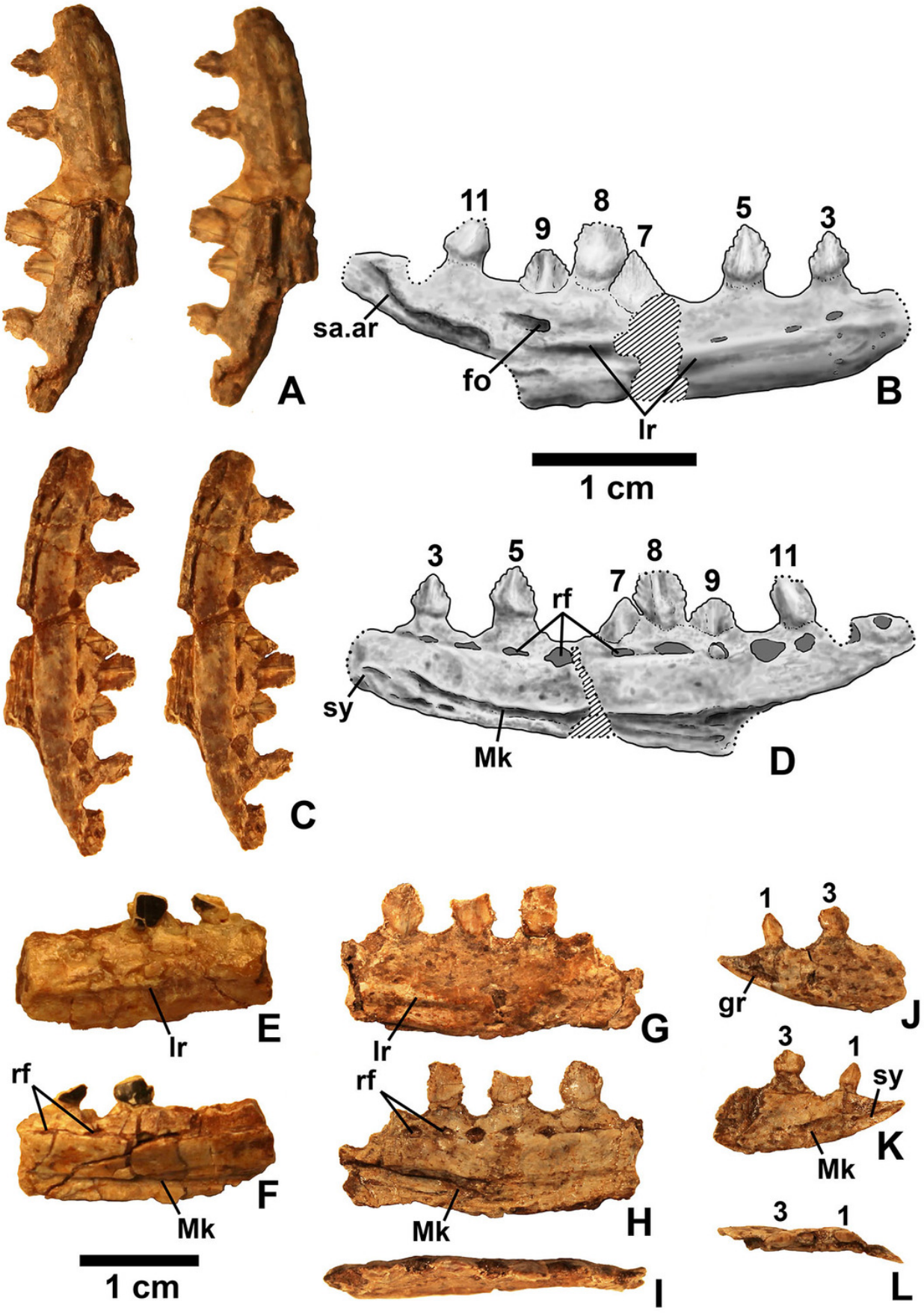
A
11
9
8
7
5
3
sa.ar
fo
lr
B
1 cm
C
3
5
8
7
9
11
rf
sy
Mk
D
lr
E
rf
Mk
F
1 cm
lr
G
rf
Mk
H
I
1
3
gr
J
3
1
sy
Mk
K
3
1
L

# Figure 13

Figure_13_Silesaurid_dentaries

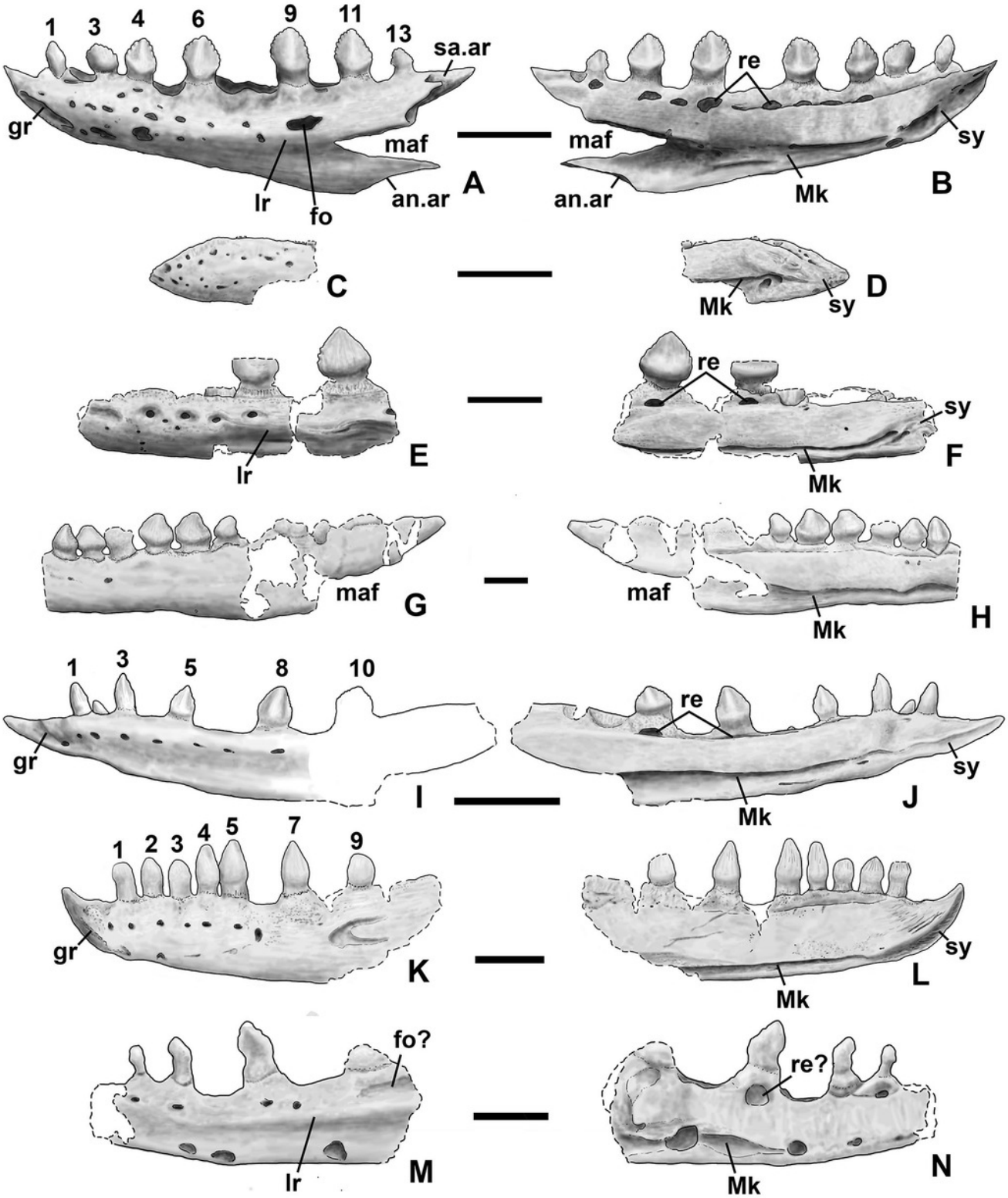
1
3
4
6
9
11
13
sa.ar
gr
maf
lr
fo
an.ar
A
re
maf
sy
an.ar
Mk
B
C
Mk
sy
D
lr
E
re
sy
Mk
F
maf
G
maf
Mk
H
1
3
5
8
10
gr
I
re
sy
Mk
J
1
2
3
4
5
7
9
gr
K
sy
Mk
L
fo?
lr
M
re?
Mk
N

# Figure 14

Figure_14_Kwanasaurus_teeth

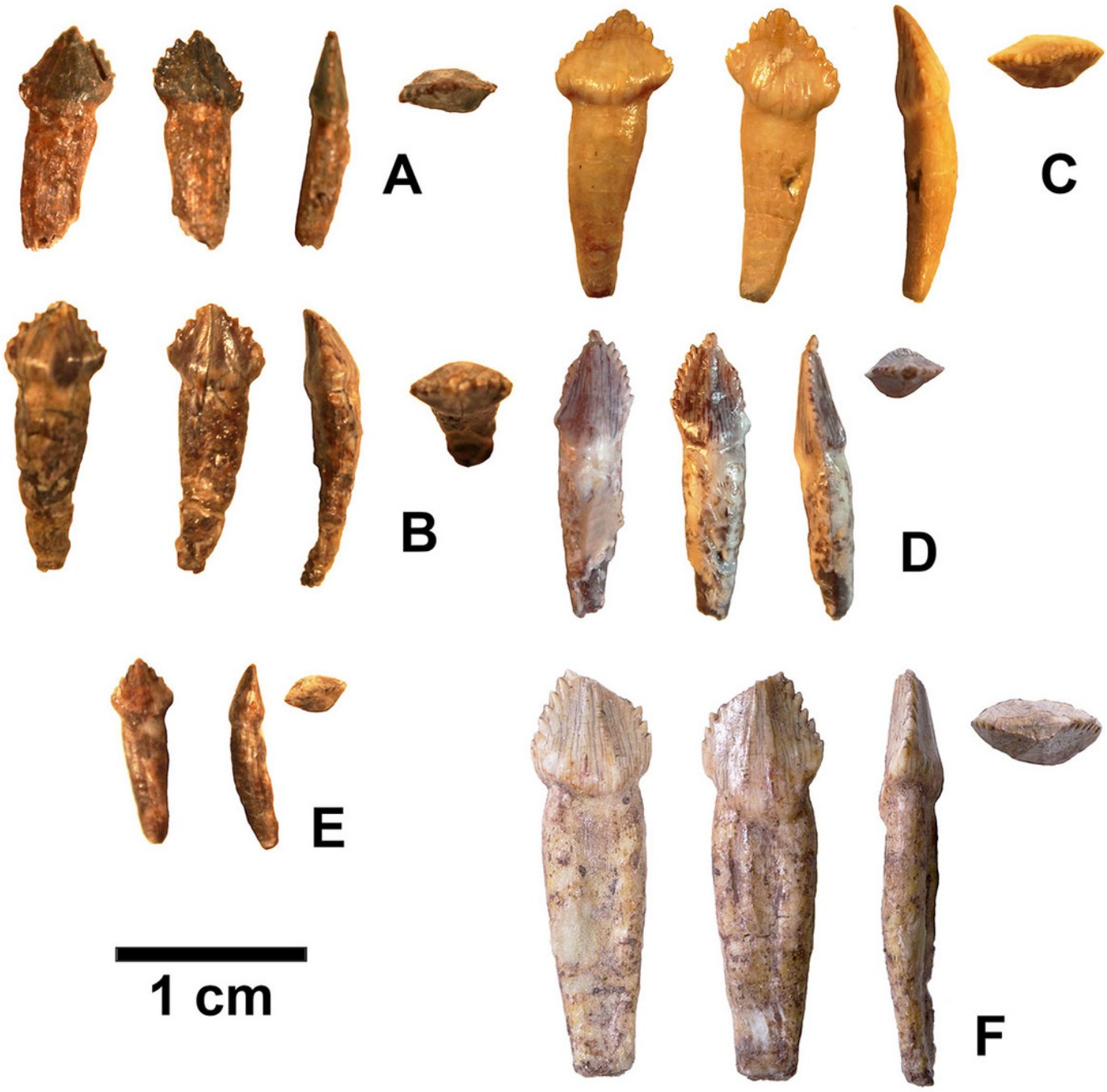

# Figure 15

Figure_15_Silesauridae_59302_(humerus)

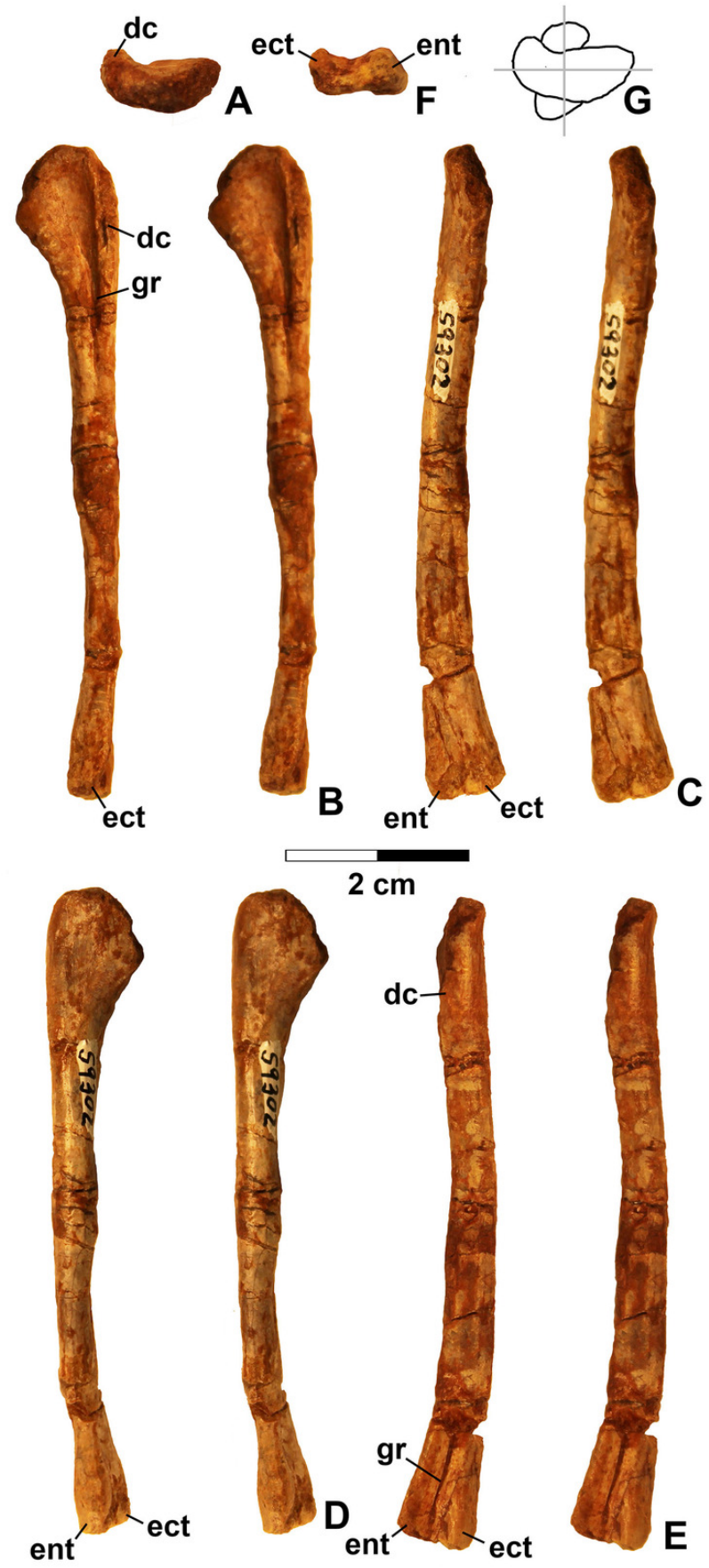
dc
ect
ent
A
F
G
dc
gr
ect
B
ent
ect
C
2 cm
ent
ect
D
dc
gr
ent
ect
E

# Figure 16

Figure_16_Silesauridae_48506_(ilium)

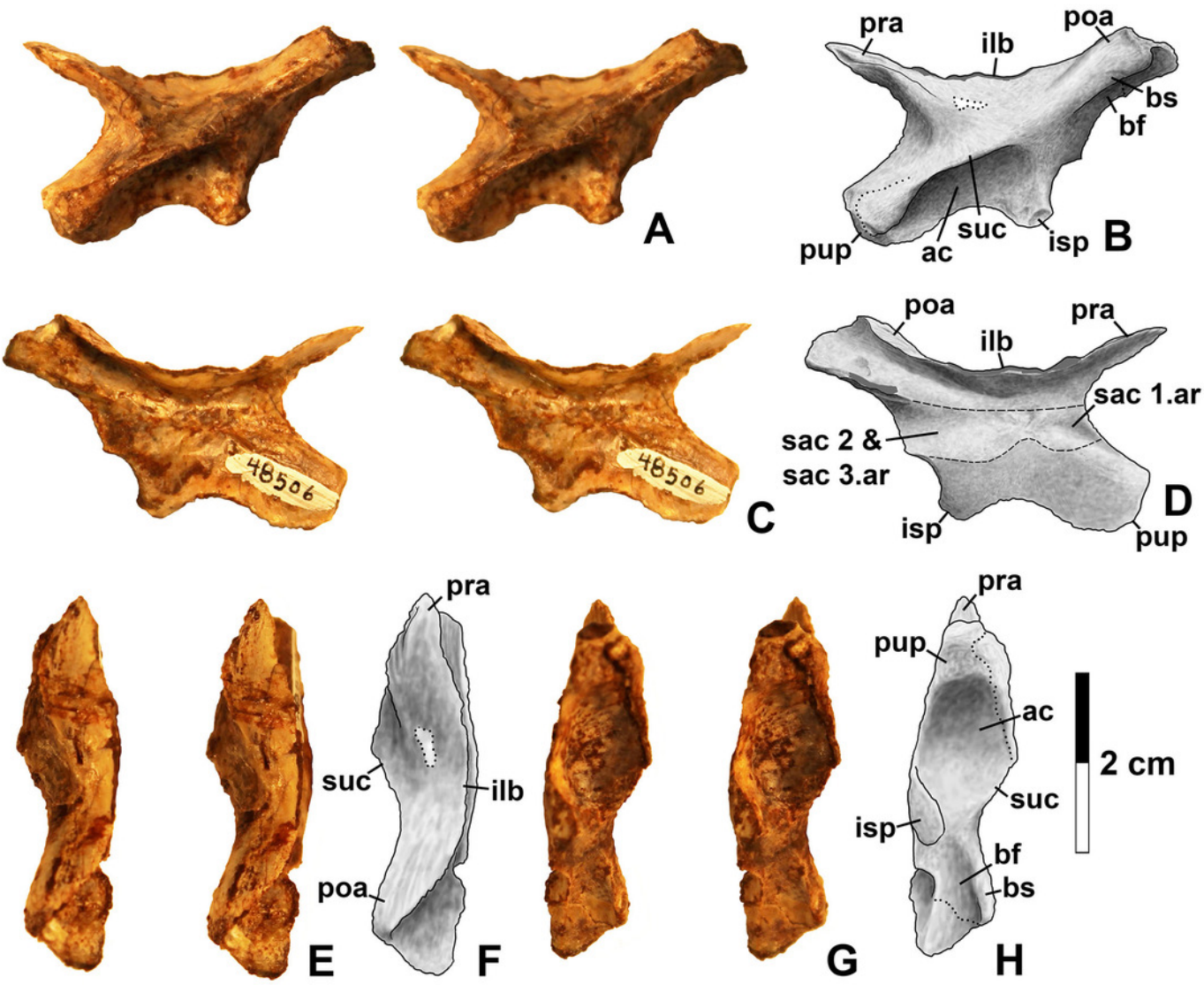

# Figure 17

Figure_17_Silesauridae_63653_&_52195_(ilium)

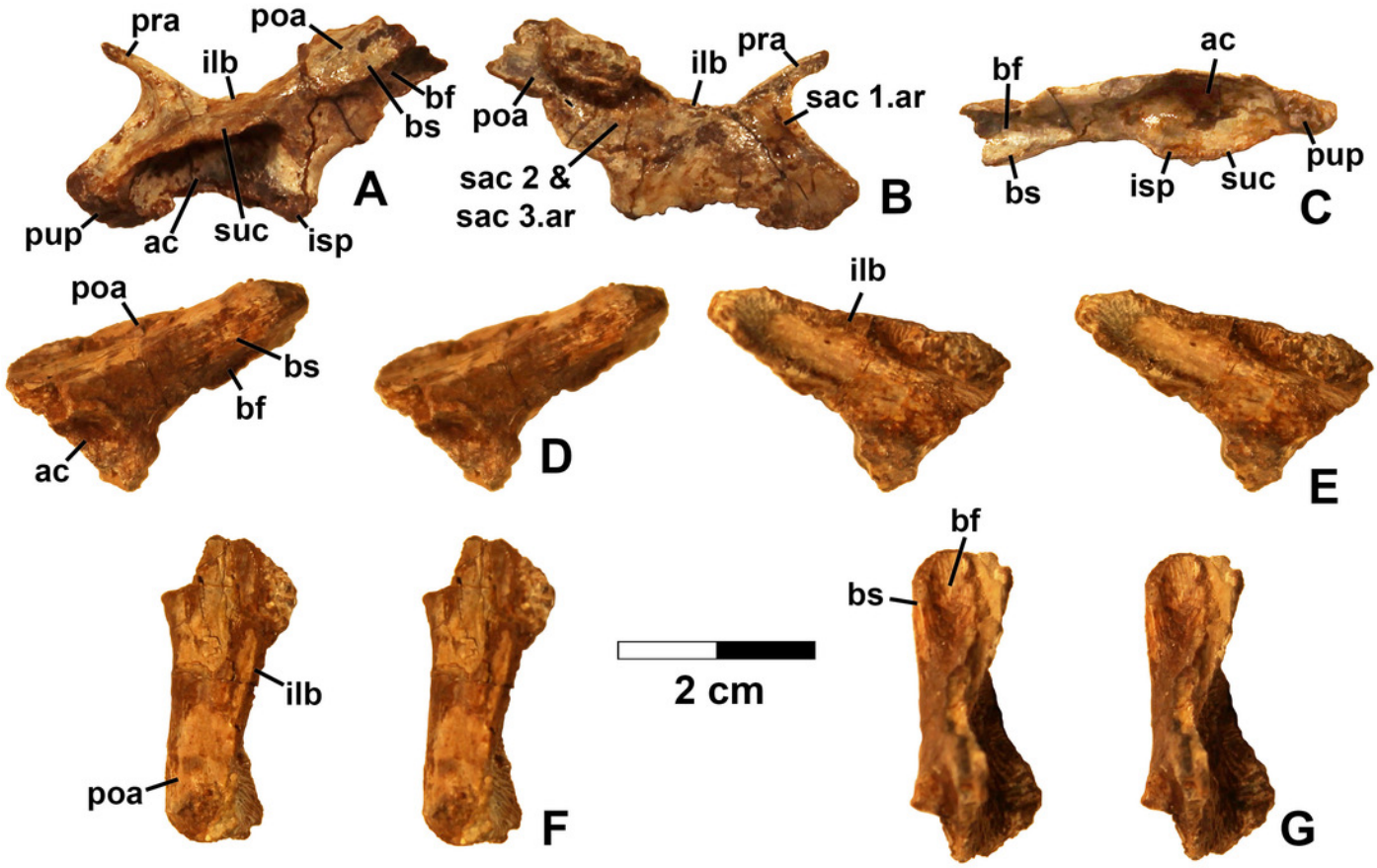

# Figure 18

Figure_18_Silesauridae_34579_(femur)

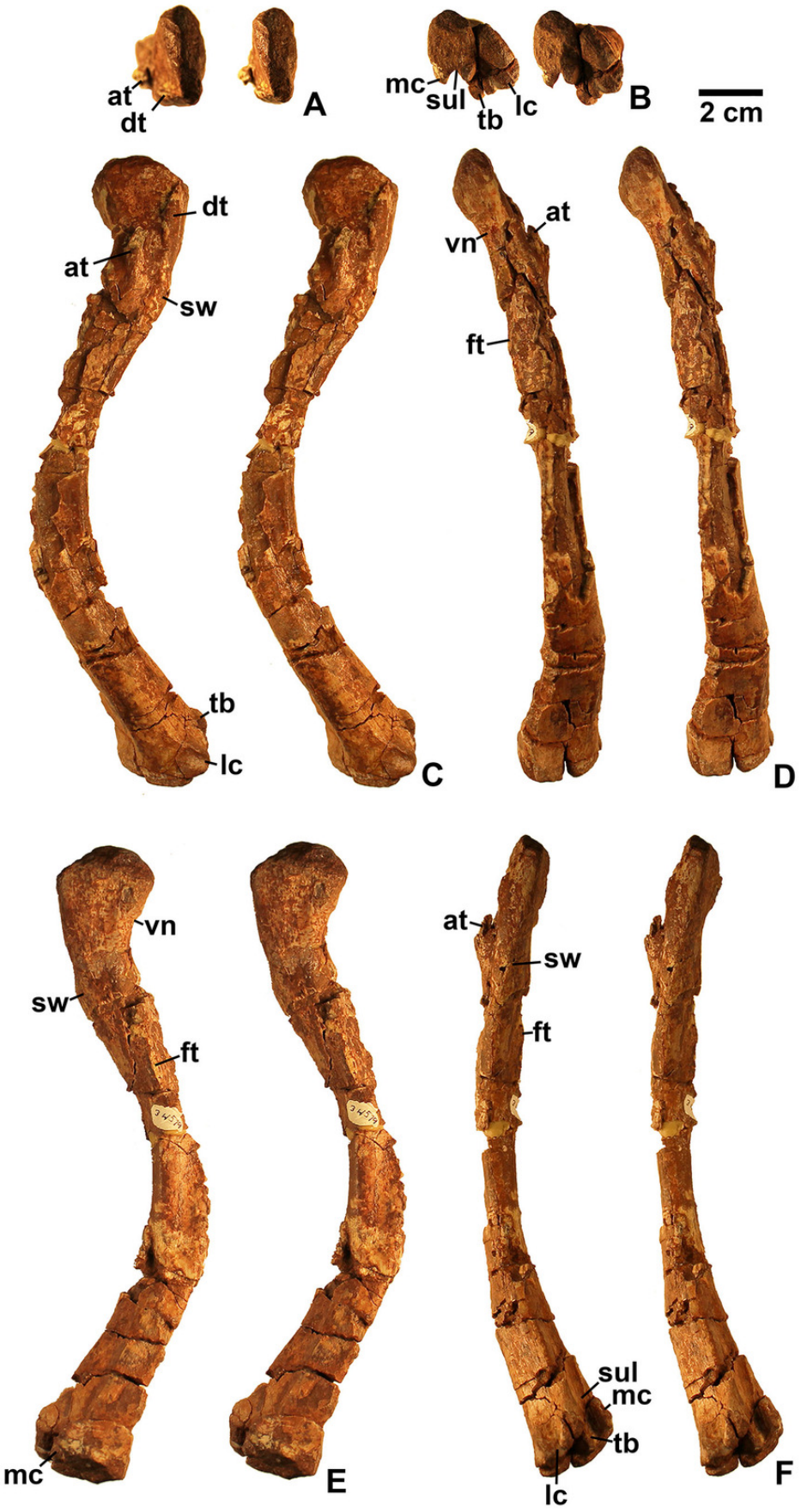
at
dt
A
mc
sul
tb
lc
B
2 cm
dt
at
sw
tb
lc
C
at
vn
ft
D
vn
sw
ft
mc
E
at
sw
ft
sul
mc
tb
lc
F

# Figure 19

Figure_19_Silesauridae_54828,_44616,_56651_(femora)

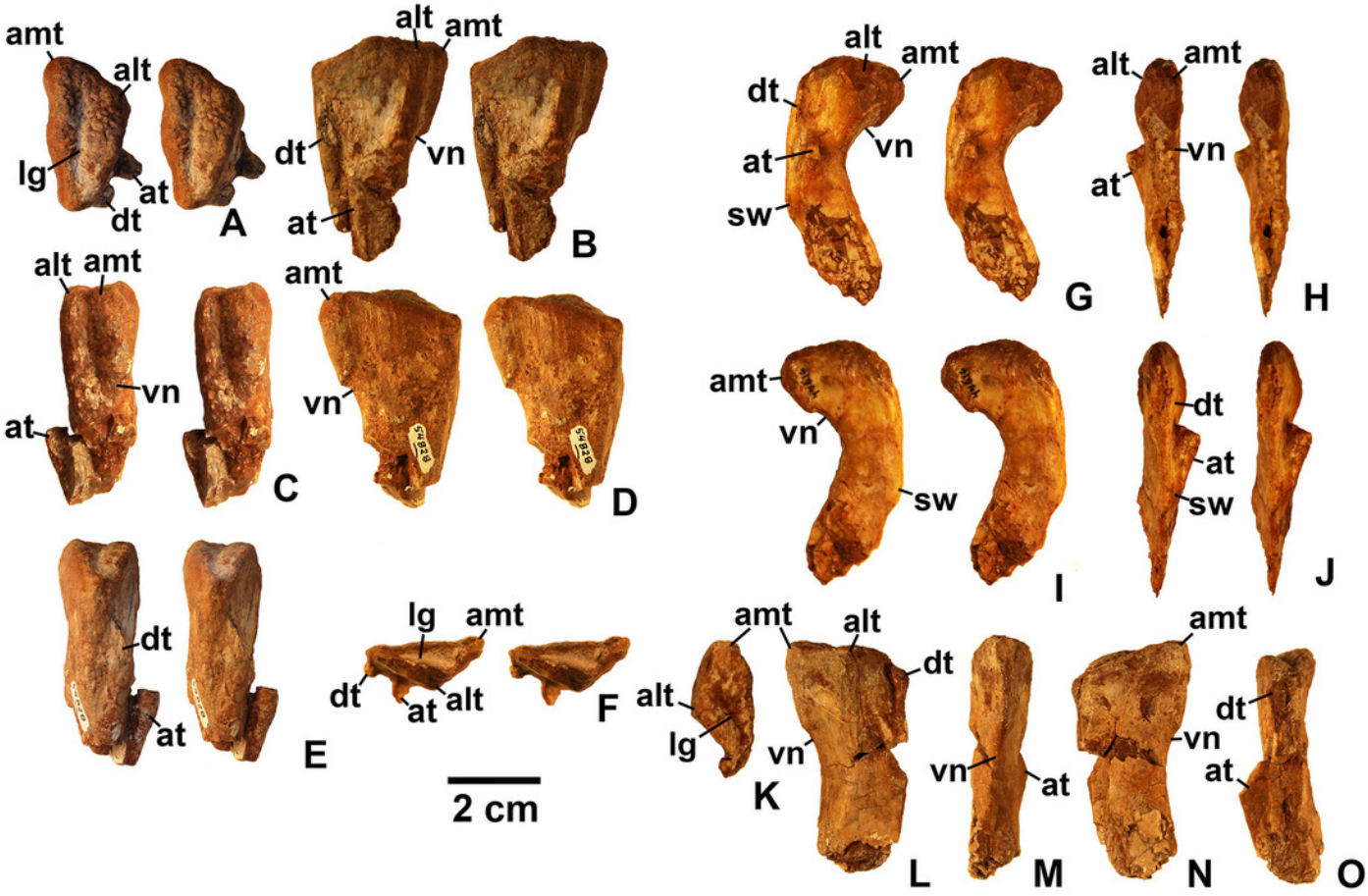

# Figure 20

Figure_20_Silesauridae_125924,_63874_(femora)

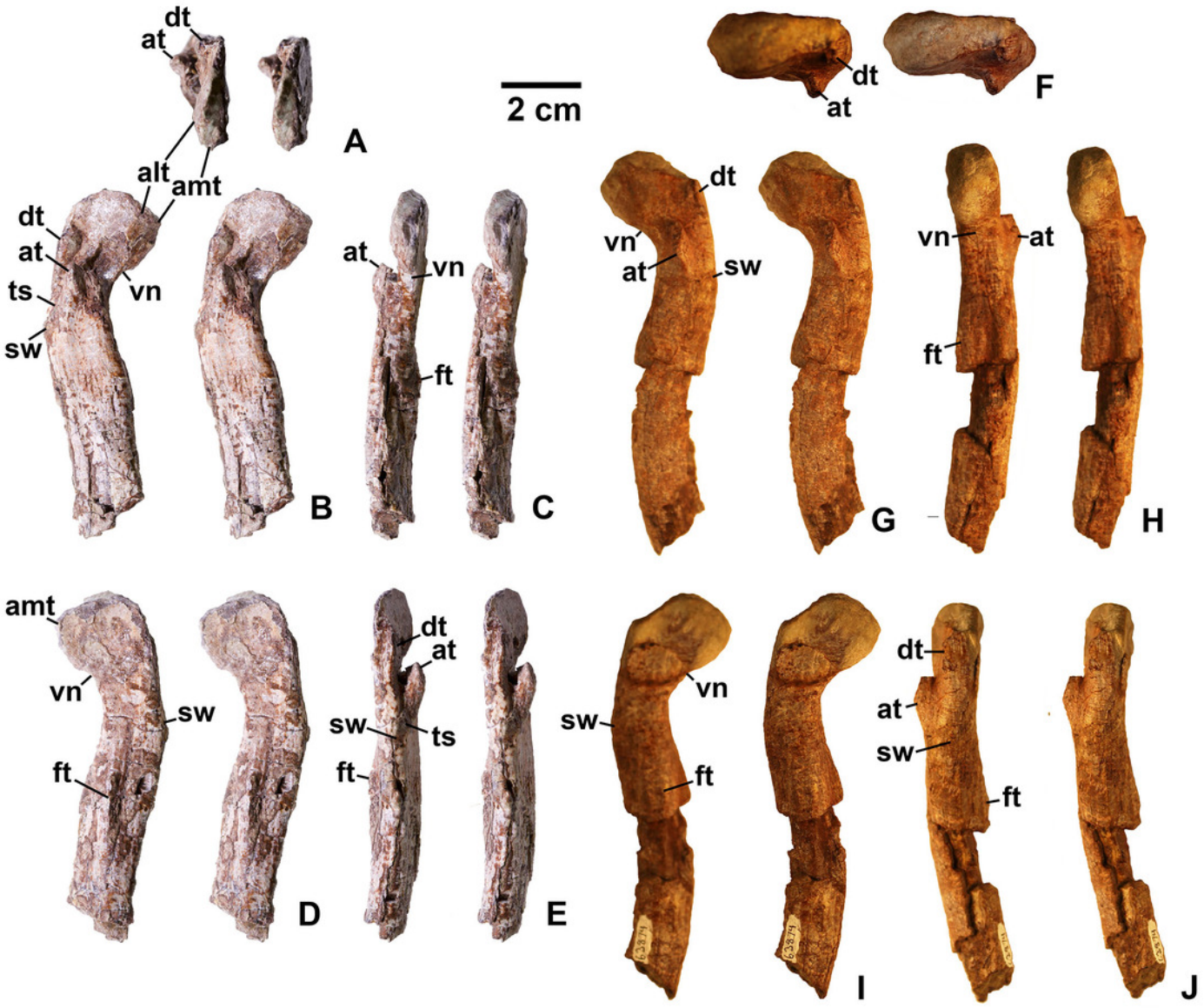

# Figure 21

Figure_21_Silesauridae_63139,_59311,_59301(femora)

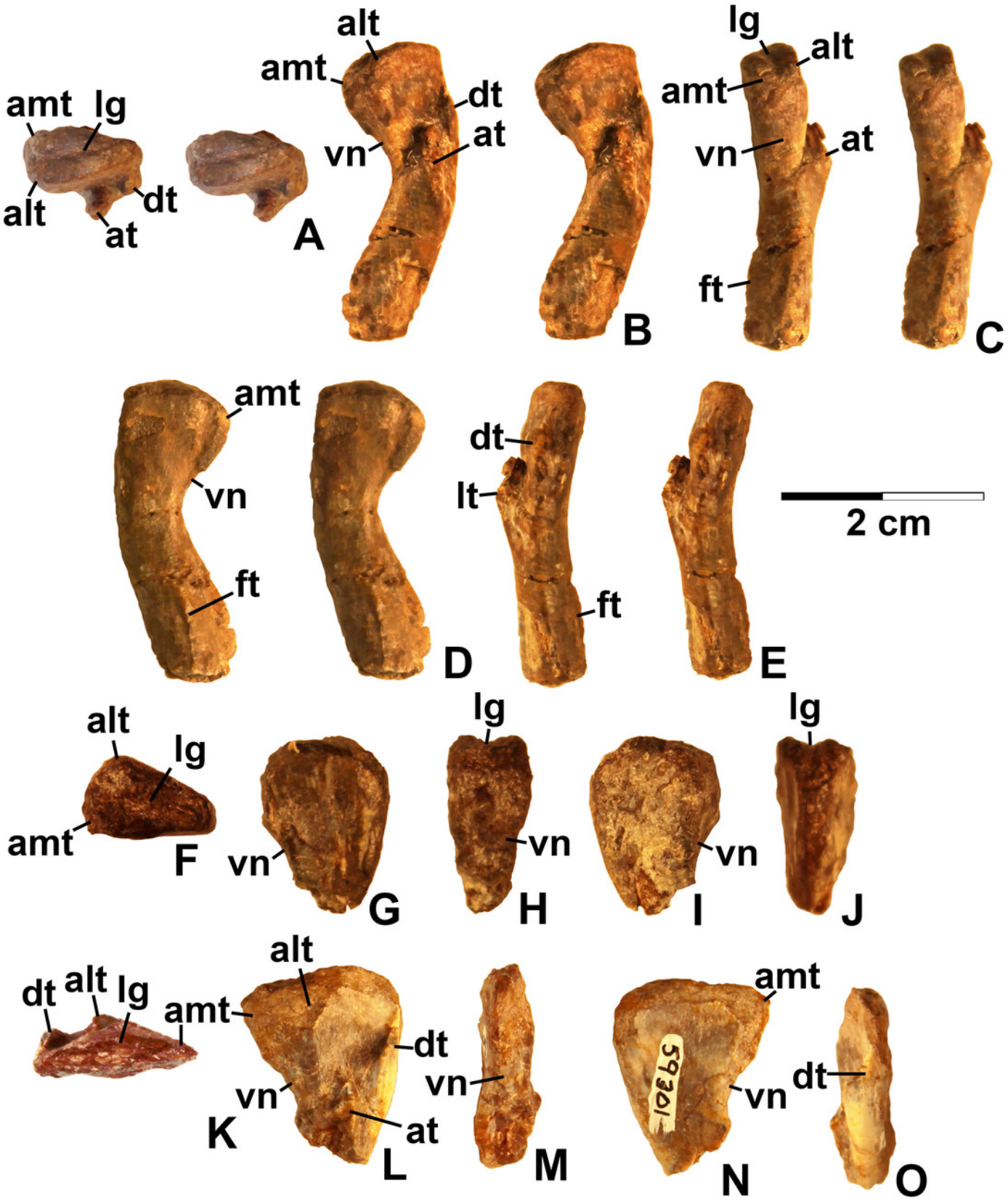
amt
lg
alt
dt
at
A
alt
amt
dt
vn
at
B
lg
alt
amt
vn
at
ft
C
amt
vn
ft
D
dt
lt
ft
E
2 cm
alt
lg
amt
F
vn
G
lg
vn
H
vn
I
lg
J
dt
alt
lg
amt
K
alt
dt
vn
at
L
vn
M
amt
vn
dt
N
O

# Figure 22

Figure_22_Silesauridae_67956_(femur)

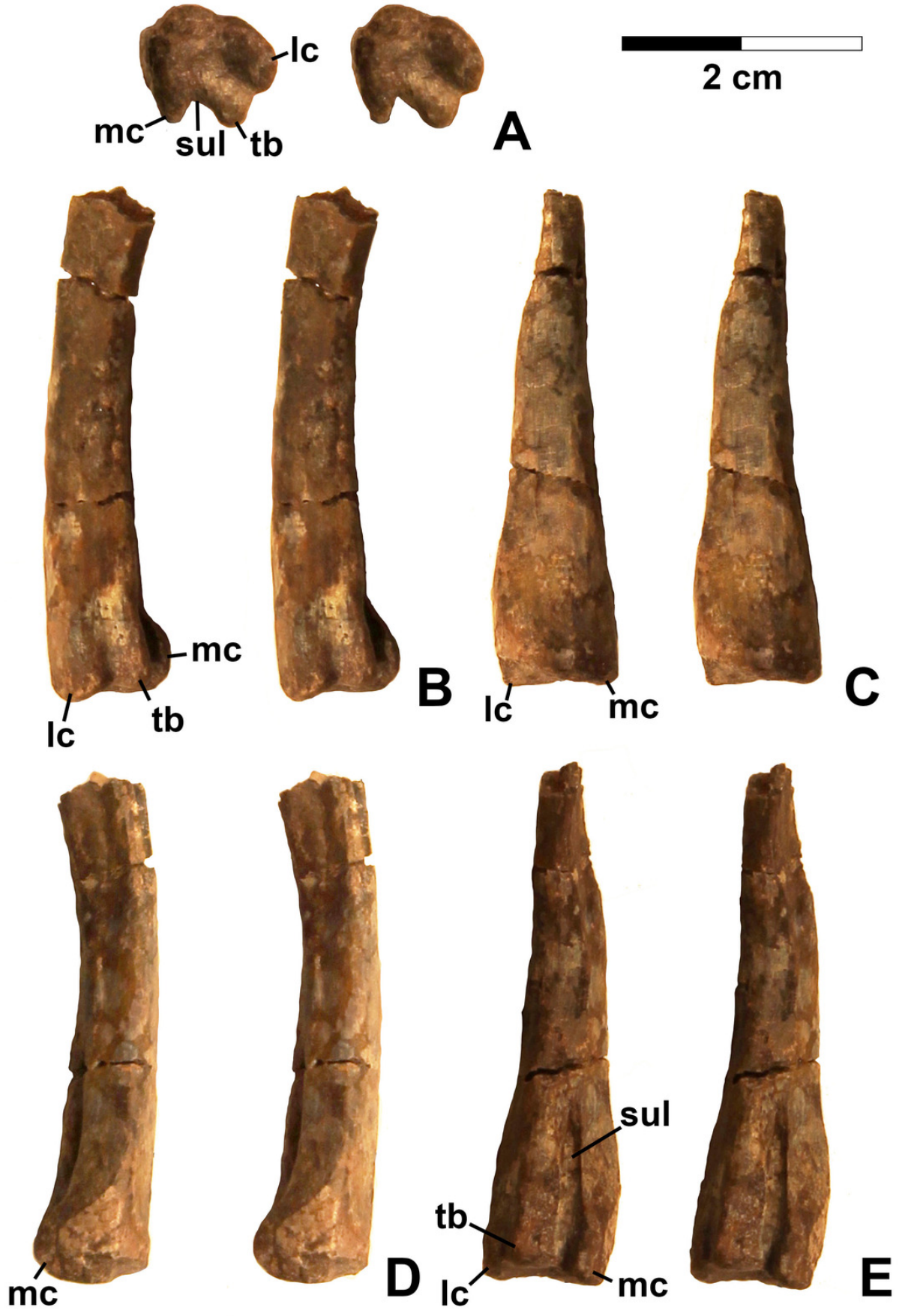
lc
mc
sul
tb
A
2 cm
mc
lc
tb
B
lc
mc
C
mc
D
sul
tb
lc
mc
E

# Figure 23

Figure_23_Phylogeny

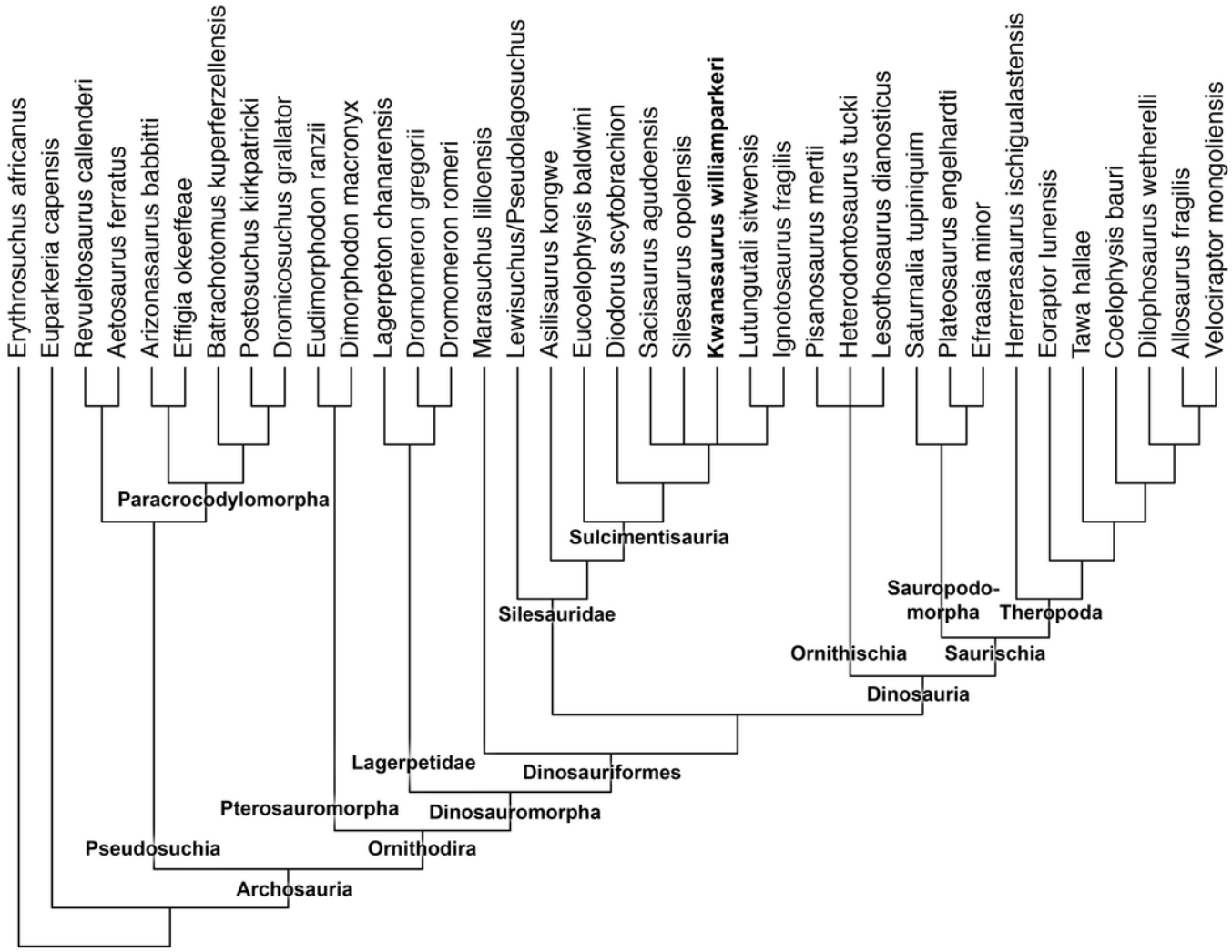

# Figure 24

Figure_24_Kwanasaurus_reconstruction

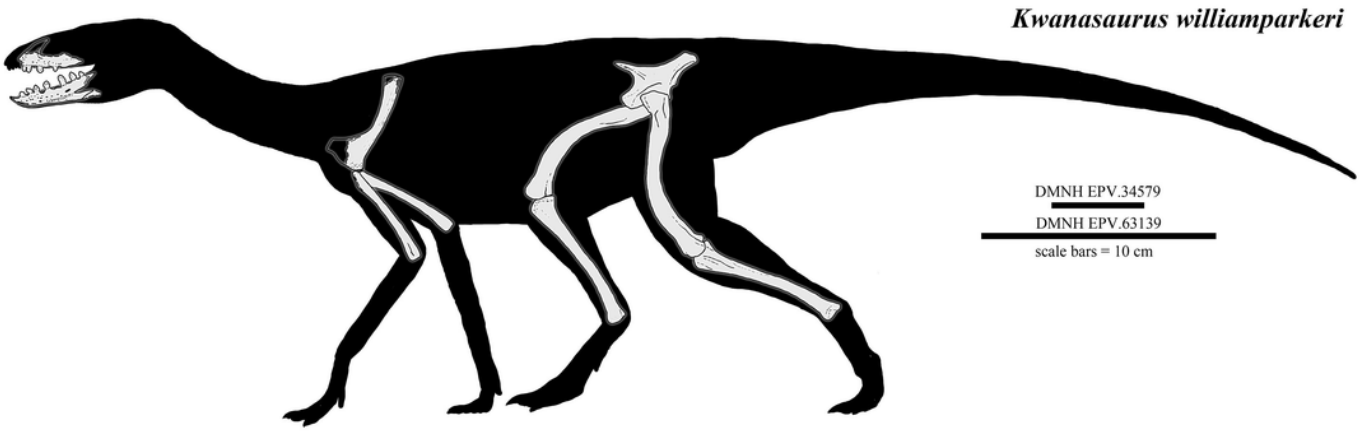

# Figure 25

Figure_25_Dinosauromorph_distribution_map

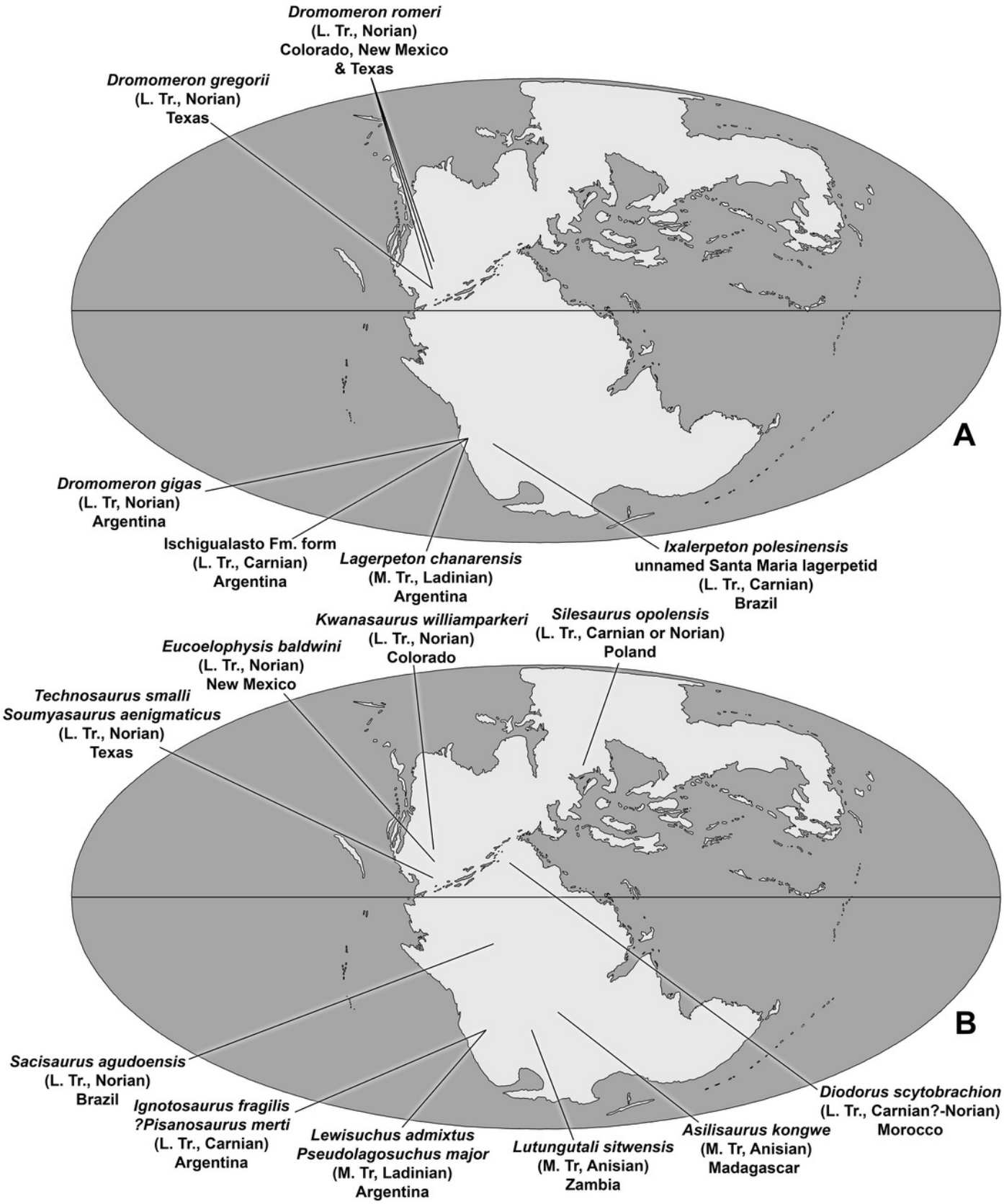
*Dromomeron romeri*
(L. Tr., Norian)
Colorado, New Mexico
& Texas
*Dromomeron gregorii*
(L. Tr., Norian)
Texas
A
*Dromomeron gigas*
(L. Tr, Norian)
Argentina
Ischigualasto Fm. form
(L. Tr., Carnian)
Argentina
*Lagerpeton chanarensis*
(M. Tr., Ladinian)
Argentina
*Ixalerpeton polesinensis*
unnamed Santa Maria lagerpetid
(L. Tr., Carnian)
Brazil
*Kwanasaurus williamparkeri*
(L. Tr., Norian)
Colorado
*Silesaurus opolensis*
(L. Tr., Carnian or Norian)
Poland
*Eucoelophysis baldwini*
(L. Tr., Norian)
New Mexico
*Technosaurus smalli*
*Soumyasaurus aenigmaticus*
(L. Tr., Norian)
Texas
B
*Sacisaurus agudoensis*
(L. Tr., Norian)
Brazil
*Ignotosaurus fragilis*
*?Pisanosaurus merti*
(L. Tr., Carnian)
Argentina
*Lewisuchus admixtus*
*Pseudolagosuchus major*
(M. Tr, Ladinian)
Argentina
*Lutungutali sitwensis*
(M. Tr, Anisian)
Zambia
*Asilisaurus kongwe*
(M. Tr, Anisian)
Madagascar
*Diodorus scytobrachion*
(L. Tr., Carnian?-Norian)
Morocco